

Doctor Thesis

Shibaura Institute of Technology

Operation Strategy and Evaluation of Battery Storage and
Power Converter towards Zero Energy in Commercial Building



A thesis submitted in partial fulfilment
for the degree of Doctor of Philosophy

2018/September

Pradita Octoviandiningrum Hadi

NA15503

Acknowledgements

It is a pleasure to thank many people who made this thesis possible.

First, I would like to thank to Prof. Dr. Goro Fujita for his guidance, also his patience and support in overcoming numerous obstacles I have been facing through my research.

Next, I gratefully acknowledge Hybrid Twinning Program of Shibaura Institute of Technology and Japanese Government (MEXT) scholarship for providing fund for my Ph.D study in Japan.

I also would like to express my gratitude to Daidan Co. Ltd., especially for Mr. Yasunobu Tanaka and Mr. Keisuke Tagami, for the research cooperation.

I convey special acknowledgement to my supervisor in Insitut Teknologi Bandung, Dr. Nanang Hariyanto. Thanks to his encouragement, I could attain this level of education.

Nevertheless, I would like to give my special thanks to my lovely mother. Without her unfailing support and continuous encouragement, I would never have the strength to reach this point.

Finally, yet importantly, I would like to thank my professors, my collages, also to everybody who has contributed to all valuable previous researches, which is important to realize this thesis successfully, as well as expressing my apology that I could not mention personally one by one.

Pradita Octoviandiningrum Hadi
na15503@shibaura-it.ac.jp
Shibaura Institute of Technology
September 2018

Abstract

Climate changes caused by emitted greenhouse gases leads to many environmental issues such as the change of water availability, highly probable of increasing extinct species, declination of food production in some areas, elevate sea level and increase floods possibility, etc. The main cause is carbon dioxide, which is majority emitted in energy utilization. Realizing this problem, many parties start to act towards energy revolution where they try to change the primary source of energy to be the clean or cleaner one. To promote the penetration of clean energy, utilities in many countries also make regulation about feed-in-tariff.

In building scale, the concept of zero energy building (ZEB) is arising there from the effort to reduce the energy consumption. ZEB concept focus on a low-energy building with considerably reduced energy consumption through efficiency gains, and then balanced the energy needs with renewable energy supplies. In order to support the realization of ZEB, we need generation system such as photovoltaic (PV) system, battery as energy storage and power converter as interface of various element in building distribution system. All of elements has lifetime, however battery has the shorter one, which is also influenced by its operation. Power converter helps to convert power in form of ac to dc and vice versa. It also can connect different voltage level of dc power. After all, additional power converter will give additional loss that has to bear with. Therefore, introduction of the operation strategy of battery and power converter is necessary. The different element to be used may also lead to different reliability system. In addition, we need to evaluate its performance economically. Expectedly, this research can give direction for building operator who want to achieve zero energy.

There are many challenges in order to realize ZEB. Many dispersed power generations that may need to be connected together with the utility grid. Increasing number of components also will give the control more complex tasks. The main challenges to realize ZEB that will be investigated in this study are including energy storage, power converter, and economic operation of system.

We proposed the control of battery charge-discharge operation by considering the battery lifetime. The aim is to make the battery lifetime longer by using carefully operation strategy. Other than using detail model simulation, we also use the proposed average model to make the simulation time shorter. We also compared the reliability system between ac-grid and dc-grid system in commercial building. The loss of load expectation (LOLE) is used to measure the reliability of system. Realizing ZEB means the need of connection between several types generation, storage, and load will increase. Based on the actual data from real system, we studied the converter loss and explained here. This study also discussed about the potential of power schedule optimization considering converter loss as the countermeasure. Finally, we introduced peak-time of electricity pricing parameters. Using the proposed peak-time pricing ratio, we done the economic evaluation using general model, also using extended model that considered the converter loss.

In conclusion, this research is addressed to answer three mains challenges to achieve ZEB: energy storage, power converter, and economic operation. Energy storage—Battery lifetime can be indicated by using some indicators, such as State of Health (SOH), State of Life (SOL), and Remaining Useful Life (RUL). By considering the lifetime parameter, we can expect the battery lifetime become longer compared to common operation. In addition, PV with battery system has a potential to reduce the electricity charge. Power converter—Avoid low power operation is necessary to keep high performance of converter. Except the sizing design, the operation controls also hold significant effect of maintaining efficiency converter in

operation condition. Considering the role of converters, the reliability evaluation in commercial building indicates reliability of dc-grids can be higher than the usual ac-grids. Economic operation—We proposed some price parameters, which can be used to evaluate the system benefit that is intended to be applied in preliminary economic study of system planning. Hence, it is still a deliberation that which system is better to be used, whether ac or dc system. This study shows that load composition has impact of the potential benefit if we change from current ac-system to dc-system. Each converter efficiency and battery size also have influence to the annual cost reduction.

Contents

Acknowledgements.....	i
Abstract.....	ii
Contents	iv
List of Tables.....	vii
List of Figures	viii
List of Abbreviations	x
Chapter 1 Introduction	1
1.1 Research Background	1
1.1.1 Environmental Issues	1
1.1.2 Energy Revolution	3
1.1.3 Feed-in-tariff (FIT) System	4
1.2 Zero Energy Building Concept	7
1.2.1 Definitions.....	7
1.2.2 Design Influence by ZEB Definition	8
1.2.3 ZEB Examples.....	9
1.3 Zero Energy Building Challenges	9
1.3.1 Energy Storage	9
1.3.2 AC System versus DC System	10
1.3.3 Economic Operation	11
1.4 Study Motivation.....	12
1.5 Thesis Structure.....	13
1.5.1 Chapter 1: Introduction	13
1.5.2 Chapter 2: Battery Charge Control by State of Health (SOH) Estimation	13
1.5.3 Chapter 3: Reliability of DC-Grids System in Commercial Building	13
1.5.4 Chapter 4: Study on Converter Loss and Optimizing Power Schedule	13
1.5.5 Chapter 5: Economic Evaluation Using Peak-Time Pricing Ratio.....	13
1.5.6 Chapter 6: Conclusion.....	13
Chapter 2 Battery Charge Control by State of Health (SOH) Estimation.....	14
2.1 Chapter Introduction.....	14

2.2	Battery Energy Storage Technology.....	14
2.2.1	Lead-Acid Battery	15
2.2.2	NiMH Battery	15
2.2.3	Li-Ion Battery	15
2.2.4	NaS Battery	15
2.2.5	Redox Flow Battery (RFB)	16
2.3	Battery Lifetime Indicator.....	16
2.3.1	Energy-throughput-based Model	16
2.3.2	Capacity Losses Model	16
2.3.3	Increasing Series Resistance Model.....	17
2.4	Battery Control Method	17
2.4.1	Detailed Model	18
2.4.2	Average Model	19
2.5	Numerical Simulations and Results.....	20
2.5.1	Detailed Model	20
2.5.2	Average Model	23
2.6	Chapter Conclusion	27
Chapter 3	Reliability of DC-Grids System in Commercial Building	28
3.1	Chapter Introduction.....	28
3.2	DC-Grids System for Building.....	28
3.2.1	Building Grid Models	29
3.2.2	Commercial Building Type	30
3.3	Reliability Analysis	31
3.3.1	System availability.....	31
3.3.2	Loss of Load Indices	32
3.4	Chapter Conclusion	33
Chapter 4	Study on Converter Loss and Optimizing Power Schedule	34
4.1	Chapter Introduction.....	34
4.2	Evaluation on Converter Loss	34
4.2.1	Evaluation Method.....	34
4.2.2	Evaluated System.....	35
4.2.3	Converter Evaluation Result.....	35
4.3	Optimizing Power Schedule in DC system of Building Power Distribution	40
4.3.1	System Architecture.....	40
4.3.2	Optimized Power Schedule Formulation	41
4.3.3	Numerical Results and Analysis.....	41
4.4	Optimizing Power Schedule Based on Converter Loss	45
4.4.1	System Architecture.....	45
4.4.2	Optimized Power Schedule Formulation	45

Contents

4.4.3	Numerical Results and Analysis	46
4.5	Chapter Conclusions	47
Chapter 5	Economic Evaluation Using Peak-Time Pricing Ratio	48
5.1	Chapter Introduction	48
5.2	Electricity Pricing System	49
5.2.1	Flat Pricing System	49
5.2.2	Block-Tariff Pricing System	49
5.2.3	Time-based Pricing System	49
5.3	Electricity Price Parameter	49
5.3.1	Price Parameter Definition	49
5.3.2	Electricity Price Parameter: Case of Japan	51
5.4	Cost Reduction	53
5.4.1	Cost Reduction Concept	53
5.4.2	Case Analysis	54
5.5	Economic Evaluation in General Model	57
5.5.1	System Model	57
5.5.2	Computational Experiments	58
5.6	Economic Evaluation in Extended Model	61
5.6.1	System Model	61
5.6.2	Cost Analysis and Results	64
5.7	Chapter Conclusions	66
Chapter 6	Conclusion	68
6.1	Alignment with Research Issues	68
6.2	Further Research Development	69
References	70
List of Publications	75

List of Tables

Table 1.1 The world’s top ten of greenhouse gas emitters based on WRI data (2013)	2
Table 1.2 Proposed emission reduction target in COP21 for various countries	2
Table 1.3 Feed-in-tariff for PV System in Japan	5
Table 1.4 List of key RE-related policies of Indonesia [8]	5
Table 1.5 Feed-in-tariff for PV System in Indonesia based on MEMR Regulation No.19/2016	6
Table 1.6 ZEB renewable energy supply option hierarchy [10]	8
Table 1.7 ZEB Example Summary [10]	9
Table 2.1 Characteristics of representative batteries[39]	15
Table 2.2 Ageing batteries coefficient for several battery technologies	17
Table 2.3 Battery Parameter	20
Table 2.4 System parameter	20
Table 2.5 Value of Delta SOH Reference	22
Table 2.6 Relative Error for Delta SOH	23
Table 2.7 Relative Error for Battery Power	23
Table 2.8 Comparison of measured Δ SOH	26
Table 2.9 Comparison of relative error for Δ SOH	26
Table 3.1 Appliances and its energy savings from avoided ac-dc power conversion losses	29
Table 3.2 The PV module and inverter characteristics[10]	30
Table 3.3 Main electric equipment in commercial buildings	31
Table 3.4 COPT of PV system running on AC (with inverter)	32
Table 3.5 COPT of PV system running on DC (without inverter)	32
Table 3.6 Comparison of LOLE value in hours/day	33
Table 4.1 Converter efficiency based on datasheet	35
Table 4.2 Efficiency analysis summary of PV converter	37
Table 4.3 Efficiency analysis summary of battery converter	39
Table 4.4 Efficiency analysis summary of DC/DC converter	40
Table 4.5 Season classification for electricity price	42
Table 4.6 Time classification for electricity price	42
Table 4.7 Unit price of electricity	43
Table 4.8 Power and loss equations	46
Table 5.1 List of considered power utility companies in Japan	51
Table 5.2 Comparison of benefit calculated by value α and real calculation	61
Table 5.3 List of converters	63
Table 5.4 Efficiency Converters	63
Table 5.5 Equations for battery and grid response in each mode	63

List of Figures

Figure 1.1 World total greenhouse gas emissions in ton of CO ₂ equivalent [1].....	1
Figure 1.2 Global emission by gas type in 2014 based on CAIT data.....	3
Figure 1.3 Global emission by sector in 2014 based on CAIT data	3
Figure 1.4 Implementation of measures to support renewable energy in major countries [7]	5
Figure 1.5 LCOE 2014 Prices and Audited 2016 BPP Numbers at Rp13,307/USD [9].....	6
Figure 1.6 Net Zero Energy Building (ZEB) categorization based on its supply-demand chart [11].....	7
Figure 1.7 Concerned aspects to schedule charge-discharge battery	10
Figure 2.1 Illustration for SOH calculation using capacity losses model	17
Figure 2.2 Bidirectional chopper (a) circuit and (b) control block for the battery	18
Figure 2.3 Control block with SOH calculation block.....	19
Figure 2.4 Detailed of additional block	19
Figure 2.5 Node position for SIM and path of circuit.....	19
Figure 2.6 Proposed SIM model.....	20
Figure 2.7 Simulation circuit for detailed model.....	21
Figure 2.8 Charge control block for detailed model	21
Figure 2.9 Actual battery power and SOH calculation block.....	21
Figure 2.10 Simulation result for discharging condition.....	22
Figure 2.11 Simulation result for charging condition	22
Figure 2.12 Simulation result for (a) discharging to charging condition, (b) charging to discharging condition	23
Figure 2.13 Simulation circuit for average model	24
Figure 2.14 SIM sub-circuit	24
Figure 2.15 Switch control block circuit for average model.....	24
Figure 2.16 Comparison of simulation result for discharging condition	25
Figure 2.17 Comparison of simulation result for charging condition	25
Figure 2.18 Magnifying of simulation result for discharging to charging condition.....	26
Figure 2.19 Magnifying of simulation result for charging to discharging condition	26
Figure 3.1 The net zero energy building concept	29
Figure 3.2 General topology in building distribution system using, (a) ac grids and (b) dc grids	29
Figure 3.3 Load curve for each commercial building type, summer and winter, ac-interface and dc-interface load	30
Figure 4.1 DC distribution grid of evaluated system	35
Figure 4.2 Data division of PV converter data	36
Figure 4.3 Power curve of PV converter.....	36
Figure 4.4 Power output (HVDC side) vs power input (solar side) curve of PV converter using data 1 ..	37
Figure 4.5 Power output (HVDC side) vs power input (solar side) curve of PV converter using data 2 ..	37
Figure 4.6 Power output (HVDC side) vs power input (solar side) curve of PV converter using data 3 ..	37
Figure 4.7 Power output (HVDC side) vs power input (solar side) curve of PV converter using data 4 ..	37
Figure 4.8 Power curve of battery converter	38
Figure 4.9 Power output (HVDC side) vs power input (battery side) curve of discharging battery for data 1	38

Figure 4.10 Power output (HVDC side) vs power input (battery side) curve of discharging battery for data 2	38
Figure 4.11 Power output (battery side) vs power input (HVDC side) curve of charging battery for data 1	39
Figure 4.12 Power output (battery side) vs power input (HVDC side) curve of charging battery for data 2	39
Figure 4.13 Power curve of DC/DC converter (Module A).....	39
Figure 4.14 Power curve of DC/DC converter (Module B)	39
Figure 4.15 Power output (DC Line side) vs power input (HVDC side) curve of DC/DC converter (Module A).....	40
Figure 4.16 Power output (DC Line side) vs power input (HVDC side) curve of DC/DC converter (Module B).....	40
Figure 4.17 System configuration and power flow.....	41
Figure 4.18 Load demand assumption	42
Figure 4.19 Season categorization for PV generation.....	42
Figure 4.20 Sample of calculation using spreadsheet	43
Figure 4.21 Monthly cost comparison result.....	44
Figure 4.22 Annual cost comparison result.....	45
Figure 4.23 System configuration and power flow including converter loss	45
Figure 4.24 Power schedule with simple ruled-base algorithm.....	47
Figure 4.25 Power schedule by minimize converter loss	47
Figure 5.1 Price illustration for one-step peak pricing.....	50
Figure 5.2 Price illustration for two-steps peak pricing	51
Figure 5.3 Electricity charge of power utility companies in Japan for summer season	52
Figure 5.4 Electricity charge of power utility companies in Japan for non-summer season	52
Figure 5.5 Price parameter of utilities in Japan for summer season	52
Figure 5.6 Price parameter of utilities in Japan for non-summer season	53
Figure 5.7 Comparison of load profile and electricity price	53
Figure 5.8 Illustration of cost reduction concept.....	54
Figure 5.9 Illustration of undesired increase of maximum power	54
Figure 5.10 Flowchart of battery charge-discharge amount for method 1	55
Figure 5.11 Flowchart of battery charge-discharge amount for method 2	55
Figure 5.12 Electricity price assumption	56
Figure 5.13 Power assumptions for (a) demand and (b) PV generation	56
Figure 5.14 Comparison of method 1 and method 2	56
Figure 5.15 Battery size analysis results	57
Figure 5.16 Electricity price in general and peak-time pricing plan.....	58
Figure 5.17 General model of power grid system for building	58
Figure 5.18 Daily load and PV generation curve.....	59
Figure 5.19 Algorithm for charging-discharging battery in scenario 1.....	60
Figure 5.20 Relation of benefit and alpha values with various size of batteries	61
Figure 5.21 Additional benefit per kWh of battery for each system.....	61
Figure 5.22 Building power grid extended model in (a) ac system and (b) dc system	62
Figure 5.23 Universal model of building power grid system	62
Figure 5.24 Flowchart for deciding battery response and power purchased from grid.....	63
Figure 5.25 Energy price for weekday in peak-time pricing plan	64
Figure 5.26 Load and PV generation curve.....	64
Figure 5.27 Comparison annual total cost by battery size	65
Figure 5.28 Total annual cost vs portion of DC load in battery size comparison.....	65
Figure 5.29 Comparison annual total cost by efficiency converter	66
Figure 5.30 Comparison annual total cost by value of alpha and battery size	66
Figure 5.31 Total annual cost vs portion of DC load for load sensitivity analysis	66

List of Abbreviations

AC	Alternating Current	GHGs	Green House Gases
ANN	Artificial Neural Network	HEPCO	Hokkaido Electric Power Company
BAU	Business-as-usual	HVAC	Heating, Ventilating, and Air Conditioning
BPP	<i>Biaya Penyediaan Pokok</i>	HVDC	High Voltage Direct Current
CAIT	Climate Access Indicators Tool	INDC	Intended Nationally Determined Contributions
CCS	Carbon Dioxide Capture and Storage	IPCC	Intergovernmental Panel on Climate Change
CfD	Contract for Different	JRC	Joint Research Centre
CHUDEN	Chubu Electric Power Company	KEPCO	Kansai Electric Power Company
CHP	Combined Heat and Power	KYUDEN	Kyushu Electric Power Company
CO ₂	Carbon Dioxide	LCOE	Levelized Cost of Electricity
COP	Conference of Parties	LOLE	Loss of Load Expectation
COPT	Capacity Outage Probability Table	MEMR	Minister of Energy and Mineral Resources
DC	Direct Current	MEP	Multistep Electricity Price
DOD	Depth-of-Discharge	MTTF	Mean Time to Failure
EDGAR	Emission Database for Global Atmospheric Research	MTTR	Mean Time to Repair
EHP	Electric Heat Pump	NDC	Nationally Determined Contributions
EPCO	Electric Power Company	NRE	New and Renewable Energy
FCCC	Framework Convention on Climate Change	NREL	National Renewable Energy Laboratory
FIP	Feed-in-Premium	OKIDEN	Okinawa Electric Power Company
FIT	Feed-in-tariff	PCS	Power Conditioner System
FOR	Forced Outage Rate	PLN	<i>Perusahaan Listrik Negara</i>
FY	Fiscal Year	PV	Photovoltaic
GA	Genetic Algorithm		
GE	Genetic Electric		

List of Abbreviations

RE	Renewable Energy	SOL	State of Life
RO	Renewable Obligation	TEPCO	Tokyo Electric Power Company
RPS	Renewable Portfolio Standard	TOU	Time-of-Use
RUL	Remaining Useful Life	WRI	World Resources Institute
RVMs	Relevance Vector Machines	YONDEN	Shikoku Electric Power Company
SIM	Switch Inductor Model	ZEB	Zero Energy Building
SOC	State-of-Charge		
SOH	State of Health		

Chapter 1

Introduction

1.1 Research Background

1.1.1 Environmental Issues

The climate change increases the global surface temperature. Various impacts may occur such as the change of water availability, highly probable for a number of species will become extinct, declination of food production in some areas, elevate sea level and increase floods possibility, also give rise to number of diseases and increase levels of premature death. The main cause of climate change is the greenhouse effect, which caused by the greenhouse gases (GHGs) include carbon dioxide (CO₂).

Based on data from Emission Database for Global Atmospheric Research (EDGAR), which is provided by European Commission, Joint Research Centre (JRC)/Netherlands Environmental Assessment Agency (PBL) [1], world total greenhouse gas emissions is increasing almost twice in the last four decades (Figure 1.1). The latest global data available (2013) from World Resources Institute (WRI) shows that the world's top three gas emitters—China, the United States and the European Union—contribute more than half of total global emission. Altogether of the top ten emitters (Table 1.1), which include Japan and Indonesia, contribute for nearly three-quarters of global emissions [2]. These listed countries need to do a significant action in order to successfully undertake the climate change challenges.

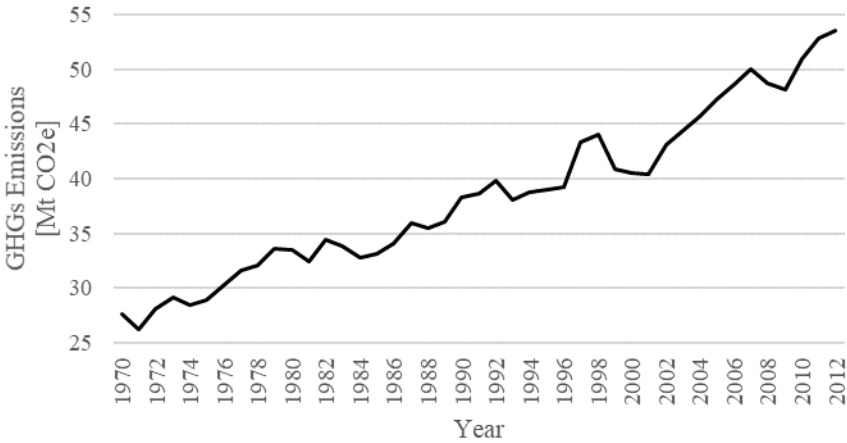


Figure 1.1 World total greenhouse gas emissions in ton of CO₂ equivalent [1]

The international concern about climate change start more than three decades ago. In 1983, US Academy of Sciences published a report on climate change. In the same year, World Commission on Environment and Development was established within the United Nations. This committee published a report called “Our Common Future” in 1987. The following conferences show how the worldwide concern to prevent dangerous climate change by trying to reduce their emission. The “Changing Atmosphere” conference which held in Toronto, Canada, in June 1988 determined the worldwide CO₂ emission should be reduced by 20% by 2005. Start in 1990, almost every five years, Intergovernmental Panel on Climate Change

(IPCC) published reports on the status of climate-change-related sciences. Second publication is in 1995, third one is in 2001, fourth in 2007, and the fifth is in 2013 and 2014.

United Nations' Conference on Environment and Development which held in Brazil, 1992, published the United Nation Framework Convention on Climate Change (UNFCCC) with main objective to prevent climate change to the dangerous state. In Kyoto Protocol (Japan, 1997), developed countries agreed to reduce their emission of GHGs by an average of 5.2% by 2008-2012 compared with the 1990 levels. In December 2015, Conference of Parties 21 (COP21) declared Paris Agreement, which is trying to hold the increase of global average temperature to below 2°C. All Parties are invited to initiate domestic preparations by submitting their own intended nationally determined contributions (INDC) to the committee in COP21. These INDCs will be considered as nationally determined contributions (NDC) after the Paris Agreement is concluded. In case of Japan, the INDC is the level of GHG emission reduction of 26.0% by fiscal year (FY) 2030 compared to FY 2013, or approximately 1042 Mt-CO₂e as 2030 emission. In order to achieve this target, the ratio of renewable energy within the total electric power generated is expected to be around 22-24%. Considering this condition, solar energy is prospected to increase by seven times. The INDCs of other countries are listed in Table 1.2.

Table 1.1 The world's top ten of greenhouse gas emitters based on WRI data (2013)

Country	GHGs [Mt CO ₂ e]
China	11,735.0
United States	6,279.8
European Union 28	4,224.5
India	2,909.1
Russia	2,199.1
Japan	1,353.3
Brazil	1,017.9
Indonesia	744.3
Canada	738.4
Mexico	733.0
Others	11,802.8

Table 1.2 Proposed emission reduction target in COP21 for various countries

Country	Proposed emission reduction target from 2020
Japan	2030: -26% (compared to 2013)
United States	2025: -26% to -28% (compared to 2005)
EU	2030: -40% (compared to 1990)
Russia	2030: -25% to 30% (compared to 1990)
Canada	2030: -30% (compared to 2005)
Australia	2030: -26% to -28% (compared to 2005)
Switzerland	2030: -50% (compared to 1990)
Norway	2030: -40% (compared to 1990)
China	2030: -60% to -65% per GDP unit (compared to 2005)
India	2030: -33% to -35% per GDP unit (compared to 2005)
Mexico	2030: -22%, conditionally -36% (compared to BAU)
South Africa	2025: -398 Mt; 2030: -614 Mt (compared to BAU)
Brazil	2025: -37%; 2030: -43% (compared to 2005)

There are several ways to reduce CO₂ emissions, such as increase share of non-carbon in primary supply, change the composition of fossil fuel to less carbon one, employ CO₂ capture and storage (CCS) system, and reduce the energy demand. Up to now, electricity generation is relying most on carbon energy source such as coal, oil, and natural gas.

Following is the way to achieve the emission targets. First is developing safe and inexpensive CCS system. Second is promoting large-scale solar plants with stable output, such as space solar power or concentrated

solar power. Third is developing nuclear fusion. However, in Japan, Fukushima accident give major effect to stop the use of nuclear fusion for generating electricity. Fourth is reduce deforestation and promote reforestation. Fifth is stabilize emissions of non-CO₂ GHGs.

Data on the Climate Access Indicators Tool (CAIT) [3] indicates the major emitted GHGs is CO₂ (Figure 1.2). Energy sector, as the largest contributor, emit approximately three-quarters of global emitted GHGs (Figure 1.3), which is including the electricity generation. By focusing in energy sector, substantial impact of emission reduction can be achieved.

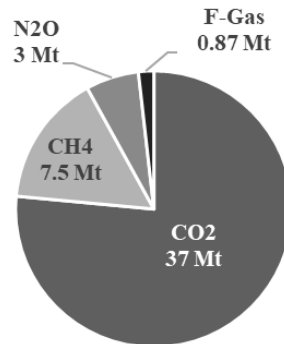


Figure 1.2 Global emission by gas type in 2014 based on CAIT data

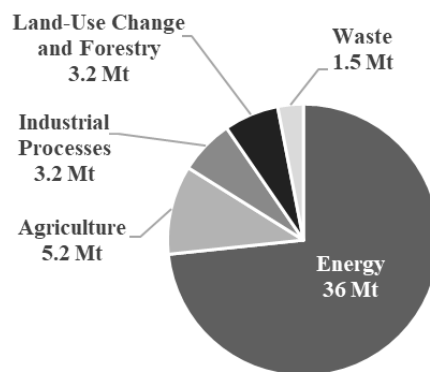


Figure 1.3 Global emission by sector in 2014 based on CAIT data

Based on IPCC report [4], in 2010, electricity and heat production give 25% of total anthropogenic GHG emissions with half is come from building sector. The share of indirect CO₂ emission of buildings almost same with industry. In total, buildings give 18.4% share, which 6.4% from direct emissions and 12% from indirect emissions. According to this fact, concerning to reduce CO₂ emission of buildings also can give significant impact in total.

1.1.2 Energy Revolution

Nowadays we are facing the revolution of energy from a fossil energy era to a new energy era. In the earliest era, there is a global primary energy transformation from wood to coal in period of 1800s. The secondary energy transformation, which is from coal to hydrocarbon sources, was happened on 1990s to 1950s period. The last transformation is the tertiary energy transformation from hydrocarbon to new energy sources. In this transformation era, the world annual oil production peak is predicted will be occurred around 2040. Besides, natural gas will reach the peak of annual production around 2060 [5].

In Japan, in the early of industrial era, domestic coal is the main primary source. In 1950s, domestic coal production dropped radically after war and hydropower compensated for the drop to some extent. In 1960s,

Japan made an energy revolution by shifting mainstream energy supply from domestic coal to imported oil. However, the dependency to imported oil brought Japan to its first oil crisis in 1973. Diversifying energy supply source is used to address these issues. Six years later, in 1979, second oil crisis occurred, then oil quota is applied for importer countries such as Japan. In 1980s, importing of steam coal expanded to full scale which is principally used for power generation. In 1990s, Japan started to put “3E” which includes energy security, economy, and environment in their energy policy. Japan declared a Basic Act on Energy Policy in 2002 for securing energy supply with environmental suitability and utilization of market mechanism. There are three plans that were published respectively in October 2003, March 2007, and June 2010. After Fukushima nuclear power plant accident happened in 2011, Japan added “S” for safety value to their energy policy than become “3E + S”. In 2012, Japan started to applied feed in tariff policy. In 2014, Strategic Energy Plan is published as fourth plan for Basic Act on Energy Policy.

In case of Indonesia, since 2004, Indonesia becomes a net oil importer, because the demand is higher than the national production. The national energy mix in 2015 is still dominated by hydrocarbon sources, which is approximately 95% of total energy. However, the new and renewable energy (NRE) is targeted to be increased to 23% in 2025 and 31% in 2050. As stated in [6], efforts to decrease GHGs emission is following these four factors. First factor is energy diversification by increasing percentage of NRE in national energy mix. Second factor is utilization of clean coal technology for electric power generation. Third one is energy transformation from oil to natural gas. The last factor is energy conservation program. Reflecting to these four factors, the GHGs emission is targeted to be decreased by 58% in 2050 compared to business-as-usual (BAU) scenario [6].

1.1.3 Feed-in-tariff (FIT) System

Feed-in-tariff (FIT) system is a supporting measure to encourage renewable power generation. Beside FIT, there is another program called Renewables Portfolio Standard (RPS), which mandates electric power resellers to have a fixed percentage of power sold from their targeted renewable energy sources. Figure 1.4 describes how the major countries implement the measures to support renewable energy. Here, another measures type is started to be introduced, such as Renewables Obligation (RO), Feed-in-Premium (FIP), and Contract for Difference (CfD). In FIP, there is a view to have renewable energy support scheme and the electric power market work together, and a bidding system in which market competition determines the level of governmental assistance. FIP, which is increasingly implemented in Europe, provides the certainty of investment, and better economic rationality. In CfD, the portion where the market price falls below the strike price will be supplemented. The uniqueness of this system is that the power generation companies reimburse the excess in cases where the market price exceeds the strike price [7].

Table 1.3 shows detail FIT for PV system in Japan from fiscal year 2012-2019. The type is divided into residential and non-residential PV system. Residential PV system contains less than 10 kW PV system. Recently, it is categorized in more detail by seeing the whether the system use power conditioner system (PCS) or not, also whether using double power generation or not. The determined tariff for each category decreases year by year. It may lead to unprofitable system when trying to sell the energy from PV generation to grid. In addition, the tariff for non-residential PV system is more unpredictable, especially if in the future, it uses kind of energy tender.

Indonesia start to concern about renewable energy on 2006. Up to now, there are several RE-related policies that is issued in Indonesia, which is summarized in Table 1.4. Indonesia has targeted that 23% of their energy mix will come from New and Renewable Energy (NRE) by 2025. Start on 2012, energy from small and medium scale renewable energy generation and excess power can be purchased by utility company in Indonesia called “*Perusahaan Listrik Negara*” (PLN). In the following years, the more detail policies about purchasing of electricity are issued.

However, FIT for PV system in Indonesia is hard to predict because the possibility of suddenly policy change is high. On July 2016, Minister of Energy and Mineral Resources (MEMR) of Indonesia published the regulation No.19/2016, which regulate the power purchase from solar photovoltaic (PV) power

generator by State Electricity Company (PT. PLN). Based on this regulation, new FIT is set with range from 14.5 – 25.0 US cent/kWh and with capacity quota depending on the region (Table 1.5).

	1998	1999	2000	2001	2002	2003	~	2010	2011	2012	2013	2014	2015	RE	Target / Plan
Japan						RPS			FIT				10.7%	2030 / 22-24%	
South Korea					FIT			RPS				3.7%	2022 / 10%		
California					RPS								20.9%	2020 / 33%+	
Spain	FIT/FIP												29.6%	2020 / 40%	
Germany			FIT								FIP		22.9%	2050 / 80%	
Italy			RPS			FIP								16.2%	2020 / 26%
UK			RO								CFD		11.4%	2020 / 31%	

Figure 1.4 Implementation of measures to support renewable energy in major countries [7]

Table 1.3 Feed-in-tariff for PV System in Japan

Type/Scale	With PCS	Double power gen. system	FY 2012	FY 2013	FY 2014	FY 2015	FY 2016	FY 2017	FY 2018	FY 2019
Residential PV Systems, <10kW	No	No	42 yen	38 yen	37 yen	33 yen	31 yen	28 yen	26 yen	24 yen
	Yes	No				35 yen	33 yen	30 yen	28 yen	26 yen
	No	Yes				25 yen	25 yen	25 yen	24 yen	24 yen
	Yes	Yes				27 yen	27 yen	27 yen	26 yen	26 yen
non-residential PV systems, 10kW-2MW			40 yen	36 yen	32 yen	29 yen 27 yen*	24 yen	21 yen	unannounced	
non-residential PV systems, >2MW									via solar tender	

*after profit consideration

Table 1.4 List of key RE-related policies of Indonesia [8]

Year	Policy Issued
2006	• National Energy Policy (NEP)
2008	• Determination of Work Area for Geothermal Mining
2009	• Law on Electricity
2010	• Tax and Custom Facility for Renewable Energy Resource Utilization
2012	• Investment General Plan • Amendment on Guideline for Geothermal Implementation • Amendment on List of Power Generation Development Project Acceleration using Renewable Energy, Coal, and Gas and Related Transmission • Electricity Purchase from Small and Medium Scale Renewable Energy and Excess Power
2013	• Purchasing of Electricity by PLN from Solar PV • Purchasing of Electricity by PLN from Municipal Solid Waste (MSW)
2014	• National Energy Policy (NEP) • Electricity Purchasing by PLN from Biomass Power Plant and Biogas Power Plant • Law on Geothermal • Amendment on the Purchasing of Electricity by PLN from Hydro • Purchasing of Electricity by PLN from Geothermal
2015	• Regulation on Hydro • Regulation on MSW
2016	• Purchasing of Electricity by PLN from Solar PV

Table 1.5 Feed-in-tariff for PV System in Indonesia based on MEMR Regulation No.19/2016

No.	Area	Capacity Quota (MWp)	Feed in Tariff (US cent/kWh)
1	DKI Jakarta	Total: 150.0	14.5
2	West Java		14.5
3	Banten		14.5
4	Central Java and Yogyakarta		14.5
5	East Java		14.5
6	Bali	5.0	16.0
7	Lampung	5.0	15.0
8	South Sumatera, Jambi, and Bengkulu	10.0	15.0
9	Aceh	5.0	17.0
10	North Sumatera	25.0	16.0
11	West Sumatera	5.0	15.5
12	Riau and Riau Archipelago	4.0	17.0
13	Bangka-Belitung	5.0	17.0
14	West Kalimantan	5.0	17.0
15	South Kalimantan and Central Kalimantan	4.0	16.0
16	East Kalimantan and North Kalimantan	3.0	16.5
17	North Sulawesi, Central Sulawesi, and Gorontalo	5.0	17.0
18	South Sulawesi, South-East Sulawesi, and West Sulawesi	5.0	16.0
19	West Nusa Tenggara	5.0	18.0
20	East Nusa Tenggara	3.5	23.0
21	Maluku and North Maluku	3.0	23.0
22	Papua and West Papua	2.5	25.0

After 6 months, on January 2017, MEMR published the new regulation No.12/2017 about utilization of renewable energy resources for electricity supply. This regulation determines a new FIT scheme, which is depending on regional supply cost of electricity (*biaya penyediaan pokok/BPP*) compare to national supply cost of electricity. The objective of this regulation is to suppress the national BPP. If regional BPP is higher than national BPP, then the tariff is defined as 85% of regional BPP in maximum. If regional BPP is lower than or equal to national BPP, then the tariff is defined as 100% of regional BPP. Figure 1.5 shows regional and national BPP, also levelized cost of electricity (LCOE) of several type of power generation. Based on this data, only two regions will have FIT for PV higher than its LCOE. However, the regulation will limit up to 85% of regional BPP, which is still lower than LCOE of solar PV.

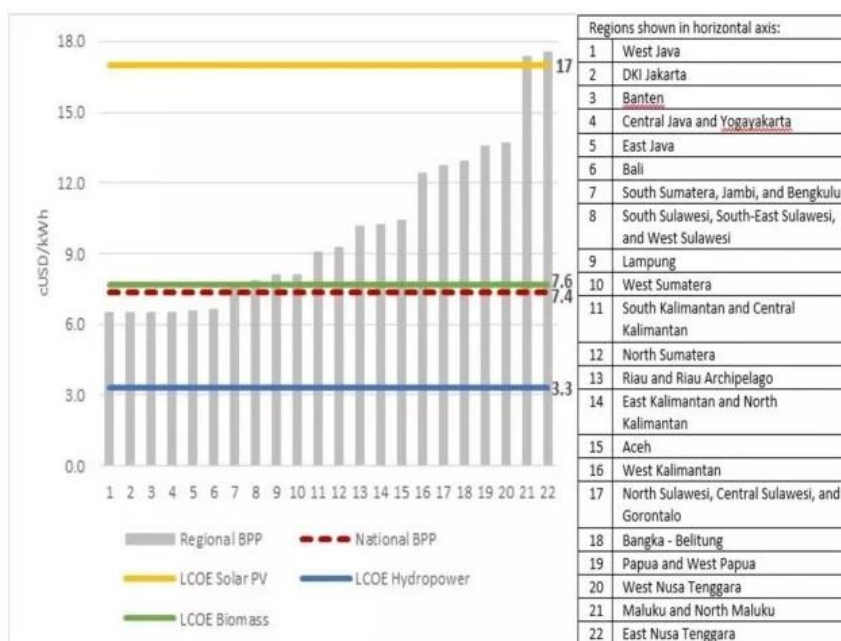


Figure 1.5 LCOE 2014 Prices and Audited 2016 BPP Numbers at Rp13,307/USD [9]

When the regulation is easy to be changed, the certainty of future tariff is low. Besides, the determined tariff itself is also low. In this condition, investment for system that intend to sell the electricity to grid is unsecured.

1.2 Zero Energy Building Concept

Zero energy building (ZEB) is recognized as the key of energy and electricity saving concept in Japan strategic documents such as the Energy Conservation Technology Strategy (2011) and the Basic Energy Plan (2014). Japan's target declared in the Basic Energy Plan for ZEB is specified into two stages. The first stage is enforcing ZEB for newly constructed public building, etc., by 2020. The second one is enforcing ZEB for an average of newly constructed buildings by 2030.

1.2.1 Definitions

The concept of ZEB is a low-energy building with considerably reduced energy consumption through efficiency gains, and then balanced the energy needs with renewable energy supplies. As shown in Figure 1.6, we can categorize the building into three general categories. First category is net minus energy building. In this category, demand total of building is less than local energy generation. However, the building should reduce its demand at least 65% of reference building. By putting effort to reduce demand and increase the local supply, we can shift the building to be ZEB oriented, ZEB ready, nearly ZEB level I, and nearly ZEB level II. To be recognized as ZEB oriented, the building should reduce the demand to 50% compare to reference building. Second category is net zero energy building, when the amount of demand and supply is equal. The last category is net plus energy building, which has larger amount of local generation compare to the demand.

How we claim the success of achieving a net zero energy building is depending on how we define the zero energy building itself. Every definition will lead to different goal. However, there is no single suitable definition for zero energy building. Based on US National Renewable Energy Laboratory (NREL) report in [10], there are four well-definitions of net zero energy building. The difference of each definition lies in the perception of the zero value that to be achieved. Following sections will explain the detail of each definition.

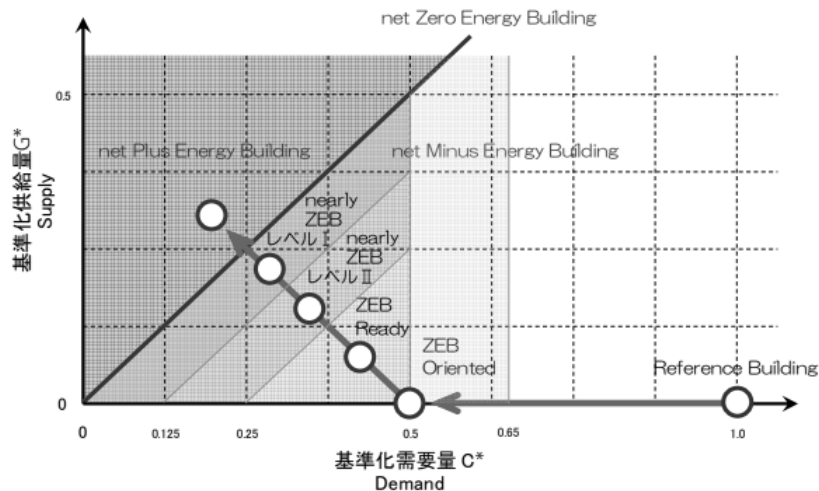


Figure 1.6 Net Zero Energy Building (ZEB) categorization based on its supply-demand chart [11]

1.2.1.1 Net Zero Site Energy

A net zero site energy building sees the site as boundary. It defines the net zero of energy in the site as the target to be achieved. In order to acquire this target, the building should produce energy at least as much energy that used in the site.

1.2.1.2 *Net Zero Source Energy*

A net zero source energy building see the energy start from its source and count the transmission loss. So that, in this definition, the net zero energy will be achieved by producing energy at least as much energy that used in the site when accounted for at the source.

1.2.1.3 *Net Zero Energy Costs*

The net zero energy costs definition is based on the value of energy in currency. The net zero energy will be achieved when income amount from selling electricity to utility is at least equal to the purchased amount that paid to utility over the year. In this definition, the amount of electricity sold and electricity purchased can be different.

1.2.1.4 *Net Zero Energy Emissions*

The last definition is based on the emitted emission. A net zero emission building produces emission-free energy from renewable source at least as much as energy used from emission-produced sources.

1.2.2 Design Influence by ZEB Definition

Each definition of ZEB will influence the design, which has its own advantages and disadvantages. Table 1.6 shows the preferred application of renewable energy supply based on [10]. The influence of each definition of ZEB will be described in following section.

1.2.2.1 *Net Zero Site Energy*

Within this definition, a site ZEB produces energy as much as it uses. Using rooftop PV (Table 1.6, Option 1) or other on-site sources but not on the building (Table 1.6, Option 2) may be available as an option to achieve a site ZEB. For determining the progress to a ZEB goal, we can do verification easily through on-site measurements. It has the fewest external fluctuation that influence the ZEB goal, and therefore provides the most repeatable and consistent definition. There is no consideration for the values of various fuels at the source here. There is also possibility that it does not realize the energy cost saving. This is the limitation of this definition.

1.2.2.2 *Net Zero Source Energy*

In this definition, we use appropriate site-to-source energy factors, as a multiplication for calculating total source energy of the building both imported and exported energy. The difference of each energy factor increases the dependence of source of energy. Different area with different energy mix will influence the design of building. Same as a site ZEB, a source ZEB also may not realize comparable energy cost savings.

1.2.2.3 *Net Zero Energy Costs*

A cost ZEB totally depends to the electricity purchased charge and sold rate. A time-of-use charge would be advantageous for a cost ZEB. If demand charges account for a significant portion of the utility bills, a net cost ZEB becomes difficult. In case two-way or net metering is not available, on-site energy storage and demand-responsive control should be included in the design.

Table 1.6 ZEB renewable energy supply option hierarchy [10]

Option Number	ZEB Supply-Side Options	Examples
0	Reduce site energy use through low-energy building technologies	Daylighting, high-efficiency HVAC equipment, natural ventilation, evaporative cooling, etc.
On-Site Supply Options		
1	Use renewable energy sources available within the building's footprint	PV, solar hot water, and wind located on the building.
2	Use renewable energy sources available at the site	PV, solar hot water, low-impact hydro, and wind located on-site, but not on the building.
Off-Site Supply Options		
3	Use renewable energy sources available off site to generate energy on site	Biomass, wood pellets, ethanol, or biodiesel that can be imported from off site, or waste streams from on-site processes that can be used on-site to generate electricity and heat.
4	Purchase off-site renewable energy sources	Utility-based wind, PV, emissions credits, or other "green" purchasing options. Hydroelectric is sometimes considered.

1.2.2.4 Net Zero Energy Emissions

An emission-based ZEB produces emissions-free energy as much as it uses from emissions-producing energy sources. Therefore, the success of achieving an emission-based ZEB depends on the energy mix from the generation source. When it is already zero emission that means it needs no effort to achieve the mission of emission-based ZEB. However, the net zero emissions ZEB definition has similar calculation difficulties as the source ZEB definition.

1.2.3 ZEB Examples

This following section will shows some examples of ZEB that have been studied in [10]. They are:

- “Oberlin”—The Adam Joseph Lewis Center for Environmental Studies, Oberlin College.
- “Zion”—The Visitor Center at Zion National Park, Springdale, Utah.
- “Cambria”—The Cambria Department of Environmental Protection Office Building, Ebensburg, Pennsylvania.
- “CBF”—The Philip Merrill Environmental Center, Chesapeake Bay Foundation, Annapolis, Maryland.
- “TTF”—The Thermal Test Facility, National Renewable Energy Laboratory, Golden, Colorado.
- “BigHorn”—The BigHorn Home Improvement Center, Silverthorne, Colorado.
- “Science House” Science Museum of Minnesota, St. Paul, Minnesota.

Table 1.7 shows the buildings with the additional PV system array area and capacity requirements to meet the ZEB goals. Some of buildings need different size of additional PV for being source or site ZEB. It shows that the ZEB definition also will influence the design requirement.

Table 1.7 ZEB Example Summary [10]

Building and PV System (DC Rating Size)	Site Energy Use (w/o PV) (MWh/yr)	Source Energy Use (w/o PV) (MWh/yr)	Actual Roof Area (footprint) (ft ²)	Flat Roof Area (ft ²) Needed for Source ZEB and Site ZEB with PV	PV System DC Size Needed for Source ZEB and Site ZEB
Oberlin-60 kW	118.8	380.2	8,500	10,800	120 kW
Zion-7.2 kW	91.6	293.1	11,726	6,100	73 kW
Cambria-17.2 kW	372.1	1,190.7	17,250	37,210	415 kW
CBF-4.2 kW	365.2	1,142.0	15,500	25,316 Source ZEB 25,640 Site ZEB	282 kW Source ZEB 286 kW Site ZEB
TTF-No PV	83.5	192.5	10,000	4,010 Source ZEB 5,550 Site ZEB	45 kW Source ZEB 62 kW Site ZEB
BigHorn-8.9 kW	490.4	901.0	38,923	18,449 Source ZEB 31,742 Site ZEB	206 KW Source ZEB 354 kW Site ZEB
Science House-8.7 kW	5.9	18.8	1,370	1,000	6 kW

1.3 Zero Energy Building Challenges

There are many challenges in order to realize ZEB. Many dispersed power generations that may need to be connected together with the utility grid. Increasing number of components also will give the control more complex tasks. The main challenges to realize ZEB that will be investigated in this study are including energy storage, power converter, and economic operation of system.

1.3.1 Energy Storage

The availability of energy generated from local power generation can be lower than the load, but in another time, it can also be higher. That is the reason why energy storage is needed to store the surplus energy, then will be used when the system lacks of power generation.

The common used energy storage is battery. In general PV system, the concerned aspect for scheduling charge-discharge power of battery (Figure 1.7) is including the objective of the scheduling itself, the battery purpose, prediction of PV generation and load. The objective of battery charge-discharge scheduling can be for minimizing cost, emission, or energy loss in system. The battery purpose is to be peak shaver or only for backup. In case for backup purpose, the scheduling becomes unnecessary. Other parameter to be concerned is the forecast of PV generation and load demand. PV generation forecast can be done by physical model or statistical model, which may include parameter such as sky clearness index (for example, clear, partially cloudy, and cloudy), ambient temperature, and wind speed. Load can be forecasted in short-term by using time-series model such as regression, stochastic, or artificial intelligence (for example Artificial Neural Network (ANN), Genetic Algorithm, (GA)). Another load forecast approach is by using similar day approach. Sample parameter that can be used for load forecast is type of day, precipitation (rain or sunny), and discomfort index, which is mainly affected by weather factor like temperature and humidity.

Realizing ZEB may require high capacity of battery storage, which lead to high investment cost. Think of the limitation of battery’s charge-discharge cycle, high repetition of charge-discharge operation will make the battery lifetime become shorter. It means the sooner it needs to be replaced which leads to additional investment cost.

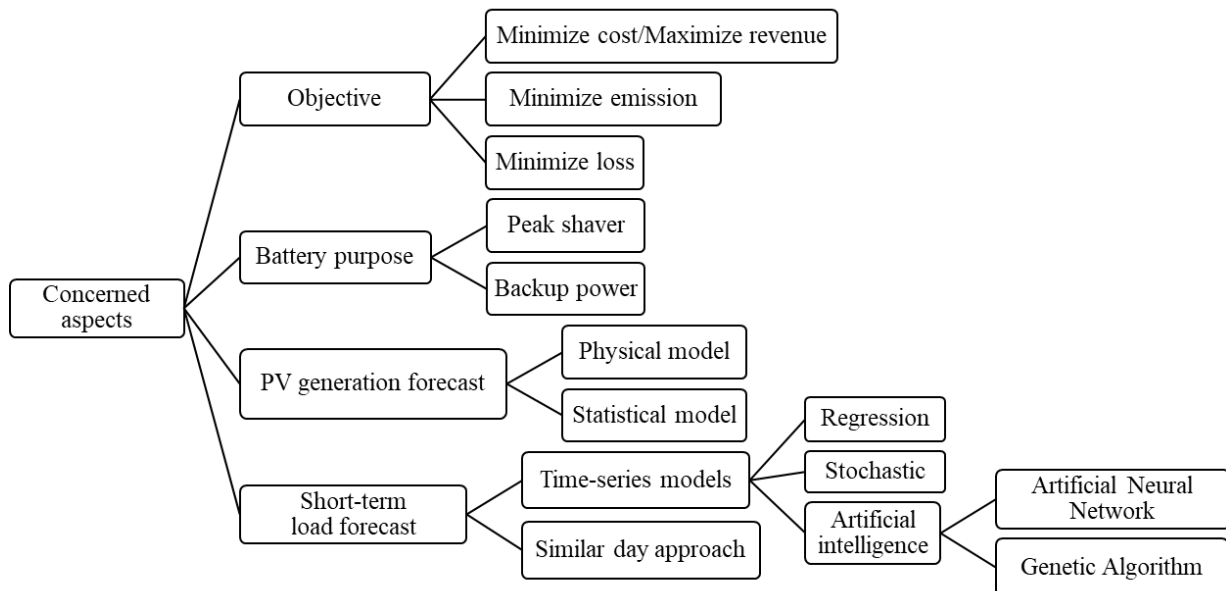


Figure 1.7 Concerned aspects to schedule charge-discharge battery

1.3.2 AC System versus DC System

“War of the Currents” was starting in the late 1880s. Thomas Edison developed direct current (DC), current that runs continually in a single direction, had a problem in that time. It cannot be converted to another level voltage, so transmission losses will be high for transferring power in long distance. While alternating current (AC) which is developed by Nikola Tesla can be easily converted to different voltage using transformer. By using higher voltage, the losses in transmission can be reduced. Besides that, Westinghouse by using Tesla's patent of AC system won bid for illuminating The Chicago World's Fair, the first all-electric fair in the world in 1893. Westinghouse won against General Electric (GE) that using Edison’s DC system by offering a more efficient and cost-effective of AC system. For the attendees, it showed that AC power would be the future system for electricity. This was the start of electricity predominantly by AC power.

Nowadays many electricity appliances start to change. Computer desktop, laptop, mobile phone, and many other electronic appliances are using DC technologies. To can be operated, they need converter to get

energy from currently system, which is an AC system. The using of converter will add some losses in the system, so more energy is needed.

We are also facing the limitation of carbon fueled energy resources. This condition leads people to exploit renewable energy in their own building, such as solar power by using photovoltaic (PV), which generate DC power. Therefore, both source and load with dc interface might be increasing. Within the context of simplicity and efficiency, it is unreasonable to use “DC-AC-DC” route from dc source to dc load [12]. It leads the dc building distribution system to be proposed.

Increasing of DC load and source leads research to evaluate the using of DC distribution system possibilities. Pang, et al. [12] evaluate possibilities of using DC electrical distribution systems in building with increasing renewable (RE) sources and DC loads by comparing efficiency of AC and DC distribution system. The calculation show replacement of current 3-phase 4-wire AC system with generic DC distribution system can save 16% of electricity. The using of DC distribution system also improves PV performance because use DC-DC converter instead of grid-connected inverter, which has better efficiency. The other benefits also have been mentioned qualitatively, such as potential material saving, power quality, reliability, and system simplicity with RE.

By using mathematical model, Starke, et al. [13] have compared loss of AC and DC distribution system in the higher voltage level, not in building level system. It showed that to get fewer losses in the pure AC load environment, DC distribution system with higher voltage level and very high DC-DC converter efficiency is required. It also showed that AC and DC distribution system could have the same merit when the loads are equal in ratio.

By realizing the current system that is using AC system, Asad & Kazemi [14] have derived quantitatively the effect of transition from AC to DC system in case of efficiency, cost, loss, and reliability. There is enormous task need to be done before this system widely used [15], including safety and investment cost. Still, there is no standard yet for constructing DC distribution system in buildings scale.

1.3.3 Economic Operation

An efficient and optimum economic operation and planning of electric power generation system has an important position in the electric power industry. The classic problem is the economic dispatch of fossil-fired generation system to achieve minimum cost. The increasing concern of environmental matters leads to the necessity of “economic dispatch” that also includes such target like minimizing pollutant and conserving various forms of fuel [16]. In the first instance, the power generation is centralized, and then the energy is transferred by using transmission and distribution system to reach the customer. Following this condition, only one side who operates the power generation and transmission can control the economic dispatch.

Currently, dispersed generator began to commonly used, which is distributed in wide area with low to medium scale of power capacity. The main purpose of dispersed generator system is to maximize the utilization of energy sources and to reduce the stress of transmission load. Some area might have small available capacity of energy source to be exploited. By using dispersed generator system concept, this small capacity still can be utilized. The low amount of generated power means it cannot be transferred to the far place. This condition would lead to the operation system that trying to supply the demand using the nearest power generation. So that, the load of transmission line can be suppressed.

Following each policy, private parties also have the chance to inject the generated or excess energy into utility grid, and then get paid for the sold electricity. However, they need to follow some rules, such as voltage deviation; in order to keep the whole system operates smoothly. Moreover, to maintain the reliability system, smaller system called microgrid is started to be used. It contains power generation, distribution system, and load, which covers smaller area. Each microgrid should has the ability to operate both independently and connected with utility.

Various control strategy for economic operation of microgrids, whether AC, DC, or hybrid AC-DC, is being developed recently, such as decentralized control [17], hierarchical optimization and control [18], [19], predictive control [20], [21], also intelligent control such as using fuzzy logic [22], and genetic algorithm [23], [24]. The main purpose of the control strategy is to achieve optimal operation strategy, which has minimum cost and balanced condition of whole system. The complexity of the control strategy depends on number of controlled variable and objective.

In the era of Internet-of-Thing (IoT), we started to learn that energy also would have the similar future called Internet-of-Energy (IoE). The framework for information exchange [25] in microgrid operation will be necessary. The security of energy internet also need to be considered, which includes security of cyber-attack and energy availability [26], [27]. Connecting many consumer and producer with complex transmission system will create a big data to be handled. In term of data analytic, the security issues that need to be concerned include impersonation, eavesdropping, data manipulation, access and authorization, and system availability [28].

In framework of ZEB, where the power generation is included in building, economic operation in building scale will be necessary. Based on the ZEB definitions that have been explained in section 1.2.1, the most affected design is a cost ZEB, which the main target is to achieve the net-zero of cost. However, in order to get the optimum design, other type of ZEB also need economic operation strategy.

There are several options of local generation that can be used in ZEB. At any rate, PV system is still a common option. In addition, we usually use the battery as the complement of PV system to overcome the uncertainty of its power generation. Price of PV and battery system installation has potential to decrease year by year, following its development stage. However, to achieve the status of zero energy, PV and battery sizing design still require high investment cost due to the necessary capacity. In order to balance the high investment cost, the operation cost need to be reduced by incessantly of optimal economic operation. In this case, we also can consider the economic operation of power distribution in building as main challenges for realizing ZEB.

The economic operation in power system had a bearing on electricity price. The variably price based on time or total consumption will lead to different behavior of optimal operation. An advanced calculation for optimal operation may need such additional expenses. For small building with low demand, it can be too expensive to bear. Therefore, kind of simple calculation using such as spreadsheet that usually they already have will be a good way to cope with this problem.

1.4 Study Motivation

In order to support the realization of ZEB, we need generation system such as PV system, battery as energy storage and power converter as interface of various element in building distribution system. All of elements has lifetime, however battery has the shorter one, which is also influenced by its operation. Power converter helps to convert power in form of ac to dc and vice versa. It also can connect different voltage level of dc power. After all, additional power converter will give additional loss that has to bear with. Therefore, introduction of the operation strategy of battery and power converter is necessary. The different element to be used may also lead to different reliability system. In addition, we need to evaluate its performance economically. Expectedly, this research can give direction for building operator who want to achieve zero energy. Followed the explanation in section 1.3, this research will focus on three points: energy storage, power converter, and economic operation in ZEB.

1.5 Thesis Structure

We organized this research into six chapters. Following are the short outline of each chapter.

1.5.1 Chapter 1: Introduction

This chapter includes background and motivation of this research. Here, we also describe the concept and main challenges of ZEB.

1.5.2 Chapter 2: Battery Charge Control by State of Health (SOH) Estimation

This chapter describes the control of battery charge-discharge operation considering the battery lifetime. The purpose is for making the battery lifetime longer by using carefully operation strategy. Other than using detail model simulation, we also use the proposed average model to make the simulation time shorter.

1.5.3 Chapter 3: Reliability of DC-Grids System in Commercial Building

Here, we discussed about the comparison of reliability system between ac-grid and dc-grid system in commercial building. The loss of load expectation (LOLE) is used to measure the reliability of system.

1.5.4 Chapter 4: Study on Converter Loss and Optimizing Power Schedule

Realizing ZEB means the need of connection between several types generation, storage, and load will increase. Based on the actual data from real system, we studied the converter loss and explained here. This chapter also discuss the potential of power schedule optimization considering converter loss as the countermeasure.

1.5.5 Chapter 5: Economic Evaluation Using Peak-Time Pricing Ratio

Section 5.2 introduces peak-time of electricity pricing parameters. Based on peak-time pricing, section 5.4 describes the cost reduction concept. Using the proposed peak-time pricing ratio, we done the economic evaluation. Section 5.5 shows the economic evaluation result of general model. Section 5.6 points out the economic evaluation result that considered the converter loss using extended model.

1.5.6 Chapter 6: Conclusion

Section 6.1 will conclude the studies covered in this thesis. The further research development will described by section 6.2.

Chapter 2

Battery Charge Control by State of Health (SOH) Estimation

2.1 Chapter Introduction

Electricity demand increases day by day. Concerning about carbon emission and global warming pumps up the need of sustainable sources such as photovoltaic (PV). It also may change the people lifestyle [29]. Recently, smart systems such as smart house and smart building are becoming more and more popular. It is necessary to use storage system such as battery for managing peak demand and improving reliability of the system [30]. It makes the used of battery increase.

Battery has shorter lifetime compare to other parts in system [31]. When reached its end-of-life (EOL), the battery need to be replaced. Generally, the limit is set to 80% of nominal capacity [32]. If there are many changes of battery along the whole system lifetime, it can increase total investment cost. Degradation of battery depends on its operation which can be influenced by the operational management [33]. Several studies proposed method to extend battery lifetime, such as optimization based on life loss cost [34] and replacement cost [35].

State of Health (SOH) is commonly used for estimating battery lifetime. There are several indications that can be used to evaluate SOH, such as series resistance [36], capability of storing energy [37], and restriction of cycle number. This study proposes additional block control, which is using decreasing of SOH as reference. Aim of this block is to control the battery power and manage battery lifetime, all at one. Further, it can be used for more advanced optimization charge control, such as to extend battery lifetime or optimize investment and operational cost.

2.2 Battery Energy Storage Technology

In the past, electrical energy has to be used as soon as it is generated. Along with the development of renewable energy utilization, energy storage is also developed as one of countermeasure of the intermittent energy. The batteries used in power system applications so far are deep cycle batteries with energy capacity ranging from 17 to 40 MWh and having efficiencies about 70-80% [38]. Representative batteries technologies include lead-acid batteries, nickel-metal-hydride (NiMH) batteries, lithium-ion (Li-ion) batteries, sodium Sulphur (NaS) batteries, and vanadium redox-flow batteries (VRBs). Each representative technologies has different characteristics as summarized in Table 2.1. Apart from price differences, each battery type may be well suited for a particular energy storage application in consequence of its own unique features and characteristics[39].

Table 2.1 Characteristics of representative batteries[39]

Type	Lead-Acid	NiMH	Li-Ion	NaS	VRB
Energy density (Wh/kg)	25-50	60-120	75-200	150-240	10-30
Power density (W/kg)	75-300	250-1,000	500-2,000	150-300	80-150
Cycle life (100% DOD)	200-1,000	180-2,000	1,000-10,000	2,500-4,000	>12,000
Round-trip efficiency (%)	75-85	~65	85-97	75-90	75-90
Self-discharge	Low	High	Medium	-	Negligible

2.2.1 Lead-Acid Battery

The lead-acid battery development is started in 1970s [40], and being the oldest rechargeable battery. In this type of battery, the positive and negative electrodes are separately made up of lead dioxide and metallic lead, which are immersed in a diluted sulphuric-acid electrolyte. The main advantages of using lead-acid batteries are high efficiency of energy, low self-discharge rate, and low up-front cost. However, the further development of lead-acid battery faces some technical drawbacks, including low depth of discharge (<20%), low cycle life, low energy density, and slow charging rate. Lead-acid batteries are still primarily employed in cases where cost effectiveness, reliability, and abuse tolerance are critical, but energy density and lifetime are not as important [39]. Safety considerations in large application of lead-acid batteries is necessary. It is reported that there is a significant number of injuries occur during the maintenance and repair of lead-acid batteries. These injuries include burns from electrical arcing and acid exposure, as well as strained muscles and crushed hand [41].

2.2.2 NiMH Battery

NiMH battery consists of a nickel-oxyhydroxide-based positive electrode, a metallic cadmium-based negative electrode, and an alkaline electrolyte (usually potassium hydroxide). This type of battery has higher power/energy density, realizes better environmental friendliness, and is less prone to undergo memory effect, compared to nickel cadmium (NiCd) battery). Nonetheless, it has several technical drawbacks, such as high self-discharge rate, limited service life, and low Coulombic efficiency (about 65%). In addition, it has a very low ability to tolerate fast charging and overcharge. Especially during fast charging, massive amounts of heat may be generated, and hydrogen buildup may cause cell rupture, leading to considerable capacity decay [39].

2.2.3 Li-Ion Battery

The Li-ion battery is an advanced rechargeable battery first commercially developed in the early 1990s. This battery is formed by lithiated metal oxide in cathode and graphitic carbon in anode with a layer structure. When charging, Li-ions are inserted into and deinserted from the negative electrode and positive electrode, respectively. The process is reversed during discharge process. Compared to other types of batteries, Li-ion batteries have advantages of high energy density, high efficiency, long cycle life, and environmental friendliness. Battery-cycle life is a key factor for grid application and affects the economic viability of energy storage [39].

2.2.4 NaS Battery

NaS battery is composed of a molten Sulphur anode, a molten sodium cathode, and separated by solid beta alumina ceramic electrolyte. The electrolyte allows only the positive sodium ions to go through it and combine with the sulfur to form sodium polysulfides. To allow the charge and discharge cycles, batteries have to be operated in temperatures over 300°C, such that Sulphur and sodium exist in a molten state. External heating is required to start the operation, whereas it is usually not needed during the charge and discharge processes, as internal heat can be generated by electrochemical reactions. NaS battery is able to provide high energy density and round-trip efficiency, long lifetime, and deep also fast discharge. Moreover, its ability to work at high temperatures allows operation within some hot and harsh environment. However, NaS battery should be taken carefully in its operation, because pure sodium is hazardous and will spontaneously burn if exposed to air and moisture. In addition, if the beta alumina ceramic electrolyte is broken, the molten sodium and Sulphur are directly mixed, incurring short-circuits and exothermic reactions [39].

2.2.5 Redox Flow Battery (RFB)

Flow battery type consists of two electrolyte reservoirs. Between these reservoirs, the electrolytes are circulated through an electrochemical cell comprising a cathode, an anode, and a membrane separator. The chemical energy is converted to electricity in the electrochemical cell, when the two electrolytes flow through. Both electrolytes are stored separately in large storage tanks outside the electrochemical cell. An RFB is a type of energy storage device consisting of separate power and energy modules. It makes the power and energy capacity completely independent each other. As the advantage, it is easy to scale up to multi-megawatts and megawatt-hours by modular design. This battery type also has an exceptionally long lifespan, with excellent safety, reliability, and large-scale applicability. Moreover, RFBs exhibit good transient, with very fast response speed. Therefore, it is well-suited for balancing highly variable renewables [39].

2.3 Battery Lifetime Indicator

Comparing to other parts in the system, battery has the shorter lifetime. The price also quite expensive for buying the new one. Obviously, the concern about battery lifetime in power management system is needed. There are several indicators for battery lifetime, such as State of Health (SOH), State of Life (SOL), and Remaining Useful Life (RUL). State of health is indicated by capacity degradation, internal resistance increase, or a combination of the two. State of life is the time when the battery must be replaced. It is similar to SOH, but quantifies the remaining time until the battery will be unable to perform. Remaining useful life is the length of time from present time to the end of useful life. This means the lower RUL indicates the shorter time to reach the end of life.

The speed of battery capacity degradation can be influence by several factors, such as deep depth-of-discharge (DOD), high or low temperature, high c-rates, extreme state-of-charge (SOC) levels, etc. By controlling the battery operation, the slower degradation speed is expected.

In this study, SOH is selected to represent the battery life. SOH can be calculated use several models, such as energy-throughput-based model, capacity losses model, and increasing series resistance model. By considering the long cycle-life and high round-trip efficiency, li-ion battery is chosen to be investigated here.

2.3.1 Energy-throughput-based Model

Energy-throughput-based model assumes that under constant operating conditions, a battery can withstand a certain amount of energy throughput, which is equivalent to a number of charge/discharge cycles, before it reaches its end-of-life. Total number of cycles before end-of-life (N) usually is stated in the datasheet. In this model, total energy-throughput is defined as multiplication of number of cycles before end-of-life and initial energy capacity of the battery, Q for charging cycle, and the same value for discharging cycle. If the total energy that flows is equal to the total energy-throughput, then the battery will reach its end-of-life. So that, amount of battery power at time t ($P(t)$) is a main factor for the degradation speed.

If $SOH(t)$ indicates SOH battery at time t , based on this model it will be calculated by (2.1). New battery, as the battery capacity equals its nominal initial value, $SOH(t)$ is equal to one. Whenever $SOH(t)$ reaches zero, it means the end-of-life of the battery is reached.

$$SOH(t) = SOH(t - \Delta t) - \frac{1}{2 \cdot N \cdot Q} \cdot \int_{t-\Delta t}^t |P(\tau)| d\tau \quad (2.1)$$

2.3.2 Capacity Losses Model

Capacity losses model defines the SOH as comparison of current battery capacity with its initial value at $t = 0$. Every time the batteries operations a discharge, capacity losses are calculated and new battery capacity at time t ($C_{bat}(t)$) is obtained. In this model, only when batteries are discharged, the capacity

losses will be calculated as illustrated in Figure 2.1. The ageing batteries coefficient (Z) of several battery type is shown in Table 2.2.

By observing the state of charge battery ($SOC(t)$) in percentage, capacity loss at time t ($\Delta C_{bat}(t)$) is defined as (2.2). Corresponding SOH at time t ($SOH(t)$) is calculated by (2.3).

$$\Delta C_{bat}(t) = C_{bat}(0) \times Z \times [SOC(t - \Delta t) - SOC(t)] \quad (2.2)$$

$$SOH(t) = \frac{C_{bat}(t) - \Delta C_{bat}(t)}{C_{bat}(0)} \quad (2.3)$$

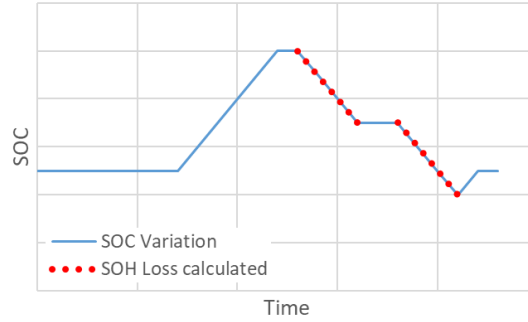


Figure 2.1 Illustration for SOH calculation using capacity losses model

Table 2.2 Ageing batteries coefficient for several battery technologies

Technologies	Z
Pb flat plate	3×10^{-4}
Pb tubular	0.5×10^{-4}
Ni-Cd	0.6×10^{-4}
Li-ion	0.17×10^{-4}

2.3.3 Increasing Series Resistance Model

Series resistance of battery will increase as the usage time. Based on this characteristic, the last model is using the increase of battery series resistance (R_0) to indicate SOH. Typically, battery series resistance at end-of-life (R_0^{EOF}) is 1.6 times higher than battery series resistance of new batteries (R_0^{New}). In this model, SOH is calculated by comparing the value of battery series resistance at time t ($R_0(t)$) with the new batteries as mentioned in (2.4). However, measuring battery internal resistance online is still quite difficult.

$$SOH(t) = \frac{R_0^{EOF} - R_0(t)}{R_0^{EOF} - R_0^{New}} \quad (2.4)$$

2.4 Battery Control Method

Bidirectional chopper circuit control the amount of battery power, as shown in Figure 2.2 (a). By adjusting duty cycle of switch T_1 and T_2 , amount of charge or discharge power can be controlled. Common power control block, as shown in Figure 2.2 (b), use battery power reference (P_B^*) value command as a reference value and, current-loop and voltage-loop as feedbacks [42]. This study proposed additional block control, which is using decreasing of SOH as reference.

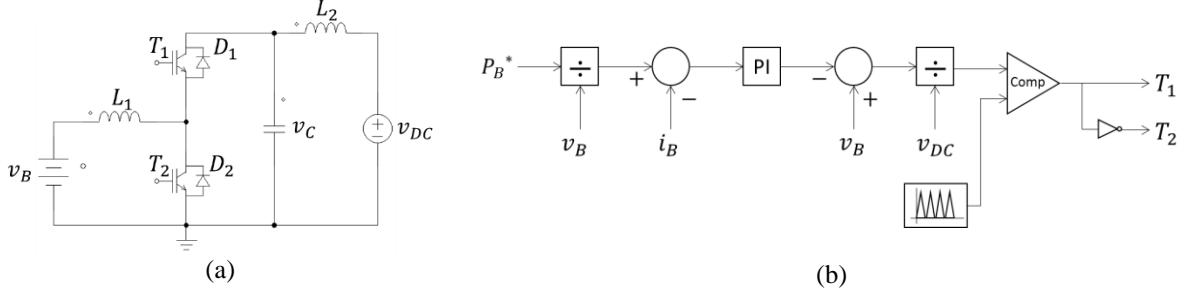


Figure 2.2 Bidirectional chopper (a) circuit and (b) control block for the battery

2.4.1 Detailed Model

This section will explain the proposed control method in detailed model.

New battery is indicated by SOH value equal to 1, and battery reached the end of life is indicated by SOH value equal to 0. Based on the simplicity and possibility of implementing, energy-throughput based of SOH estimation is chosen here. We define (2.5) to calculate SOH at $t + \Delta t$.

$$SOH(t + \Delta t) = SOH(t) - \frac{1}{2 \cdot N \cdot Q_{new}} \cdot \int_t^{t+\Delta t} \frac{|P_B(\tau)|}{3600} d\tau \quad (2.5)$$

Where, t indicates time in second, $SOH(0)$ indicates battery state of health initial value, N is a total number of cycles before end-of-life, Q_{new} is initial energy capacity of the new battery in kWh, and $P_B(t)$ is charge or discharge power of battery at time t in kW. In order to distinguish charge and discharge condition, positive value is defined as discharge power and negative value is defined as charge power. Generally, value of N is not constant. It depends on battery operating condition [43]. However, in order to keep the simplicity of this study, value of N is assumed to be constant.

Equation (2.6) shows that the value of SOH always decrease time by time. For simplicity in calculation, decreasing value of SOH, $\Delta SOH(t + \Delta t)$, is defined by (2.7).

$$SOH(t + \Delta t) - SOH(t) = - \frac{1}{2 \cdot N \cdot Q_{new}} \cdot \int_t^{t+\Delta t} \frac{|P_B(\tau)|}{3600} d\tau \quad (2.6)$$

$$\Delta SOH(t + \Delta t) = \frac{1}{2 \cdot N \cdot Q_{new}} \cdot \int_t^{t+\Delta t} \frac{|P_B(\tau)|}{3600} d\tau \quad (2.7)$$

By time discretization, equation (2.8) can be derived from (2.7) for calculating P_B along period of Δt . Here, reference of battery power can be driven by desired decreasing value of SOH. However, other command is necessary to decide the battery flow, whether to charge or discharge. This command is defined by $P_{B,flow}$ as shown in (2.9), where positive value for discharging and negative value for charging.

In order to control the battery charging and discharging process by using decreasing value of SOH as reference, an additional calculation block is proposed as shown in Figure 2.3. The function of this block is to calculate the value of P_B^* . The calculation block is defined by referring to (2.8) and (2.9). Figure 2.4 shows the detail calculation of the additional block. This block will calculate battery power reference value based on desired value of ΔSOH , Δt , and $P_{B,flow}$. The value of P_B^* is determined by how much SOH is allowed to decrease along period of Δt . While $P_{B,flow}$ gives command for the direction of power flow, which is to charge or discharge.

For evaluating the proposed control block, measured voltage and current of the battery is used for calculating instantaneous value of P_B . Then this value is used for calculating the estimation of decreasing SOH by modifying (2.8).

$$|P_B(t)| = \frac{2 \cdot N \cdot Q_{new} \cdot 3600 \cdot \Delta SOH(t + \Delta t)}{\Delta t} \quad (2.8)$$

$$P_{B,flow} = \begin{cases} +1, & \text{for discharging} \\ -1, & \text{for charging} \end{cases} \quad (2.9)$$

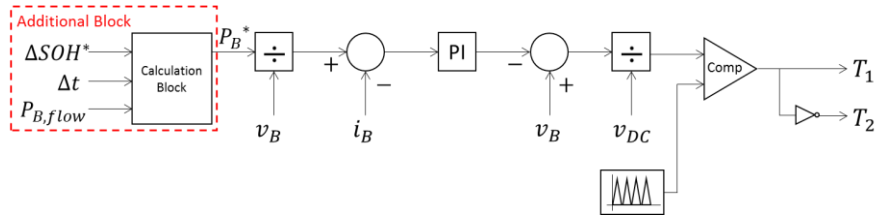


Figure 2.3 Control block with SOH calculation block

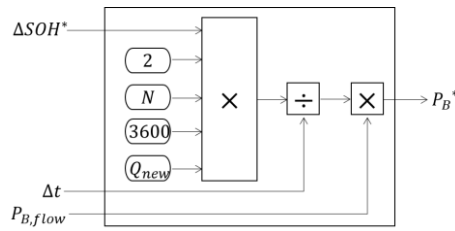


Figure 2.4 Detailed of additional block

2.4.2 Average Model

Switch mode DC-DC converter relies on a switched inductor as a temporary energy storage between input and output terminal. Switch Inductor Model (SIM) as average model for boost converter is proposed in [44]. Based on it, the average model for bidirectional chopper is developed in this study. In this model, the converter is substitute by 3-ports block, which represent the node at side of switched inductor (node a) and each end of switch (node b and c) as shown in Figure 2.5. The path of circuit when switch T_1 on is shown by blue line and for switch T_2 on is shown by red line.

By using continuous current mode, this bidirectional DC-DC converter is represented in its average value based on (2.10) to (2.14). $D_{1,on}$ and $D_{2,on}$ are duty cycle of switch T_1 and T_2 to be on, respectively. Figure 2.6 shows the average model of SIM.

$$D_{1,on} = 1 - D_{2,on} \quad (2.10)$$

$$E_L = V_{ab} \cdot D_{1,on} + V_{ac} \cdot D_{2,on} \quad (2.11)$$

$$I_a = I_L \quad (2.12)$$

$$I_b = I_L \cdot D_{1,on} \quad (2.13)$$

$$I_c = I_L \cdot (1 - D_{1,on}) = I_L \cdot D_{2,on} \quad (2.14)$$

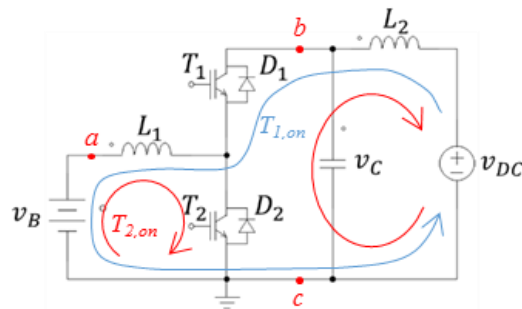


Figure 2.5 Node position for SIM and path of circuit

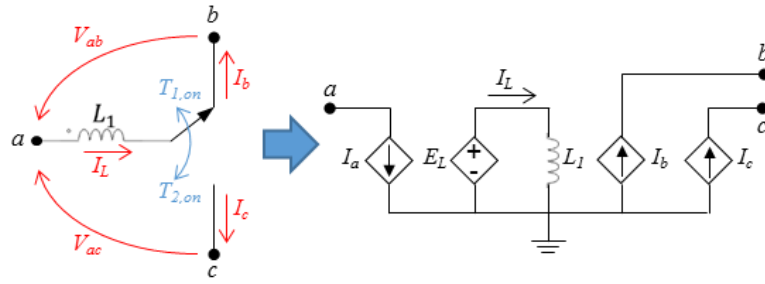


Figure 2.6 Proposed SIM model

2.5 Numerical Simulations and Results

To evaluate the proposed model, battery charge system is built by using PSIM software 64-bit Version 10.0, which is running on computer with Intel® Core™ i5-6500 CPU @ 3.20GHz processor and 4 GB RAM. Parameter of battery is shown by Table 2.3. For the numerical simulation, the assumption for total number of cycles before end-of-life is 4000 cycles. Initial energy capacity of the new battery in total is 4800 kWh. Whole system parameter is shown by Table 2.4.

Table 2.3 Battery Parameter

Parameter	Value	Unit
Rated voltage	48	V
Discharge cut-off voltage	32	V
Rated capacity	20	Ah
Internal resistance	0.05	Ohm
Full voltage	57.6	V
Exponential point voltage	54	V
Nominal voltage	51.2	V
Maximum capacity	24	Ah
Exponential point capacity	5	Ah
Nominal capacity	22	Ah
Initial SOC	80%	

Table 2.4 System parameter

Parameter	Value	Unit
L_1	4	mH
L_2	0.1	mH
C_1	4000	μ F
DC bus voltage	400	V
Number of batteries in series	4	

2.5.1 Detailed Model

In order to validate the performance of the proposed design, following simulation procedure is used. Battery system as shown in Figure 2.7 is built. In this system, lithium ion battery model is adopted then connected to DC bus by bidirectional converter. Bidirectional converter is used to charge and discharge the battery, which is controlled by switch T_1 and T_2 . Figure 2.8 depicts the battery charge control block that gives the command to by switch T_1 and T_2 . Input values of ΔSOH , Δt , and $P_{B,flow}$ are entered to generate battery power reference. The measured values of battery voltage, vb and current, ib are used for feedback loops. Proportional-Integral (PI) controller is set with gain 10 and time constant 0.1. The control block will generate signal reference to control the switches in bidirectional converter. The block may

generate control signal that makes the circuit produce the current higher than rating capacity. In order to avoid this higher current flow through the circuit, a current limiter is added in the control block.

For evaluating the proposed control block, calculation block in Figure 2.9 is used. This block will calculate the actual estimation of SOH by using actual output of battery power which is obtained from measured values of battery voltage, v_b and current, i_b .

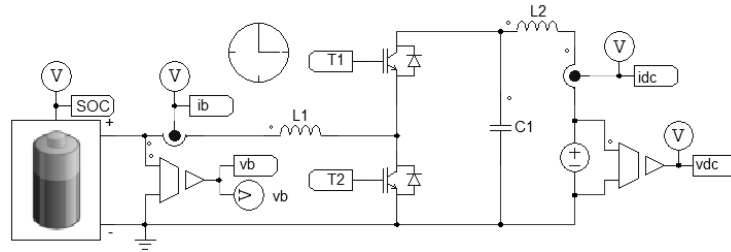


Figure 2.7 Simulation circuit for detailed model

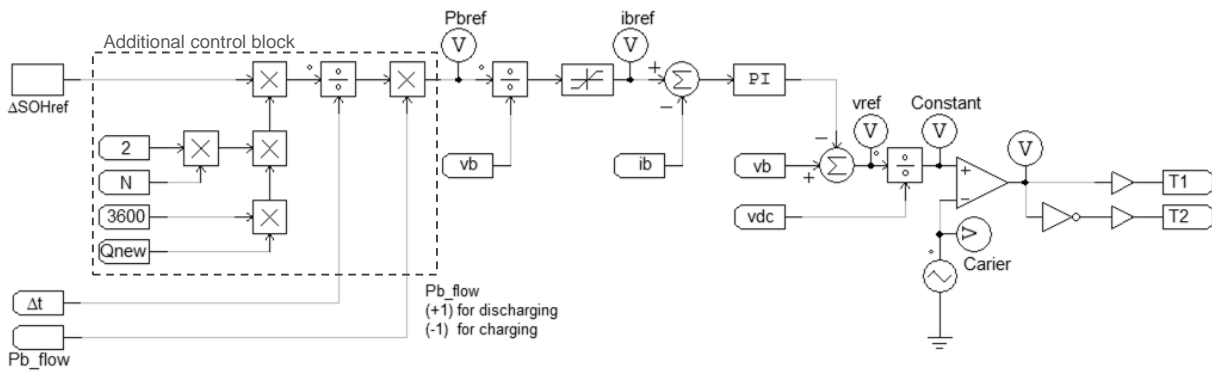


Figure 2.8 Charge control block for detailed model

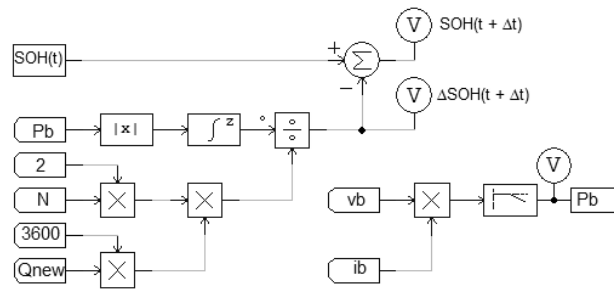


Figure 2.9 Actual battery power and SOH calculation block

Three cases of delta SOH reference value (as shown in Table 2.5) are demonstrated for each operating condition, charge and discharge. This delta SOH reference value is claimed as decreasing amount of SOH along simulation duration, which is 60 seconds. Each simulation takes around 45 minutes to simulate 60 seconds of operation.

Simulation results are shown for both battery conditions, discharging (Figure 2.10) and charging (Figure 2.11) conditions. These plots show that the proposed additional block control is successful to control discharging and charging power output by using decreasing of SOH as reference. Greater allocated value of delta SOH obtains higher power discharge or charge amount as expected.

Table 2.5 Value of Delta SOH Reference

Case	ΔSOH^*
Case 1	0.5×10^{-6}
Case 2	1.0×10^{-6}
Case 3	1.5×10^{-6}

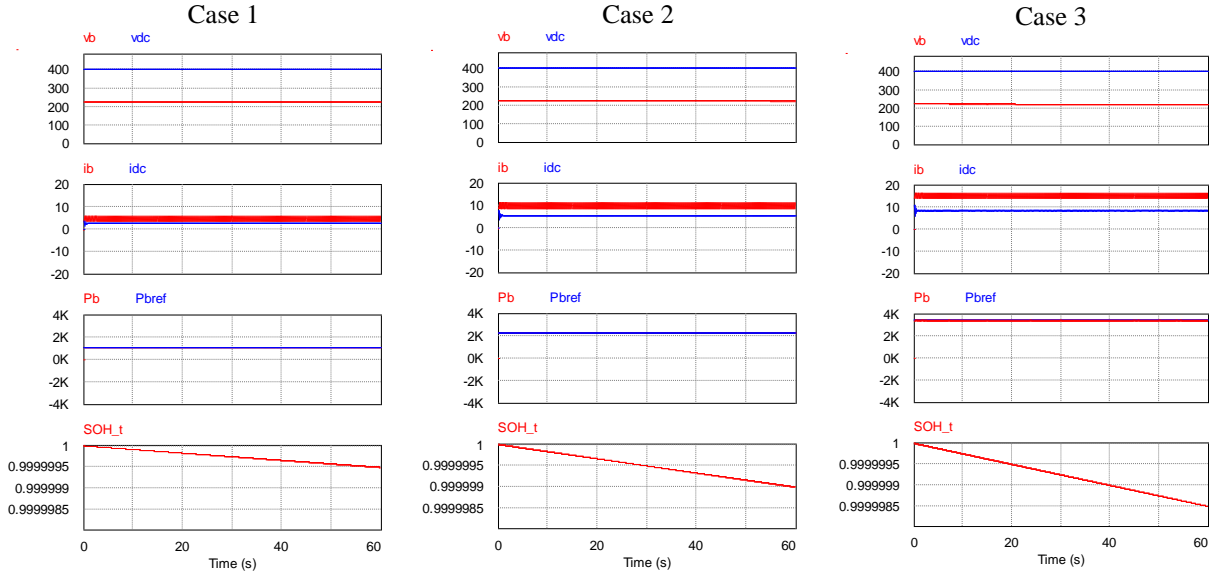


Figure 2.10 Simulation result for discharging condition

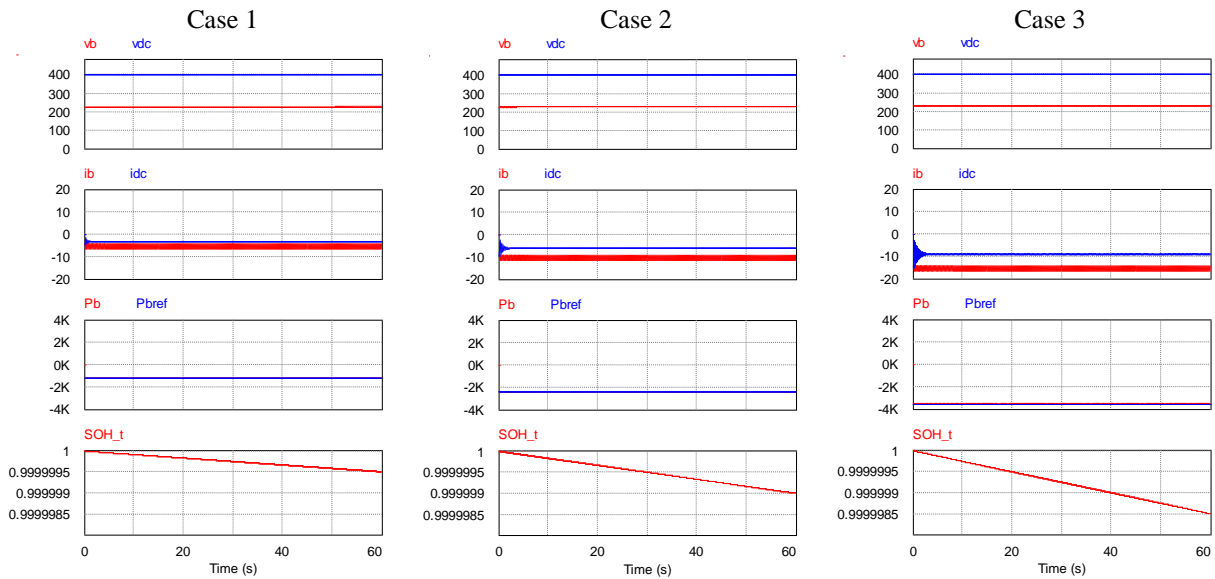


Figure 2.11 Simulation result for charging condition(2.15)

Table 2.6 and Table 2.7 present comparison between the relative error for delta SOH and battery power in discharge and charge condition. The relative error is calculated by using (2.15). Measured value for delta SOH is the value in the end of simulation, and for battery power is the average value in steady state (in this study, it is assumed start from 50 ms).

$$relative\ error = \left| \frac{measured - reference}{measured} \right| \tag{2.15}$$

Table 2.6 Relative Error for Delta SOH

Case	Discharge			Charge		
	ΔSOH^*	ΔSOH	error	ΔSOH^*	ΔSOH	error
Case 1	0.5×10^{-6}	0.509×10^{-6}	1.72%	0.5×10^{-6}	0.491×10^{-6}	1.83%
Case 2	1.0×10^{-6}	0.991×10^{-6}	0.91%	1.0×10^{-6}	0.991×10^{-6}	0.91%
Case 3	1.5×10^{-6}	1.509×10^{-6}	0.57%	1.5×10^{-6}	1.491×10^{-6}	0.61%

Table 2.7 Relative Error for Battery Power

Case	Discharge			Charge		
	$P_{B,ref}$ (W)	$P_{B,ave}$ (W)	error	$P_{B,ref}$ (W)	$P_{B,ave}$ (W)	error
Case 1	1,152	1,162	0.83%	-1,152	-1,142	0.84%
Case 2	2,304	2,314	0.41%	-2,304	-2,294	0.42%
Case 3	3,456	3,466	0.27%	-3,456	-3,446	0.28%

There is no significant different of relative error value between discharging and charging condition, both in delta SOH and Battery power. In these cases, value of relative error is less than 2% for delta SOH and less than 1% for battery power. Besides the decreasing trend of error value is seen in quadratic trend with increasing of delta SOH.

The changing conditions of discharge-to-charge, and vice versa are also simulated, but only for case 1 is shown (Figure 2.12). These figures show that the proposed control block is also successfully used to control the system. When the command changed from discharge to charge, current fluctuated less than 150 ms, and power fluctuated around 50 ms.

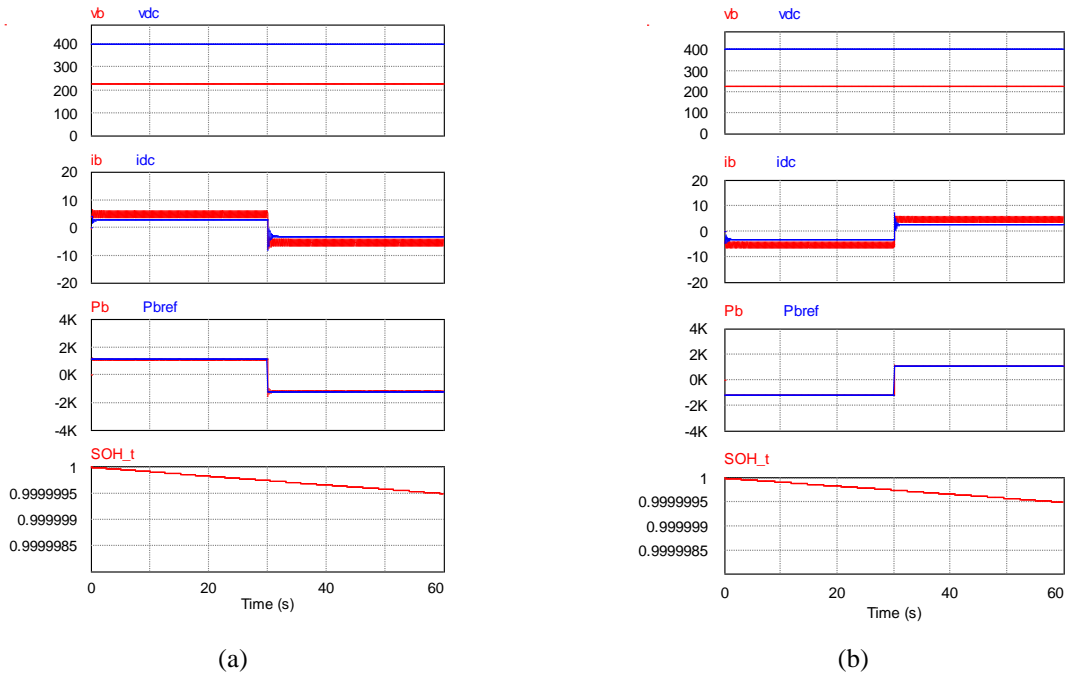


Figure 2.12 Simulation result for (a) discharging to charging condition, (b) charging to discharging condition

2.5.2 Average Model

To evaluate the proposed model, battery system is built as shown in Figure 2.13. In this system, lithium ion battery model is also adopted then connected to DC bus by bidirectional converter which is modeled by SIM. The detail of SIM sub-circuit is shown in Figure 2.14.

Bidirectional converter is used to charge and discharge the battery, which is controlled by switch T_1 and T_2 . The switch control is shown by Figure 2.15. Input values of ΔSOH , Δt , and $P_{B,flow}$ are entered to generate

battery power reference. The measured values of battery voltage, v_b and current, i_b are used for feedback loops. Proportional-Integral (PI) controller is set with gain 10 and time constant 0.1. The control block will generate signal reference to control the switches in bidirectional converter. In order to avoid this higher current flow through the circuit, a current limiter is added in the control block. For evaluating the proposed control block, the actual estimation of SOH will be calculated by using actual output of battery power which is obtained from measured values of v_b and i_b .

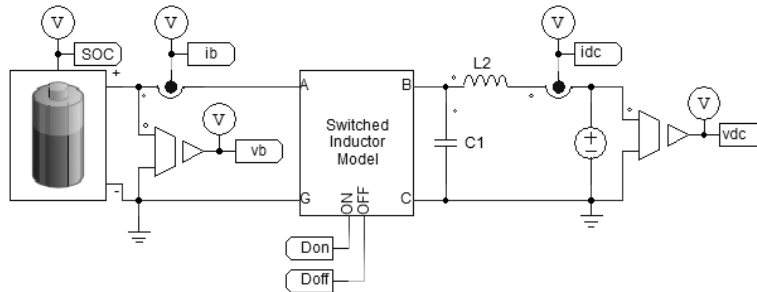


Figure 2.13 Simulation circuit for average model

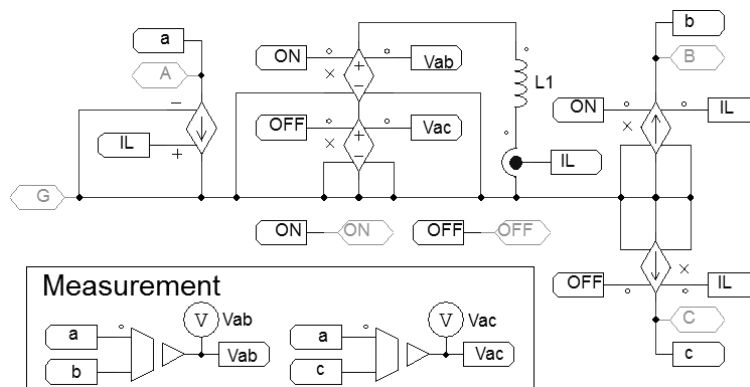


Figure 2.14 SIM sub-circuit

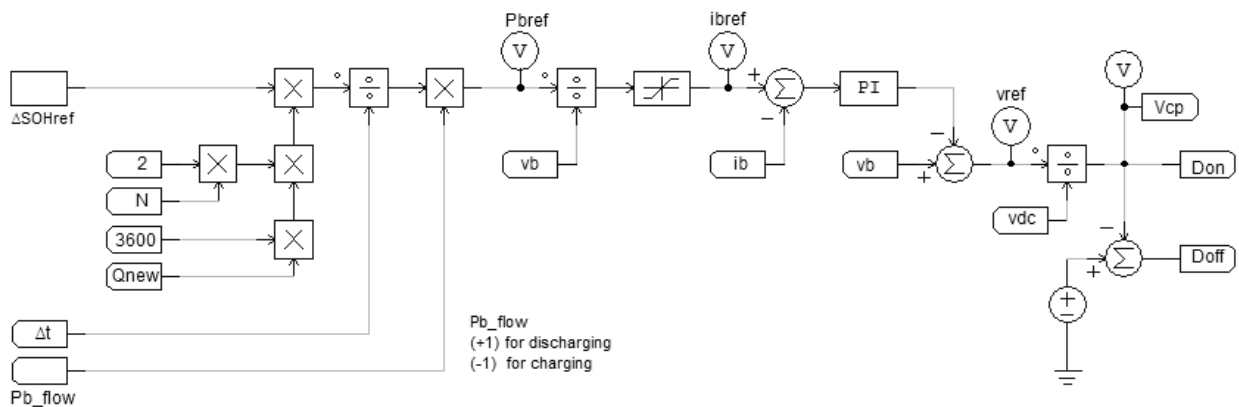


Figure 2.15 Switch control block circuit for average model

To evaluate the proposed model, three cases of delta SOH are used for each condition, discharging and charging. They are 0.5×10^{-6} , 1.0×10^{-6} , and 1.5×10^{-6} . This delta SOH reference value is claimed as decreasing amount of SOH along simulation duration, which is 60 seconds. The simulation takes only 27 seconds, which means reduced by 98% compares to the detailed model which takes 45 minutes for the same case.

By comparing with the result of detailed model, the numerical results are shown for discharging (Figure 2.16) and charging (Figure 2.17) condition. Based on these results, the average model produces similar

amount of power output. However, the proposed model gives smoother battery current because the average value is used in the model.

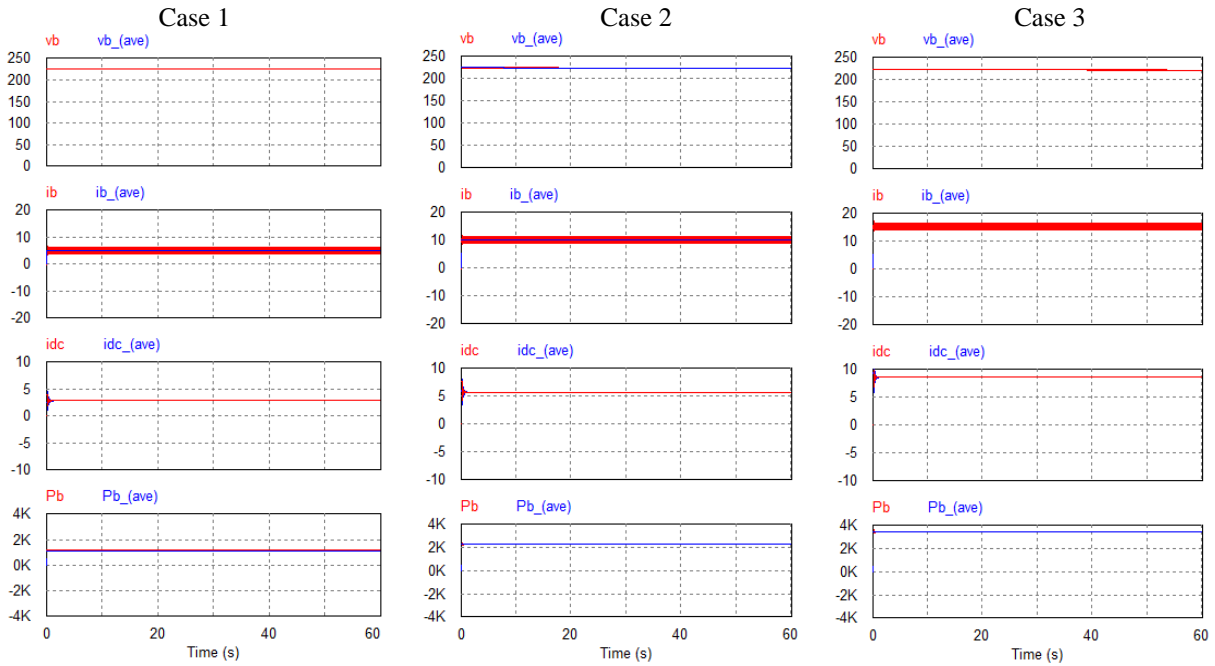


Figure 2.16 Comparison of simulation result for discharging condition

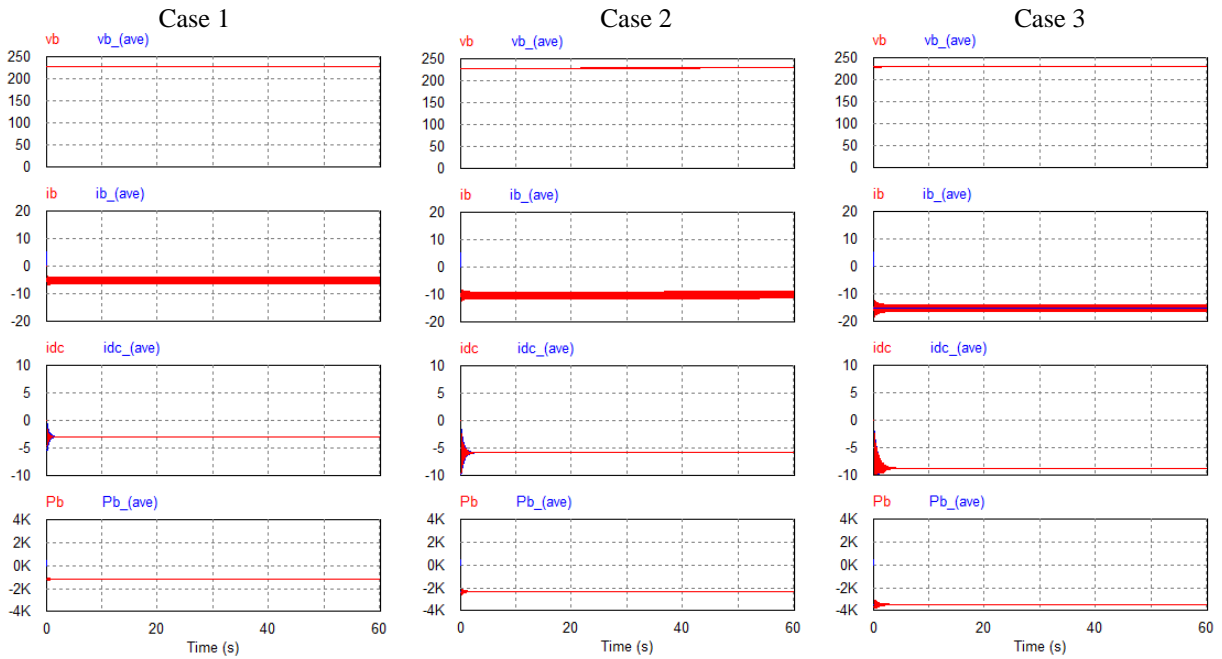


Figure 2.17 Comparison of simulation result for charging condition

In order to see more detail of the comparison of average model with the detailed model, the changing conditions of discharge-to-charge and vice versa are also simulated. The change of $P_{B,flow}$ is set on 30 s. By using case 1 for the value of desired delta SOH, the magnifying results at 29.5 to 31.5 s are shown in Figure 2.18 for discharge-to-charge condition and Figure 2.19 for charge-to-discharge condition. These results show the differences are found at the transition condition, especially in term of dc bus current, i_{dc} . Battery current is forcedly being constant by current source as the value of inductor L_I current. This value is being constant in this model as a response in the SIM sub-circuit. As the result, it supposes to eliminate the feedback process of control block, then dc bus current, i_{dc} , oscillates in high frequency.

Comparing to the detailed model, Table 2.8 presents measured delta SOH and Table 2.9 presents its relative error. The average model gives the measured delta SOH very close to the reference value with only 0.01% difference. Due to the slightly difference of v_b and i_b , since these values are used in calculation, the measured delta SOH is not same as the original model. In long-term condition, the difference value can be accumulated and might need to be adjusted.

Table 2.8 Comparison of measured Δ SOH

Case	Discharge		Charge	
	Detailed Model	Average Model	Detailed Model	Average Model
Case 1	5.088E-7	5.000E-7	4.910E-7	5.000E-7
Case 2	9.909E-7	9.999E-7	9.909E-7	9.999E-7
Case 3	1.509E-6	1.500E-6	1.491E-6	1.500E-6

Table 2.9 Comparison of relative error for Δ SOH

Case	Discharge		Charge	
	Detailed Model	Detailed Model	Detailed Model	Average Model
Case 1	1.72%	0.01%	1.83%	0.01%
Case 2	0.91%	0.01%	0.91%	0.01%
Case 3	0.57%	0.01%	0.61%	0.01%

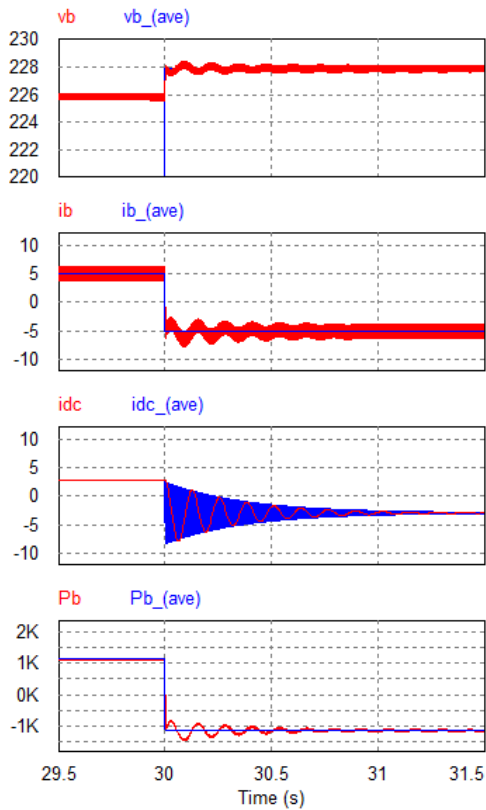


Figure 2.18 Magnifying of simulation result for discharging to charging condition

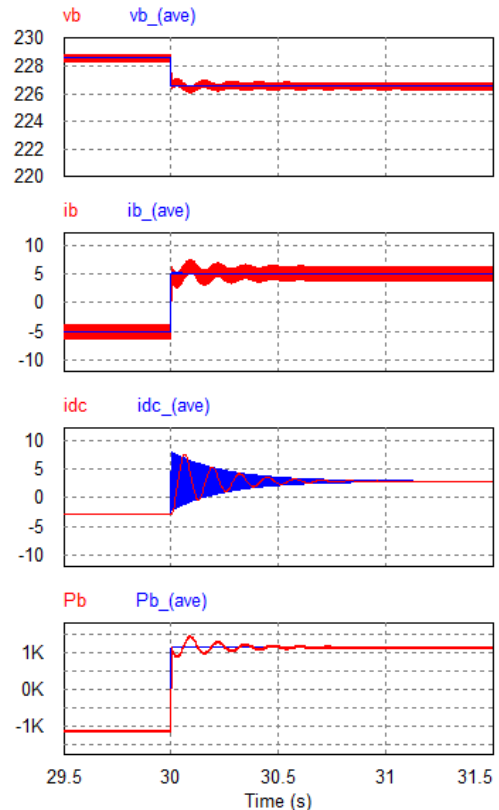


Figure 2.19 Magnifying of simulation result for charging to discharging condition

2.6 Chapter Conclusion

Battery lifetime can be indicated by using some indicators, such as State of Health (SOH), State of Life (SOL), and Remaining Useful Life (RUL). Battery operation will influence the speed of battery capacity degradation. So that, by controlling the battery operation, the longer battery lifetime is expected.

As battery lifetime decreasing depends on the discharge-charge cycle, the profile of SOH can be one of the indicator to manage the energy system in order to extend battery lifetime. Considering this condition, the battery charge control based on SOH estimation is proposed in this study. Battery system, which is connected to DC bus by bidirectional converter, is used to implement the proposed control block.

Using the detailed model, numerical simulation results show that the proposed block control is successfully used. Moreover, the control block gives relative error less than 2% for delta SOH and less than 1% for battery power. There is also no significant different between discharging and charging condition. However, by using the detailed model, the simulation is required long time.

The average model is proposed as modification of charge control simulation to reduce simulation time. Bidirectional chopper circuit is substituted by switch inductor model (SIM). Switched inductor circuit is seen as three-port circuit block. Average voltage and current of inductor is used to substitute switch circuit. By using this average model, simulation time can be reduced by 98%. The average model gives the measured delta SOH very close to the reference value with only 0.01% difference. Due to the slightly difference of v_b and i_b , since these values are used in calculation, the measured delta SOH is not same as the original model. In long-term condition, the difference value can be accumulated and might need to be adjusted. It is also needed a strategy to overcome the high oscillation in dc bus side in order to achieve the closely output result with the conventional model which is more represented the real circuit.

As future work, the energy management system, which includes SOH consideration, can be developed by using this proposed control. This kind of management system is expected will extend battery lifetime while optimizing the operation cost.

Chapter 3

Reliability of DC-Grids System in Commercial Building

3.1 Chapter Introduction

Sustainable system development becomes more popular for facing climate issues. For supporting the sustainable system development, renewable energy (RE) sources would be suitable choices to supply the energy demand in the future. In the other hand, the use of dc appliances is also gaining. So that, both of source and load with dc interface might be increasing. Within the context of simplicity and efficiency, it is unreasonable to use “DC-AC-DC” route from dc source to dc load [12]. It leads the dc building distribution system to be proposed.

The low voltage of dc power distribution has long been used for telecommunication equipment (e.g. 12, 24, or 48 V dc). Currently, the use of dc appliances become wider in other sectors and also bigger in power demand. To deal with the greater power demand, the higher voltage dc can be an option to distribute power in buildings. The research and development of equipment for supporting the higher voltage dc power distribution system has been started, such as rectifier [45], [46], power supply [47], plug and socket-outlet [48].

The reliability calculation for dc-grids in commercial building is presented in order to compare with the ac-grids that is commonly used now. The appliances in building that used in this study are referred to [49]. They are assumed to be identical in every way other than their front-end power interface. The dc appliances are defined as the basis sets, then the ac appliances are the dc appliances with an ac-dc converter.

3.2 DC-Grids System for Building

The sustainable system development should lead to resolve the energy issues. It can be pursued by reducing the need of energy, using energy more efficiently, and using RE [50]. One of the ways to reduce energy need is to build the net zero energy building (ZEB). The concept of ZEB (Figure 3.1) is minimizing energy consumptions by efficiency gains, then generating local power with RE source-on-site such as wind and solar energy [10]. Most of RE technologies is dc-connected preferred. It is one of the reasons that dc-grids system in building is started to be proposed.

Another reason is the use of dc-internal loads that is also increasing. Then the idea for avoiding dc-ac-dc conversions lead to propose the using of dc-grids system for electrical distribution in building. Reference [49] explains about potential of future dc products and estimates the energy saving by avoiding ac-dc conversion losses in the dc appliances. Table 3.1 shows groups of main appliances in commercial buildings and its energy saving from avoiding ac-dc conversion in their front-end power interface.

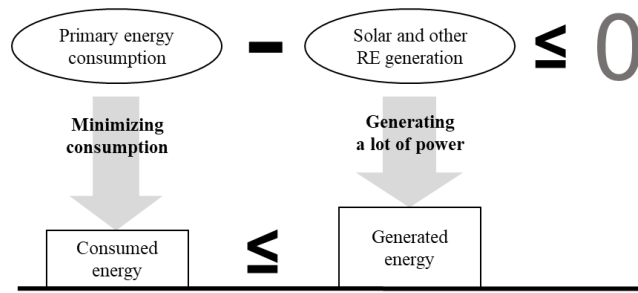


Figure 3.1 The net zero energy building concept

Table 3.1 Appliances and its energy savings from avoided ac-dc power conversion losses

Appliances	The main energy consumption equipment	Energy saving [49]
Lighting & Power Outlet	Lighting equipment, office equipment	18%
Heat source equipment	Chiller, boiler, circulation pump, electric water heater	13%
Heat source auxiliary	Cooling water pump, hot and cold water primary pump	12%
Heat Transfer	Hot and cold water secondary pump	12%
EHP	Electric Heat Pump	12%
Air Transfer	Air conditioner, fan coil unit, other	11%

3.2.1 Building Grid Models

There are various RE technologies can be applied in commercial buildings, such as photovoltaic (PV), small wind turbine, fuel cell, etc. This study limit to use only roof-top PV technologies in building. Then the PV scale constrain is roof area. Utility grid would supply the lack of power.

The PV modules can be configured in central inverter system, string inverter system, or module integrated inverter system. The reliability of module integrated inverter system is higher than other configuration [50]. The string inverter system is used in this study in order to compare the impact of using inverters.

For comparing ac-grids and dc-grids, energy saving from avoided ac-dc converter internal load is implemented in calculating dc load. Figure 3.2 gives the brief illustration for building grid system.

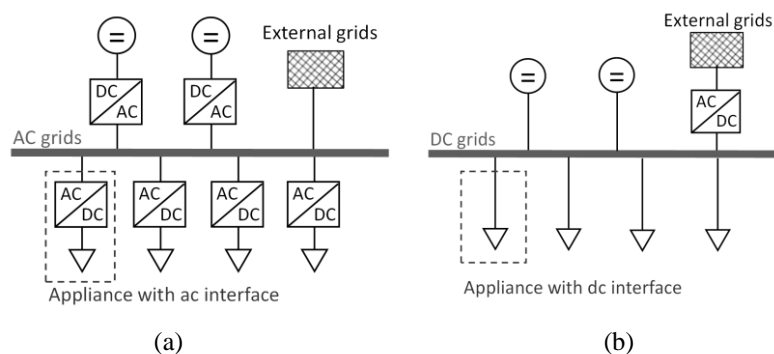


Figure 3.2 General topology in building distribution system using, (a) ac grids and (b) dc grids

The sizing criteria of PV array is detail described in [51]. PV system that consist of 437 modules (19 modules in series and 23 array in parallel) with nominal power output 100 kW is used as base. The PV system is arranged in string configuration to build the larger power output. For ac-grids, each string is connected to one inverter. Table 3.2 shows the PV module and inverter characteristics.

Expected life time for each PV module is assumed to be 25 years and inverter is 10 years. The mean time to repair (MTTR) of all of system is very short compare to the mean time to failure (MTTF) then it is assumed to be one day.

Table 3.2 The PV module and inverter characteristics[10]

Inverter (100 kW)	PV Module (230 W)
$V_{mpp,min} = 450 \text{ V}$	$I_{SC} = 8.24 \text{ A}$
$V_{mpp,max} = 820 \text{ V}$	$V_{OC} = 37.2 \text{ V}$
$V_{max} = 1000 \text{ V}$	$I_{mpp} = 7.60 \text{ A}$
$I_{DC,max} = 230 \text{ A}$	$V_{mpp} = 30.2 \text{ V}$

3.2.2 Commercial Building Type

Commercial buildings can be categorized into several type. This study encompasses four group of commercial buildings: department store, hospital, hotel, and office. Load data is adapted from [52], used the building data with 10.000 m² for average floor area. The dominant number of floor of each building group is different. Hotel and office have more number of floor than hospital and department store. It gives different space of roof area that would be used for installing PV system. In this study, the department store is assumed can install PV system up to 5x100 kW, hospital 2x100 kW, then hotel and office only 1x100 kW.

Table 3.3 shows the main electric equipment that is used in commercial buildings. These main appliances power give different shape of the hourly load curve for each building type. The typical load curve for each building group (Figure 3.3) is adapted from [53] for summer, and [54] for winter. The saving energy from avoided ac-dc converter is used to shape the load curve of dc-interface load.

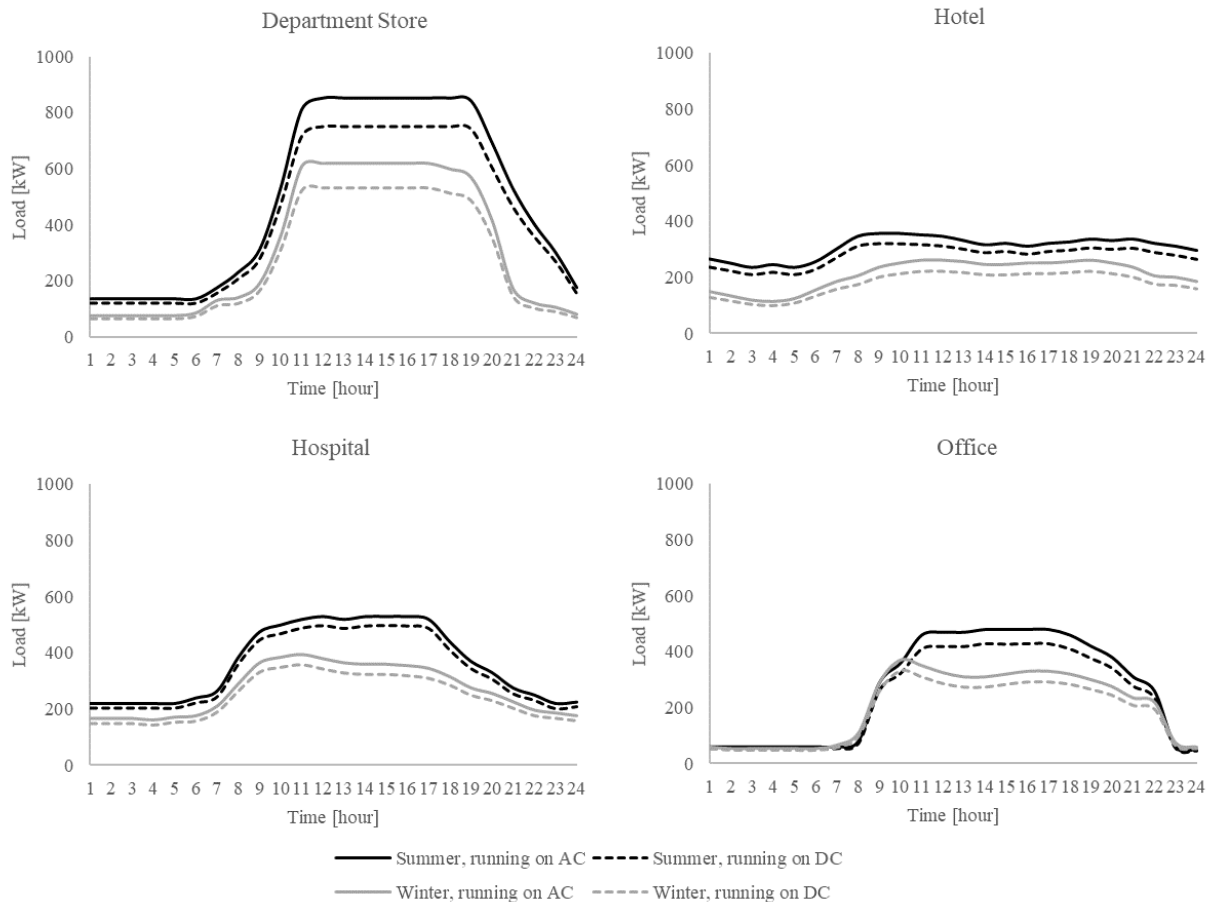


Figure 3.3 Load curve for each commercial building type, summer and winter, ac-interface and dc-interface load

Table 3.3 Main electric equipment in commercial buildings

	Department Store	Hospital	Hotel	Office
Lighting & Power Outlet	v	v	v	v
Heat source equipment	-	v	v	v
Heat source auxiliary	-	v	v	-
Heat Transfer	v	v	v	v
EHP	v	-	v	-
Air Transfer	v	-	v	-

3.3 Reliability Analysis

System reliability indexes represent the ability of system to supply the load. The load interruption frequency and the expected duration of load interruption events are commonly used. These basic indexes can be used to compute other useful indexes, such as total expected interruption time per period, system availability or unavailability, expected demanded – but unsupplied – energy per time period. The reliability in each building type is calculated in case to compare performing of dc-grids and ac-grids in building.

3.3.1 System availability

System availability (A) is determined by the probability of system that can perform satisfactory services for supplying the load. It can be calculated by (3.1), with μ and λ are system repair and failure rates, respectively. The MTTF is the average useful life = $1/\lambda$ and MTTR is average time for repairing = $1/\mu$. The forced outage rate (FOR) or unavailability (U) is defined as $1-A$.

$$A = \frac{\mu}{\lambda + \mu} \quad (3.1)$$

The failure rate is assumed constant for each component and the exponential distribution is used to describe the behavior of the component. The reliability in time function, $R(t)$, is calculated by (3.2). The reliability for n series components is obtained using (3.3). In case of n series identical components, the reliability of entire system is determined using (3.4). Equation (3.5) obtain reliability for m parallel components. In case of m parallel identical components, the reliability of entire system is obtained by (3.6). By combining (3.4) and (3.6), reliability of PV array that contained $m \times n$ size can be calculated by (3.7). In addition of inverter, the reliability for PV system should be multiply by reliability of inverter, $R_i(t)$, as mentioned in (3.8).

$$R(t) = e^{-\lambda t} \quad (3.2)$$

$$R_s(t) = R_1(t) \times R_2(t) \times \dots \times R_n(t) \quad (3.3)$$

$$R_{sn}(t) = e^{-n\lambda t} \quad (3.4)$$

$$R_p(t) = 1 - [(1 - R_1(t))(1 - R_2(t)) \dots (1 - R_n(t))] \quad (3.5)$$

$$R_{pn}(t) = 1 - (1 - e^{-\lambda t})^m \quad (3.6)$$

$$R_{PVarray}(t) = 1 - (1 - e^{-n\lambda t})^m \quad (3.7)$$

$$R_{PVsys}(t) = [1 - (1 - e^{-n\lambda t})^m][R_i(t)] \quad (3.8)$$

We use (3.9) to obtain the MTTF value of system as the average useful life. As the calculation result, the MTTF and FOR of PV system with inverter is 3.88 years and 0.071%, without inverter is 4.91 years and 0.056%, respectively.

$$MTTF = \int_0^{\infty} R(t) \cdot dt \quad (3.9)$$

3.3.2 Loss of Load Indices

A ‘loss of load’ will occur when the remaining capacity is below the load level. The calculation of loss of load expectation (LOLE) needs combination of system capacity outage probability table (COPT) and load characteristics. The ‘capacity outage’ (cap out) indicates the loss generation and not depend on the system load. There are some approach to calculate the capacity outage probability that detail describe in [55]. Table 3.4 and Table 3.5 show the individual probability of capacity outage for PV system running on ac and dc, respectively.

Table 3.4 COPT of PV system running on AC (with inverter)

Cap. out (kW)	1x100 kW	2x100 kW	5x100 kW
0	0.9992943832909960	0.9985892644769330	0.9964768918923920
100	0.0007056167090036	0.0014102376281272	0.0035181361809501
200		0.0000004978949400	0.0000049684171458
300			0.000000035082737
400			0.000000000012386
500			0.0000000000000002
	1.0000000000000000	1.0000000000000000	1.0000000000000000

Table 3.5 COPT of PV system running on DC (without inverter)

Cap. out (kW)	1x100 kW	2x100 kW	5x100 kW
0	0.9994427191959550	0.9988857489538050	0.9972166998685020
100	0.0005572808040448	0.0011139404843005	0.0027801979725098
200		0.0000003105618946	0.0000031004297330
300			0.0000000017287734
400			0.000000000004820
500			0.0000000000000001
	1.0000000000000000	1.0000000000000000	1.0000000000000000

The building grid system has no batteries, so PV systems and utility grid are the only supply. PV system is assumed can operates 6 hours in summer from 9 a.m. to 3 p.m. and 4 hours in winter from 10 a.m. to 2 p.m. Output power percentage to power rated of PV system can achieve 90% in summer and 70% in winter [56]. For the rest load should be supplied by grid that has outage averages four minutes each year [57]. Then the power contracted has to cover the highest peak for a whole year that uncovered by PV system. The final COPT should combine the outage probability of PV systems and grid.

The value of LOLE can be obtained by (3.10), with C_i and L_i are available capacity and forecast peak load on hour i , respectively, $P_i(C_i - L_i)$ is probability of loss of load on hour i , then a is number of hours. If the calculations of LOLE use the hourly peak load, then the value of LOLE should also in hour [58]. This calculation is to encompass the operation time of PV systems, which is different between summer and winter period.

$$LOLE = \sum_{i=1}^a P_i(C_i - L_i) \tag{3.10}$$

Table 3.6 shows the LOLE value comparison of ac-grids and dc-grids. The combinations of reduced load by avoiding ac-dc inverter in front-end interface and directly connected PV system to building grid deliver most LOLE value of dc-grids to be lower than ac-grids. The significant difference occurred for hotel and office building type in summer season. In office building type, there is about 50% potential of LOLE reduction by changing into the dc-grids. Meanwhile, in hotel building type, there is almost 80% potential of LOLE reduction. However, the LOLE reduction for all building type is not significant in winter season.

Table 3.6 Comparison of LOLE value in hours/day

Building Type	AC-grids		DC-grids	
	Summer	Winter	Summer	Winter
Department store	0.014280	0.010757	0.011319	0.008536
Hospital	0.004416	0.001595	0.003526	0.001298
Hotel	0.000888	0.001594	0.000183	0.001297
Office	0.001594	0.000183	0.000740	0.000183

3.4 Chapter Conclusion

The reliability evaluation the use of dc-grids in comparing to the usual ac-grids in commercial building is presented in this chapter. The observed differences of dc-grids and ac-grids are in the front-end interface of load and connection of on-site generation. The limitation of study is to use only PV system as on-site generation and without any batteries. The result shows that the avoidance of inverter in PV array increase the average useful life of PV system from 3.88 years to 4.91 years and decrease the FOR value from 0.071% to 0.056%. The LOLE value of dc-grids building always lower than or equal to ac-grids. It indicates that the reliability of dc-grids can be higher than ac-grids. Potential of LOLE reduction is high in summer season. Nevertheless, the practical experiment is still needed. Furthermore, the study can be expanded to cover more on-site generation types and their state of conditions.

Chapter 4

Study on Converter Loss and Optimizing Power Schedule

4.1 Chapter Introduction

Environment issues such as limited primary energy sources and emission limitation lead us to develop power system by including sustainable principle. Sustainable development needs capability of being not harmful to the environment or depleting natural resources in long term. In building scale, zero energy building is started introduced to fulfill the sustainability requirements [10], [50]. The aim of energy management system in the building is to achieve net zero energy, which means the generation energy equal to consumption energy. In order to realize this condition, the buildings should generate energy using clean sources. The common power is photovoltaic, which does not generate energy in a whole day. Hence, battery storage is needed to compensate. Using photovoltaic, battery storage, and grid as power sources in building is necessary to use energy management system. This system schedules the power flow to supply the load.

Photovoltaic generates DC power. Battery storage also discharges DC power and charges by DC power. Besides, usage of DC load is increasing too. By using current system which is AC system, the power needs to be converted to AC, then to DC again [12]. These conditions intrigue to discover which system is better to be used, AC or DC system. Many studies have shown DC system can lessen loss in conversion, such as [49] and [59].

In this study, converter loss for AC and DC system is evaluated. Besides, by using DC system, optimizing power schedule of grid connected PV system with batteries is also formulated based on converter loss. The power schedule will be achieved by minimizing the converter loss.

4.2 Evaluation on Converter Loss

In ZEB environment, different type of power generation, energy storage, and load need converter to connect each to another. This section will evaluate the converter loss of real system.

4.2.1 Evaluation Method

Evaluation method for the converter loss follow these three steps.

Step 1. Calculate power input and output using measured voltage and current data.

For each converter, the measured voltage and current data is available for both side, input and output. The data is instantaneous voltage ($V(t)$) and current ($I(t)$). Using these data, the instantaneous power ($P(t)$) of input and output side is calculated by (4.1).

$$P(t) = V(t) \times I(t) \quad (4.1)$$

Step 2. Plot power output versus power input.

Using the calculation result of Step 1, we plot the power input as x-axis and power output as y-axis.

Step 3. Determine efficiency converter by using linear trend line of power output versus power input curve.

Using the plot from Step 2, efficiency of each converter is evaluated using linear trend line (4.2), where m is the slope and b is the intercept. Two approaches are used here, whether it is neglecting or considering the standby loss of each converter.

$$y = mx + b \tag{4.2}$$

Approach 1: Neglecting standby loss. By neglecting the standby loss in the converter, the intercept of linear trend line is set as zero.

Approach 2: Considering standby loss. By considering the standby loss in the converter, the intercept is defined as standby loss, which will have a constant value for every input power.

4.2.2 Evaluated System

The evaluated system follows Figure 4.1. The system is a dc power distribution system in building which is using HVDC 380 Volt as main bus. The main supply is from PV panels. The batteries are for storing the surplus power from PV panels and for supply the load whenever the PV panels lacks of energy generation and the batteries have energy to be discharged. If the energy from PV panels or batteries cannot fulfill all load, the AC grid will supply the rest. Referring to the datasheet, Table 4.1 summarizes efficiency of each converter.

Table 4.1 Converter efficiency based on datasheet

Converter	Max. Power Output [kW]	Efficiency
PV converter	5	95%
Battery converter	5	93% / 93% (charge / discharge)
DC/DC converter	1.2	95%

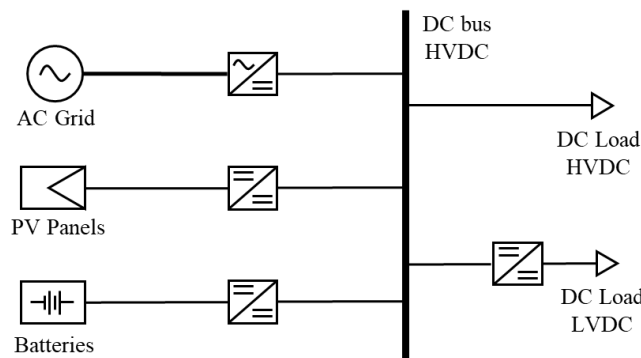


Figure 4.1 DC distribution grid of evaluated system

4.2.3 Converter Evaluation Result

Recorded data is available every minute for voltage and current of both side of each converter. We evaluated the efficiency of each converter based on these data.

4.2.3.1 PV Converter

In this system, PV converter converts power from low voltage dc in PV side to high voltage dc in main bus. PV converter will deliver high power when the PV panels get high radiation, which will happen on the daytime. Considering this condition, as shown in Figure 4.2, we evaluated PV converter efficiency using four type data as mentioned below:

Data 1. Whole data

Data 2. Only data after sunrise and before sunset (daytime)

Data 3. Using data 30 minutes after sunrise and 30 minutes before sunset

Data 4. Using data 1 hour after sunrise and 1 hour before sunset

For the evaluation of PV converter, we used the calculated power curve of PV converter as shown in Figure 4.3, and following the altitude of sun in the respective time for the data division.

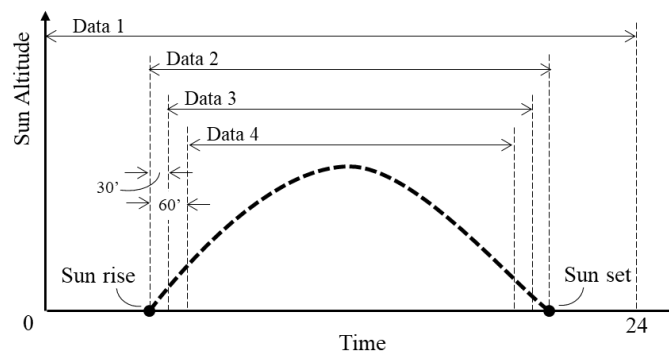


Figure 4.2 Data division of PV converter data

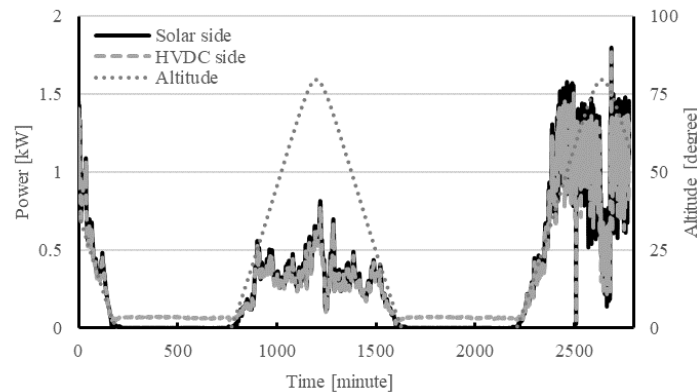


Figure 4.3 Power curve of PV converter

As for the analysis, Figure 4.4 to Figure 4.7 show the plot of PV converter power output (HVDC side) versus power input (solar side) for Data 1 to Data 4 respectively. Each plot contains two approaches trend line completed with its equation and R-square value. Dashed line represents trend line of approach 1, and dotted line represents trend line of approach 2.

Table 4.2 summarizes the efficiency analysis this converter. Based on the efficiency analysis result, trend line in approach 1 gives the closer value to represent the data form datasheet. Whereas, trend line in approach 2 gives positive value for the intercept, which means a negative value for constant loss. However, this negative value cannot be accepted, because loss is never negative.

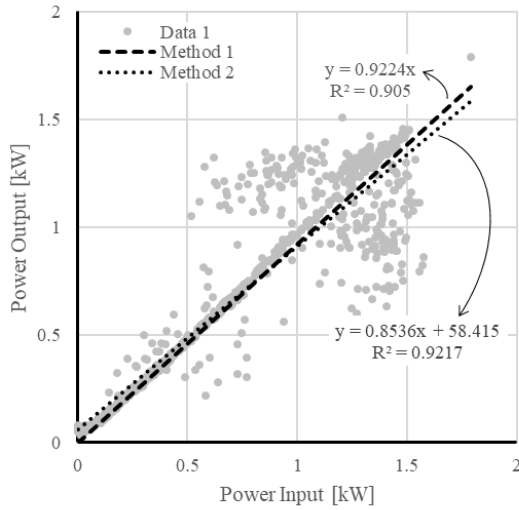


Figure 4.4 Power output (HVDC side) vs power input (solar side) curve of PV converter using data 1

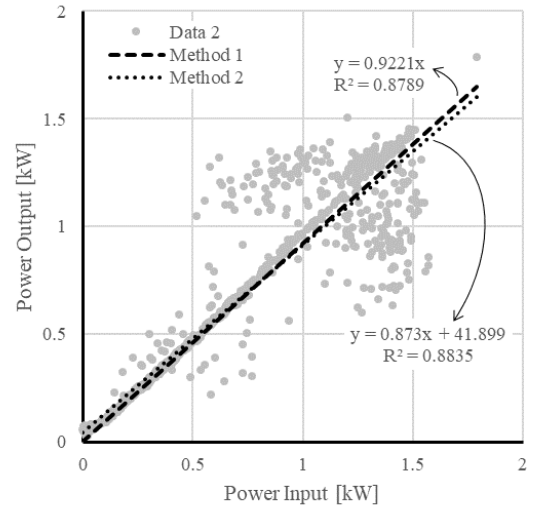


Figure 4.5 Power output (HVDC side) vs power input (solar side) curve of PV converter using data 2

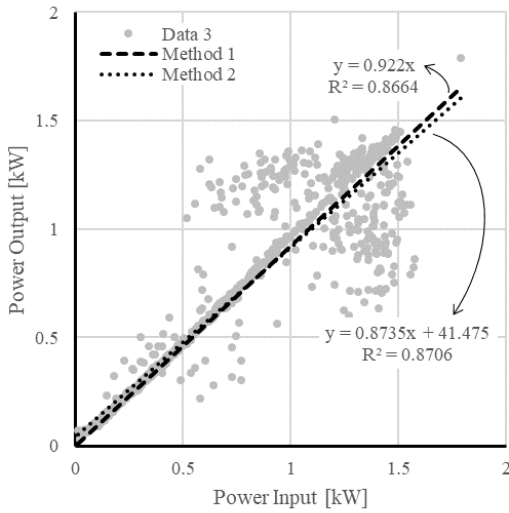


Figure 4.6 Power output (HVDC side) vs power input (solar side) curve of PV converter using data 3

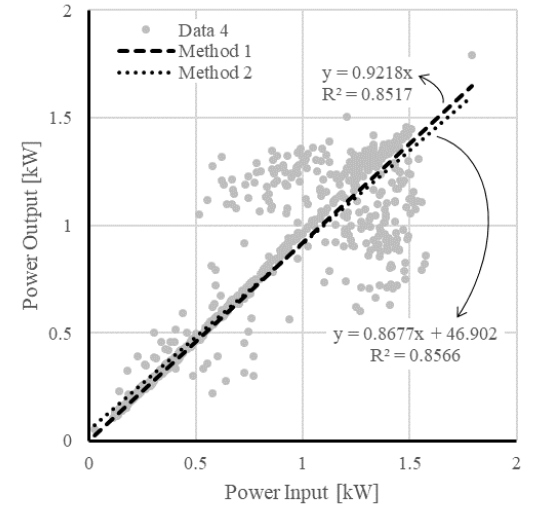


Figure 4.7 Power output (HVDC side) vs power input (solar side) curve of PV converter using data 4

Table 4.2 Efficiency analysis summary of PV converter

	Data 1	Data 2	Data 3	Data 4
Reference efficiency in datasheet	95%			
Measured efficiency by method 1	92.24%	92.21%	92.2%	92.18%
Measured efficiency by method 2	85.36%	87.3%	87.35%	86.77%
Constant loss by method 2	-58.4 Watt	-41.9 Watt	-41.5 Watt	-46.9 Watt

4.2.3.2 Battery Converter

In the evaluated system, battery converter connects the battery system to the high voltage dc of main bus. The calculated power curve of battery converter is shown in Figure 4.8. However, the calculation of recorded voltage and current data give some negative value in result. Considering this, we evaluated battery converter efficiency using two type data as mentioned below:

Data 1. Whole positive output data

Data 2. Data with output greater than 50 Watt

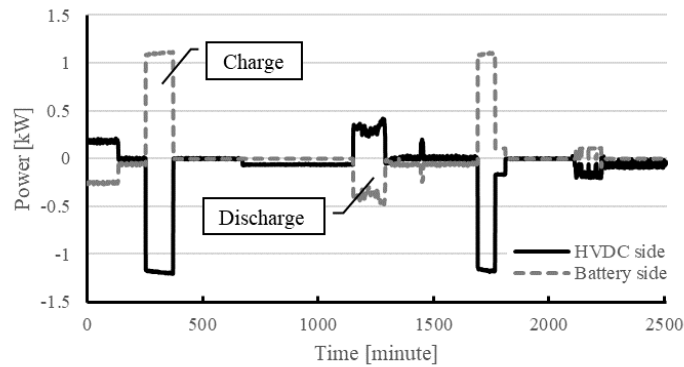


Figure 4.8 Power curve of battery converter

As for the analysis, Figure 4.9 and Figure 4.10 show the plot of power output versus power input of battery converter in discharging phase for Data 1 and Data 2 respectively. Meanwhile, for charging phase, the plot of power output versus power input of battery converter is shown by Figure 4.11 and Figure 4.12 for Data 1 and Data 2 respectively. Each plot contains two approaches trend line completed with its equation and R-square value. Dashed line represents trend line of approach 1, and dotted line represents trend line of approach 2.

Table 4.3 summarizes the efficiency analysis this converter. The efficiency analysis result shows that battery converter has significant constant loss compared to other converter. Based on the measured result, efficiency value that is stated in datasheet is closer to approach 1 for charging condition. The measured efficiency by approach 2 gives close result for discharge and charge condition by using data 2.

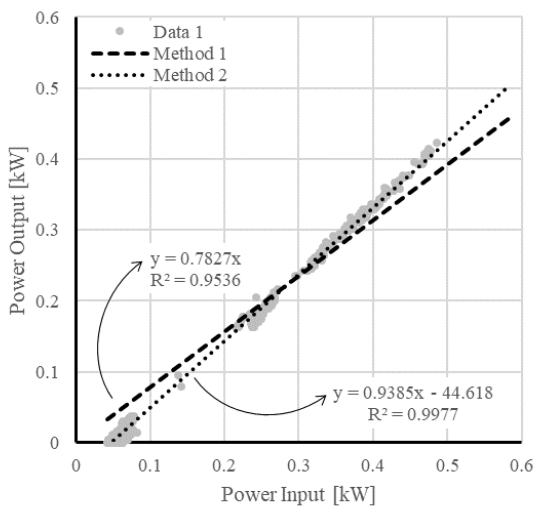


Figure 4.9 Power output (HVDC side) vs power input (battery side) curve of discharging battery for data 1

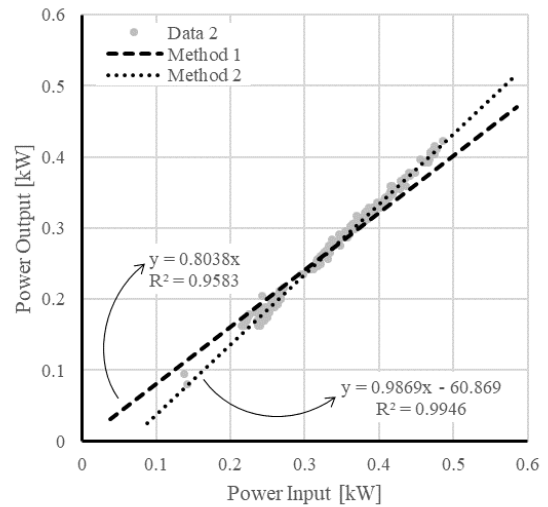


Figure 4.10 Power output (HVDC side) vs power input (battery side) curve of discharging battery for data 2

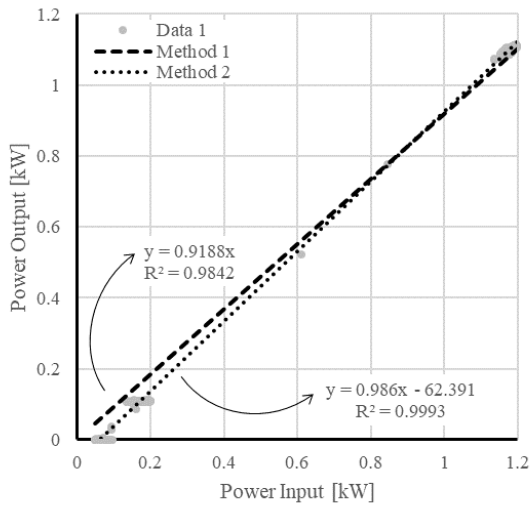


Figure 4.11 Power output (battery side) vs power input (HVDC side) curve of charging battery for data 1

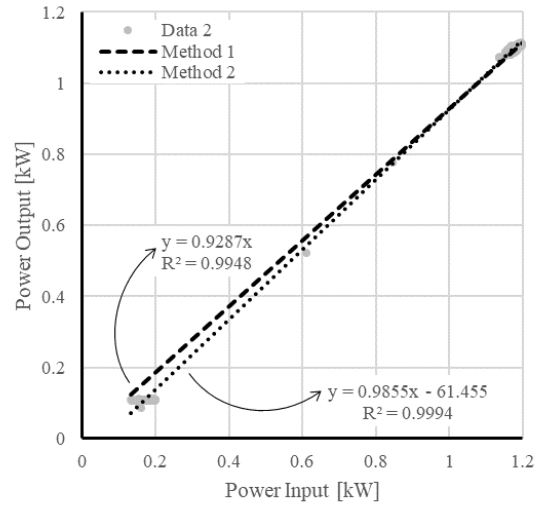


Figure 4.12 Power output (battery side) vs power input (HVDC side) curve of charging battery for data 2

Table 4.3 Efficiency analysis summary of battery converter

	Battery Discharge		Battery Charge	
	Data 1	Data 2	Data 1	Data 2
Reference efficiency in datasheet	93%		93%	
Measured efficiency by method 1	78.27%	80.38%	91.88%	92.87%
Measured efficiency by method 2	93.85%	98.69%	98.6%	98.55%
Constant loss by method 2	44.6 Watt	60.9 Watt	62.4 Watt	61.4 Watt

4.2.3.3 DC/DC Converter

In this system, dc/dc converter is used to convert the power from high voltage dc in main bus to supply the load in low voltage dc. There are two modules of dc/dc converter that will be evaluated here, named Module A and Module B. Figure 4.13 shows the calculated power curve of battery converter for Module A and Figure 4.14 shows the one for Module B.

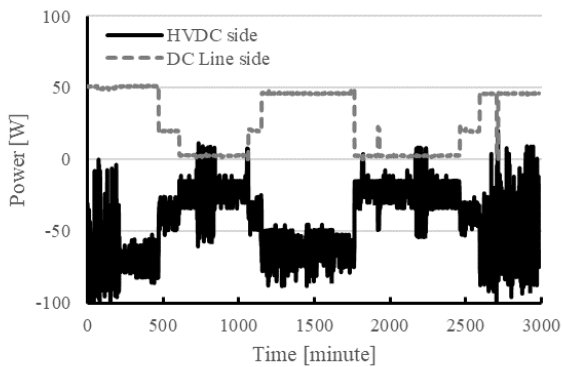


Figure 4.13 Power curve of DC/DC converter (Module A)

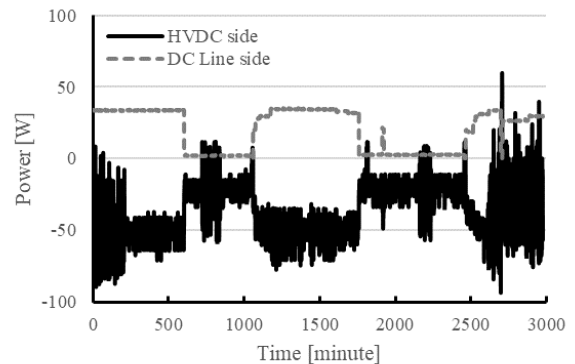


Figure 4.14 Power curve of DC/DC converter (Module B)

As for the analysis, Figure 4.15 and Figure 4.16 show the plot of dc/dc converter power output versus power input for Module A and Module B respectively. Each plot contains two approaches trend line completed with its equation and R-square value. Red line represents trend line of approach 1, and purple line represents trend line of approach 2.

Table 4.4 summarizes the efficiency analysis of dc/dc converter. In this converter, recorded data is available for low power only. As the result, measured efficiency is very low if compared to the efficiency written in datasheet.

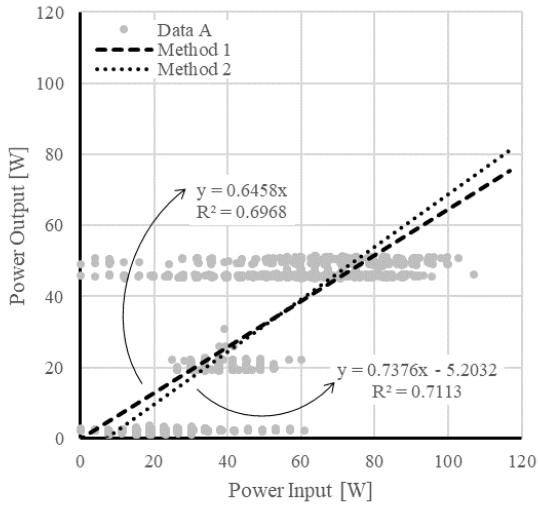


Figure 4.15 Power output (DC Line side) vs power input (HVDC side) curve of DC/DC converter (Module A)

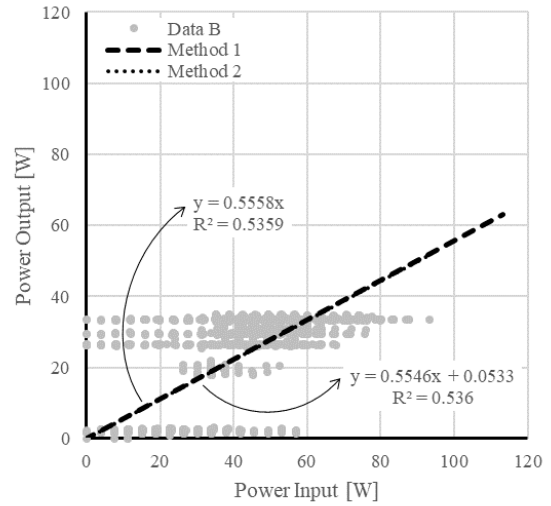


Figure 4.16 Power output (DC Line side) vs power input (HVDC side) curve of DC/DC converter (Module B)

Table 4.4 Efficiency analysis summary of DC/DC converter

	Module A	Module B
Reference efficiency in datasheet	95%	95%
Measured efficiency by method 1	64.58%	55.58%
Measured efficiency by method 2	73.76%	55.46%
Constant loss by method 2	5.20 Watt	-0.05 Watt

4.3 Optimizing Power Schedule in DC system of Building Power Distribution

This section will discuss about potential of cost reduction in DC system of building power distribution. The optimization is based on the purchased electricity form grid.

4.3.1 System Architecture

PV System with batteries is installed in building that uses DC for distribution system. Configuration of the system is shown in Figure 4.17. Positive value of grid power (P_g) refers to exchange power from grid to building and vice versa. Positive value of battery power (P_{bat}) represents power for charging battery, while negative value represents discharging power.

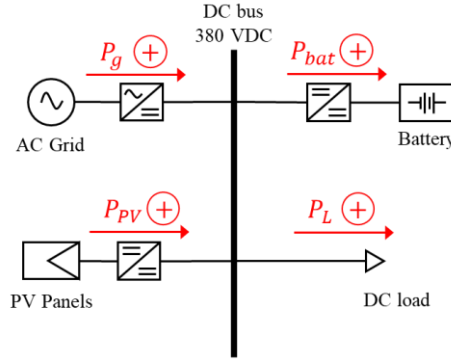


Figure 4.17 System configuration and power flow

4.3.2 Optimized Power Schedule Formulation

To optimize the power schedule, we put minimization of total payment to electric utility as objective function as shown in (4.3). Total payment is calculated by summation hourly payment based on electricity price for every time t ($C(t)$) in period of time (T). Calculation is for optimizing charge schedule in hourly for one day.

$$\min(\sum_{t=1}^T C(t) \times P_g(t)) \quad (4.3)$$

The objective function is subjected to constraints as follow description. Battery power is limited by (4.4), while power from/to grid is limited by (4.5). Power generation from PV ($P_{PV}(t)$) depends on weather and season. Battery SOC is limited by (4.6), and the battery power is calculated by changed of SOC as shown in (4.7). Power flow in the system is determined by (4.8).

$$P_{bat(min)} \leq P_{bat}(t) \leq P_{bat(max)} \quad (4.4)$$

$$P_{g(min)} \leq P_g(t) \leq P_{g(max)} \quad (4.5)$$

$$SOC_{(min)} \leq SOC(t) \leq SOC_{(max)} \quad (4.6)$$

$$P_{bat}(t) = \Delta SOC(t) \times Cap_{bat} \quad (4.7)$$

$$P_g(t) + P_{PV}(t) = P_{bat}(t) + P_L(t) \quad (4.8)$$

4.3.3 Numerical Results and Analysis

For numerical calculation, load demand assumption is divided for weekday (Monday to Friday) and weekend (Saturday and Sunday) or holiday as shown in Figure 4.18. The load is assumed by constant patterns and following the day of week, but not influenced by the weather. Analysis is done by comparing between four type of systems. First system is the system without PV nor battery. This system will be seen as a base system. Second one is the system including PV system. Third one is system including both PV and battery system. In the fourth system, the system is not only including both PV and battery system, but also align with optimization power scheduling. For the system with PV, power generation of PV follows three patterns (“Sunny A”, “Sunny B”, and “Rain” pattern) as shown in Figure 4.19, which is categorized by season and weather. Based on calendar day, the season is divided into four types: winter (1st January – 31st March), spring (1st April – 30th June), summer (1st July – 30th September), and autumn (1st October – 31st December). PV power generation on sunny day follows “Sunny A” pattern in spring and summer season, and follows “Sunny B” pattern in autumn and winter season. In case of rainy day, PV power generation follows “Rain” pattern, no matter what season it is. For the system with battery, the battery capacity (Cap_{bat}) is assumed to be 5 kWh.

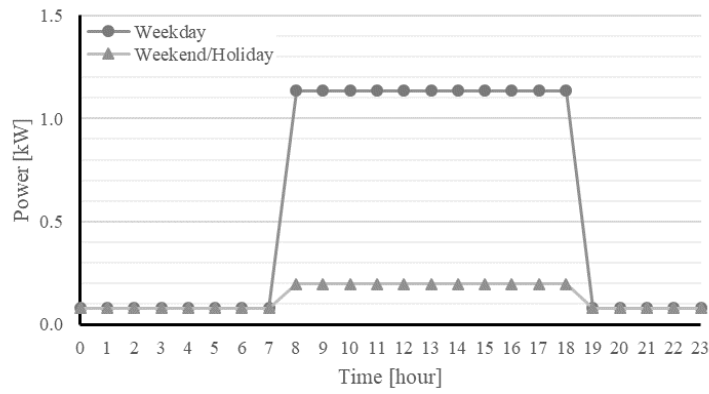


Figure 4.18 Load demand assumption

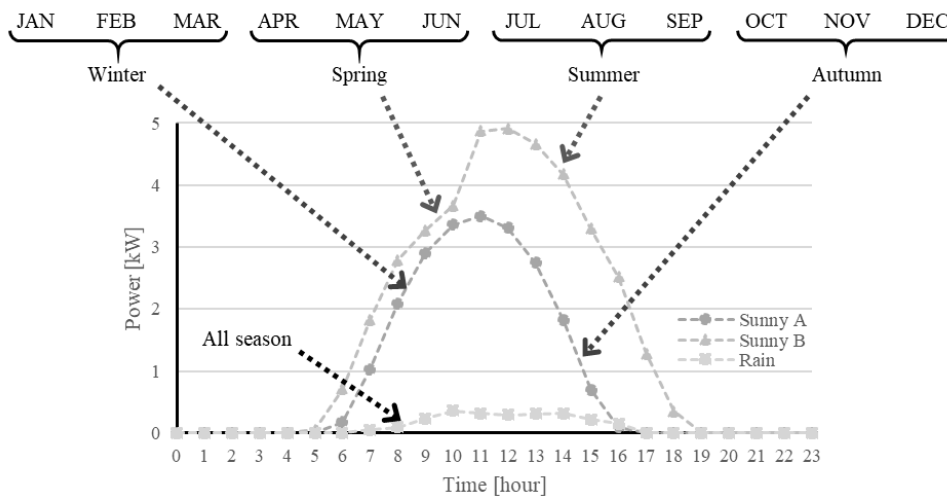


Figure 4.19 Season categorization for PV generation

Electricity price is following the price from Tokyo Electric Power Company (TEPCO) for commercial building with power contract less than 500 kW that is using seasonal time zone [60]. The price is classified into two types of season as stated in Table 4.5. Table 4.6 describes the detail of time classification for electricity price. Finally, the unit price of electricity that is used in this study is as shown in Table 4.7.

Table 4.5 Season classification for electricity price

Season	Range Date
Summer	From 1 July to 30 September.
Other seasons	From 1 October to 30 June of following year.

Table 4.6 Time classification for electricity price

Type	Description
Peak Time	Weekday in summer (including Saturday), from 1 pm to 4 pm.
Day Time	Weekday (including Saturday), from 8 am to 10 pm. However, exclude the time corresponding to the peak time.
Night Time	Exclude peak and day time, but applied throughout the day for Sunday and National holiday, and also on 2 & 3 Jan, 30 Apr, 1 & 2 May, 30 & 31 Dec.

Table 4.7 Unit price of electricity

			Unit	Charge (incl. tax)
Basic charge			1 kW	1,684.80 yen
Energy charge	Peak time		1 kWh	20.06 yen
	Day time	Summer season	1 kWh	19.36 yen
		Other seasons	1 kWh	17.96 yen
Night time		1 kWh	12.45 yen	

The numerical calculation is done in hourly base by using spreadsheet. The sample of calculation sheet is shown in Figure 4.20. The constraints are written as defined. For every designated day, the day parameter is set, then the dependent variable will change automatically. To optimize the changing variable, which is the amount of charging or discharging battery, a solver is used by setting the objective function into its minimum value. In this solver, we select evolutionary as the solving method.

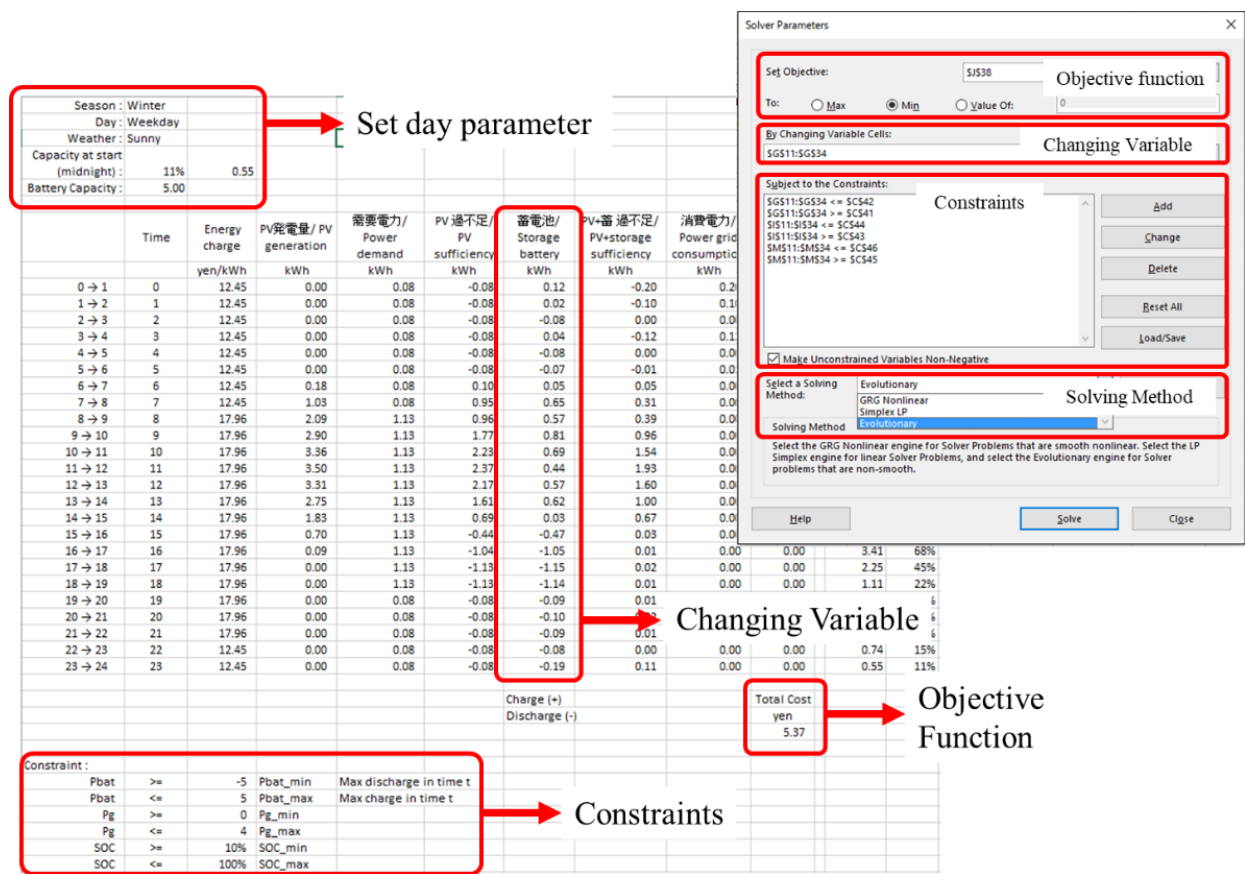


Figure 4.20 Sample of calculation using spreadsheet

Figure 4.21 shows the monthly comparison result of system with additional PV, battery, and optimization system. In this framework system, by equipping the system with PV, it can reduce 60.2% of monthly electricity charge in average comparing to system without PV. By adding battery storage system, the monthly electricity charge reduction can be increase 16.5% in average. Then, additional optimization system increases the monthly electricity charge reduction by 2% in average. Annually, system with PV can save the electricity cost nearly 40,000 yen compared to the base system (Figure 4.22). Using PV system equipped with battery storage can save around 50.000 yen per year in total. By adding the optimization of battery charge-discharge schedule, the saving money increases by 2% annually.

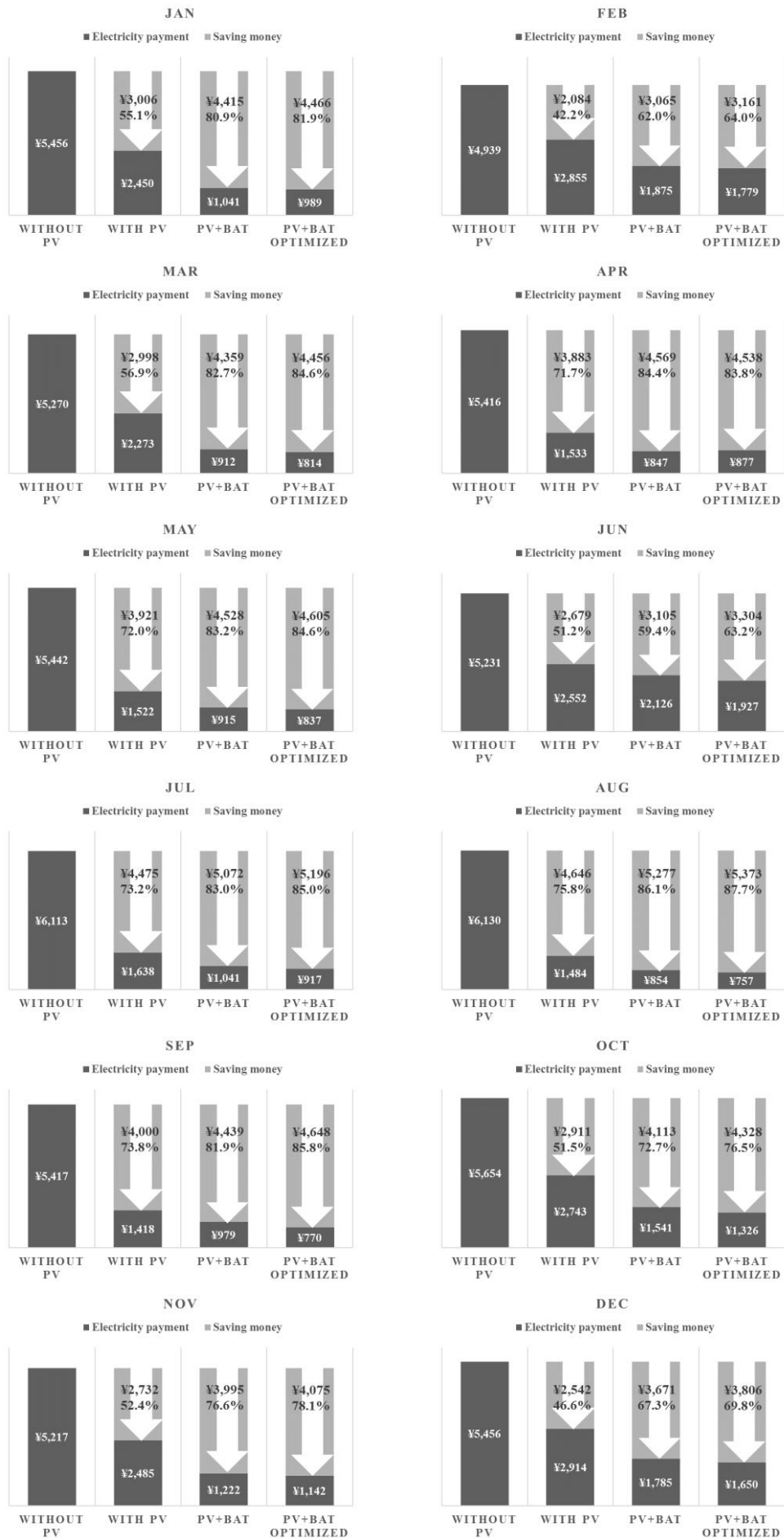


Figure 4.21 Monthly cost comparison result

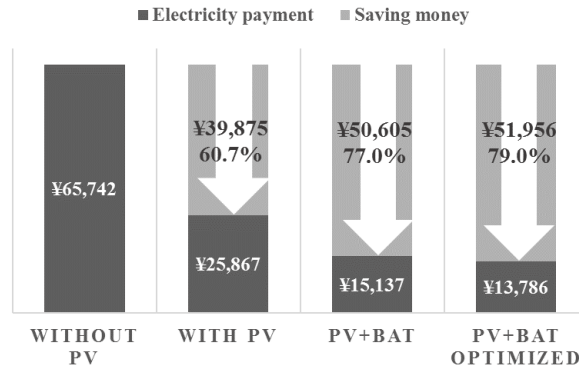


Figure 4.22 Annual cost comparison result

4.4 Optimizing Power Schedule Based on Converter Loss

In this section, optimizing power schedule will be done based on the converter loss.

4.4.1 System Architecture

PV System with batteries is installed in building that uses DC for distribution system. Configuration of the system is shown in Figure 4.23. Positive value of grid power, P_G , refers to exchange power from grid to building and vice versa. Positive value of battery power, P_B , represents power for charging battery, while negative value represents discharging power.

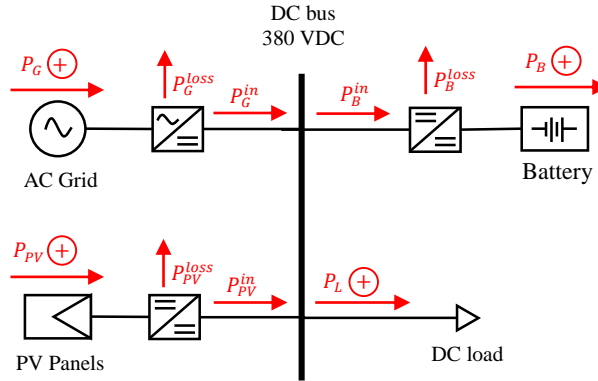


Figure 4.23 System configuration and power flow including converter loss

4.4.2 Optimized Power Schedule Formulation

An optimized power schedule is formulated, then implemented in spreadsheet using Solver for optimization. The following assumptions are used to formulate the problem:

- Predicted loads (P_L) and PV generations (P_{PV}) are available for hourly intervals.
- Power exchanges from/to grid have to be constant each hour.
- Characteristics of loss (μ) are given for each converter.
- Battery characteristics are also known.
- Cable loss is neglected.

The objective of optimization is to minimize loss in converters in duration T by time interval Δt . The objective function is defined as (4.9).

$$\min \left(\sum_{t=1}^T \left(P_G^{loss}(t) + P_{PV}^{loss}(t) + P_B^{loss}(t) \right) \right) \quad (4.9)$$

Power loss value is always positive. It does not matter whether power direction is toward to or out of the system. This objective function is subjected to constraints as follow description. Power from/to grid is limited by (4.10), while battery power is limited by (4.11). Battery SOC is limited by (4.12), and the relation between battery power, state of charge (*SOC*), and its capacity (Q_B) is calculated by (4.13). Power flow in the system is determined by (4.14). Table 4.8 shows the relation of power sources and loss in each converter and condition.

Table 4.8 Power and loss equations

	Condition	Power	Loss
PV		$P_{PV}^{in} = P_{PV} \times \eta_{PV}$	$P_{PV} - P_{PV}^{in}$
Grid	$P_G^{in} \geq 0$	$P_G = P_G^{in} / \eta_G^{fromGRID}$	$P_G - P_G^{in}$
	$P_G^{in} < 0$	$P_G = P_G^{in} \times \eta_G^{toGRID}$	
Battery	$P_B^{in} \geq 0$	$P_B = P_B^{in} \times \eta_B^{charge}$	$P_B^{in} - P_B$
	$P_B^{in} < 0$	$P_B = P_B^{in} / \eta_B^{discharge}$	

$$P_G^{min} \leq P_G(t) \leq P_G^{max} \quad (4.10)$$

$$P_B^{min} \leq P_B(t) \leq P_B^{max} \quad (4.11)$$

$$SOC^{min} \leq SOC(t) \leq SOC^{max} \quad (4.12)$$

$$P_B(t) = \frac{(SOC(t) - SOC(t-1)) \times Q_B}{\Delta t} \quad (4.13)$$

$$P_G^{in}(t) + P_{PV}^{in}(t) = P_B^{in}(t) + P_L(t) \quad (4.14)$$

4.4.3 Numerical Results and Analysis

In order to evaluate the presented method, building system is dimensioned as:

- PV panels with 6 kW power output are installed.
- Total battery capacity is 4.4 kWh.
- A grid connection of 4 kW is provided and can receive the same amount for reverse power.
- Efficiency of PV converter is 95%, battery converter is 93%/93% (charge/discharge), and grid converter 86%/93% (AC to DC/DC to AC).
- SOC_{min} is 10% and SOC_{max} is 100%.

As comparison, power schedule with simple ruled-base algorithm is used. This simple ruled-base algorithm allows battery to charge until SOC_{max} if surplus PV power is available, and discharge until SOC_{min} if PV power is not enough for supplying load. Grid power will fulfill the lack of power in the system.

The numerical result shows, using the simple ruled-base algorithm to supply total demand 13.51 kWh, generate 2.3 kWh loss in converters. It is about 14.6% of total required energy. Using proposed algorithm to schedule the power flow in the system creates almost the same amount of converter loss.

However, the power schedule is different for each algorithm. Power schedule with simple ruled-base algorithm is shown in Figure 4.24. In this algorithm, the battery is charged to full in the early morning by using the PV surplus power. Because the algorithm gives the priority of PV surplus power to charge the battery first, then send the excess power to the grid. Optimized power schedule based on converter loss by proposed algorithm is shown in Figure 4.25. The proposed algorithm allows the battery to be charged gradually. It also keeps the SOC enough for supplying the demand until rest of the day.

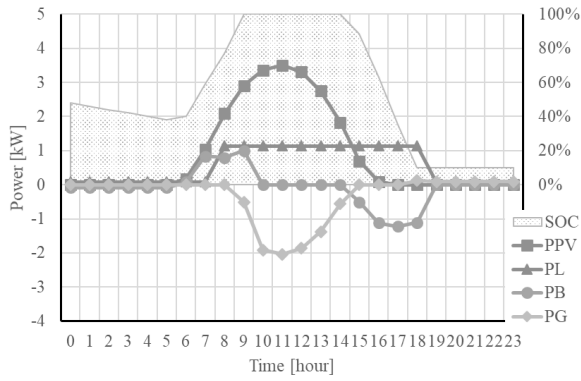


Figure 4.24 Power schedule with simple ruled-base algorithm

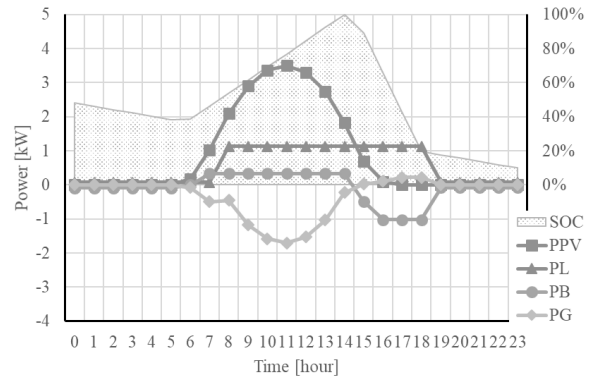


Figure 4.25 Power schedule by minimize converter loss

4.5 Chapter Conclusions

Significant constant loss is found in battery converter. In the other hand, datasheet will show the efficiency average in rating power operation. Nevertheless, analysis result of recorded data shows that operation in power lower than its rating bring low efficiency. In case designing the system contains several converters, consideration of converter rating to avoid the low power utilization is necessary.

Additional PV and battery system gives a potential reduction of electricity charge. However, the optimization of battery charge-discharge schedule may increase its potential. Besides by minimizing the total electricity charge, optimizing power schedule of PV system with batteries also can be achieved by minimizing converter loss. In this case study, converter loss total is almost equal compared to simple ruled-base algorithm. However, the power schedule of batteries is different for each algorithm. In the simple ruled-base algorithm, the battery is charged to full in the early morning by using the PV surplus power. The proposed algorithm allows the battery to be charged gradually and keeps the SOC enough for supplying the demand until rest of the day.

Chapter 5

Economic Evaluation Using Peak-Time Pricing Ratio

5.1 Chapter Introduction

The electricity pricing is not only observed from the operation cost alone. It includes the investment cost for building the power plant. To ensure the safe supply of energy, the installed generating capacity that can satisfy the peak load is also needed to be considered, as well as the reserve capacity that must be available at all times. In addition, electricity demand in a certain hour is closely related to the grid load level, where high demand will play a major role in raising the market price and applies also for vice versa [61]. The utility usually hide the fluctuating generation cost with a flat electricity tariff for the user [62]. However, to reduce peak-time electricity usage, utility or smart grid owner normally will set time-varying prices for the sale of electricity to consumers [63], because it will encourage less use of energy consumption in peak time or shift consumption to off-peak hours [64], [65].

Integrating photovoltaic (PV) power generation and energy storage systems has become a particularly interesting problem with the introduction of dynamic electricity energy pricing. Since consumers can minimize their electricity bill by using their PV-based energy generation and controllable energy storage devices for peak shaving on their power demand profile [66]. With the development of smart grid, the utilization of dispersed generator becomes more popular. Many advanced research is already conducted in order to determine electricity price, for instance one-dimensional and two-dimensional of multistep electricity price (MEP) [67], continuous-time marginal [68], game-theoretic approach of time-of-use (TOU) pricing [69], dynamic pricing [70], relevance vector machines (RVMs) pricing [71], day-ahead pricing [64], [72], [73], and so on.

Electricity price might be various depend on places. Thus, in consumers' point of view, if there is possibility to select the utility/retailer, which may offer different prices, they will try to find the one that can give more benefit to them. In this study, three parameters of peak-time electricity price will be introduced that can be used for economic evaluation of building's power grids system. By using a general model of power grids system, which contains PV generation and battery system as energy storage, the parameters will be validated. As a study case, various electricity prices from utility company in Japan with the same duration and period of peak-time is used.

When the source and load with dc interface is commencing to be used in building power grid system, by considering the simplicity and efficiency, it is unreasonable to use "dc-ac-dc" route from dc source to dc load [12]. Some studies show that dc system can reduce total conversion loss [49], [59]. So that, the idea of using dc system becomes more popular. Hence, it is still a deliberation that which system is better to be used, whether ac or dc system.

In order to cover peak-time pricing in general, we will introduce parameter α (peak-time electricity price ratio), parameter β (peak-time electricity price to standard charge ratio), and parameter γ (average price to standard charge ratio). Finally, we will evaluate the dc grid system by seeing its benefit compares to ac

grid system in term of ratio change between ac load and dc load. In this study, the efficiency of each converter will be considered.

5.2 Electricity Pricing System

Electricity market type might be different for each country. Some countries apply a perfect market with wholesale or retail power trade, such as US. Through the competitive market, market will control the price. Some other countries need to face natural monopolies, in where state-owned power grid companies are in charge of the power transmission, distribution, and retailing for the whole country. Here, the transactions are under the government-regulated tariffs that is usually used as government policy tool.

5.2.1 Flat Pricing System

A flat pricing system is common to be used for electricity pricing. In flat pricing system, there is no different tariff for each costumer type. It is also no difference price along the time. This pricing system is recognized as the simplest one because any fluctuation of generation cost will be hidden in the flat price.

5.2.2 Block-Tariff Pricing System

By using block-tariff pricing system, the electricity price is differentiated based on the amount of energy consumption. In general, it is divided into some blocks using some range of energy consumption. First block usually has the cheapest price. More energy used, the price will be higher.

5.2.3 Time-based Pricing System

5.2.3.1 Time-of-Use Pricing System

Time-of-use (TOU) pricing is a rate where usage unit prices vary by time period, and where the time periods are typically longer than one hour within a 24-hour day [74]. For utility companies, TOU pricing will help to improve their load shape by the response of customer in shifting usage from peak hours to off-peak hours. The flat load shape can reduce the utilization of peak-hour power plants that have higher marginal cost. Therefore, it can save cost for the utilities. Furthermore, reducing peak demand can help utilities delay some capital investment. It also gives opportunities for customers to save on their electricity bills by responding to the on-peak and off-peak prices [75]. Implementation of TOU pricing is suitable for DR program and requires least technological transformation [76].

5.2.3.2 Real-Time Pricing System

In real-time pricing (RTP) system, the electricity price is defined for shorter periods of time and reflecting the changes in the wholesale price of electricity. Customers usually have the price information on a day-ahead or hour-ahead basis [77].

5.2.3.3 Critical Peak Pricing System

Critical peak pricing (CPP) system is a hybrid system of TOU and RTP. Under the tight demand-supply balance, CCP tries to control electricity demand and alleviate the tight balance. In order to press the load at peak hours, CCP increases the electricity price at that time on critical days that announced beforehand. As the response to CCP, customer may change their demand pattern [78]. This system is harder to implement compared to others two time-based pricing systems [77].

5.3 Electricity Price Parameter

5.3.1 Price Parameter Definition

In this study, the parameter α (peak-time electricity price ratio), parameter β (peak-time electricity price to standard charge ratio), and parameter γ (average price to standard charge ratio) are introduced to identify electricity pricing plan. Peak-time price ratio, α , is defined as ratio of others-time price (P_2) to peak-time price (P_1). Peak-base ratio parameter, β , is defined as ratio of peak-time price (P_1) to base price (B) in general plan that is using standard charge. Average-base ratio parameter, γ , is defined as ratio of average price in peak-time pricing plan to standard charge in general plan.

5.3.1.1 Case one-step peak pricing

In case of only one step of peak in electricity price (Figure 5.1), we will have only one parameter α as defined by (5.1). Parameter β is determined by (5.2). As for parameter γ , (5.3) is used as the definition with total time follows (5.4).

$$\alpha = \frac{P_2}{P_1} \tag{5.1}$$

$$\beta = \frac{P_1}{B} \tag{5.2}$$

$$\gamma = \frac{1}{24} \times \frac{(P_1 \times \Delta t_1 + P_2 \times \Delta t_2)}{B} \tag{5.3}$$

$$\Delta t_1 + \Delta t_2 = 24 \tag{5.4}$$

5.3.1.2 Case two-step peak pricing

In case of two steps of peak in electricity price (Figure 5.2), we will have two parameters α as defined by (5.5). Parameter β is determined by (5.6). As for parameter γ , (5.7) is used as the definition with total time follows (5.8).

$$\alpha_1 = \frac{P_2}{P_1}; \alpha_2 = \frac{P_3}{P_1} \tag{5.5}$$

$$\beta = \frac{P_1}{B} \tag{5.6}$$

$$\gamma = \frac{1}{24} \times \frac{(P_1 \times \Delta t_1 + P_2 \times \Delta t_2 + P_3 \times \Delta t_3)}{B} \tag{5.7}$$

$$\Delta t_1 + \Delta t_2 + \Delta t_3 = 24 \tag{5.8}$$

5.3.1.3 General peak pricing

Based on case of one-step and two-steps peak pricing, following equations are defined each parameter in general form. In case N-steps of peak pricing, for every $n \in \{1, 2, \dots, N - 1\}$, parameter α_n is defined by (5.9). Parameter β is determined by (5.10). As for parameter γ , (5.11) is used as the definition with total time follows (5.12).

$$\alpha_n = \frac{P_{n+1}}{\text{Max}(P_1, P_2, \dots, P_N)} \tag{5.9}$$

$$\beta = \frac{\text{Max}(P_1, P_2, \dots, P_N)}{B} \tag{5.10}$$

$$\gamma = \frac{1}{24} \times \frac{\sum_{n=1}^N (P_n \times \Delta t_n)}{B} \tag{5.11}$$

$$\sum_{n=1}^N \Delta t_n = 24 \tag{5.12}$$

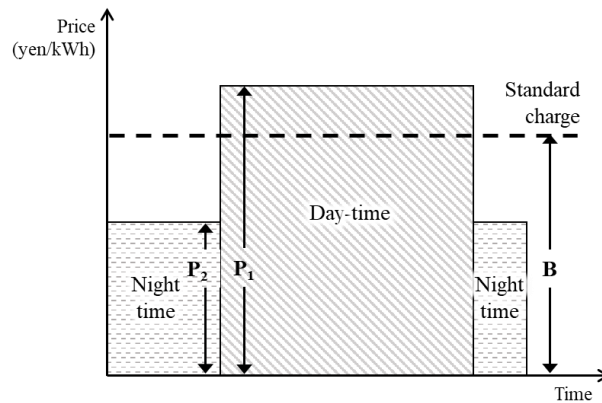


Figure 5.1 Price illustration for one-step peak pricing

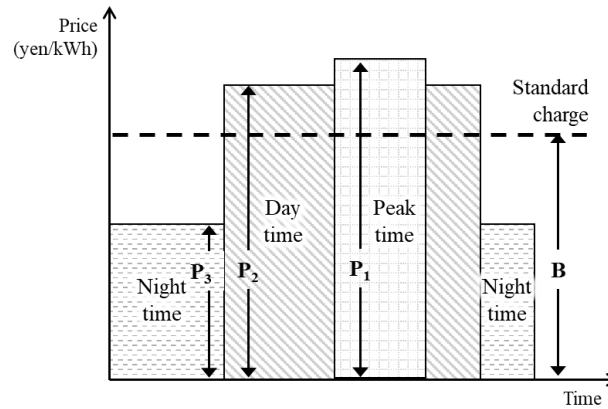


Figure 5.2 Price illustration for two-steps peak pricing

5.3.2 Electricity Price Parameter: Case of Japan

The electricity price parameter is implemented for case of Japan. There are several power utility companies in Japan. For this study, we select nine companies as listed in Table 5.1. Electricity charge of these companies is shown in Figure 5.3 for summer season, and in Figure 5.4 for other seasons.

Table 5.1 List of considered power utility companies in Japan

Company Name	
TEPCO	Tokyo Electric Power Company
Tohoku-EPCO	Tohoku Electric Power Company
KEPCO	Kansai Electric Power Company
YONDEN	Shikoku Electric Power Company
ENERGIA	Chugoku Electric Power Company
KYUDEN	Kyushu Electric Power Company
OKIDEN	Okinawa Electric Power Company
HEPCO	Hokkaido Electric Power Company
CHUDEN	Chubu Electric Power Company

As the note, HEPCO does not differentiate summer and non-summer season (no peak-time in summer). Meanwhile, CHUDEN has 3 plans for general plan (low, moderate, and high utilization rate) and 2 plans for peak-time pricing plan (low and high utilization rate), and also has different time of peak-time price which is 10 am - 5 pm. “CHUDEN 1” represent the low utilization rate plan. “CHUDEN 2” represent the high utilization rate plan. Moderate utilization rate plan in standard plan is not presented here.

The result of price parameter calculation is shown in Figure 5.5 for summer season and in Figure 5.6 for other season. YONDEN has the lowest α (peak-time price ratio) in both summer and other season, compared to other companies. This condition gives high potential to provide benefit by shift the load from day-time to night-time in YONDEN’s service area. However, YONDEN has the highest β (peak-to-base ratio), and parameter γ (average-to-base ratio) also in both summer and other season. Consequently, the carefully operation is necessary to evade undesired payment of used electricity.

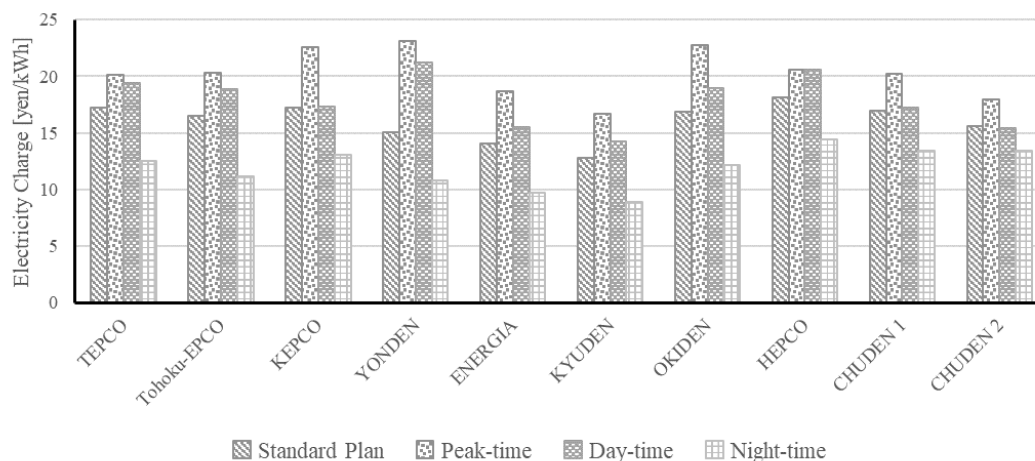


Figure 5.3 Electricity charge of power utility companies in Japan for summer season

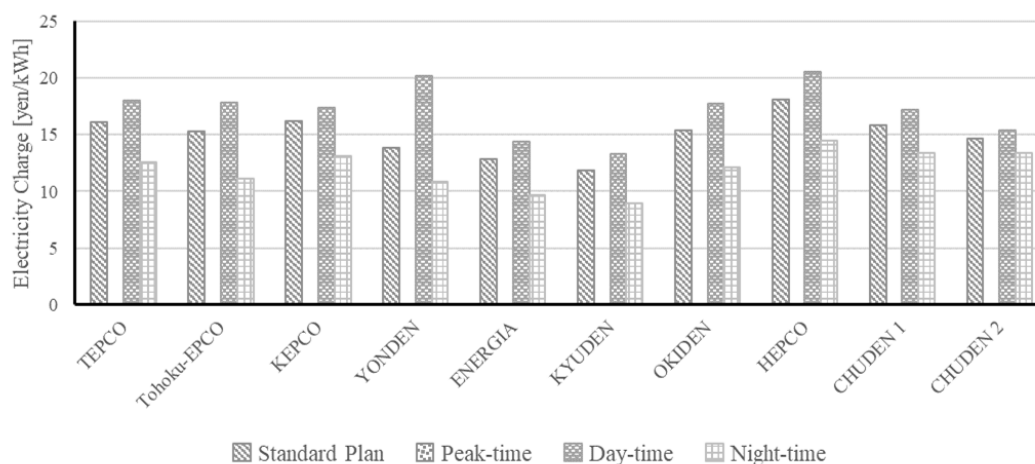


Figure 5.4 Electricity charge of power utility companies in Japan for non-summer season

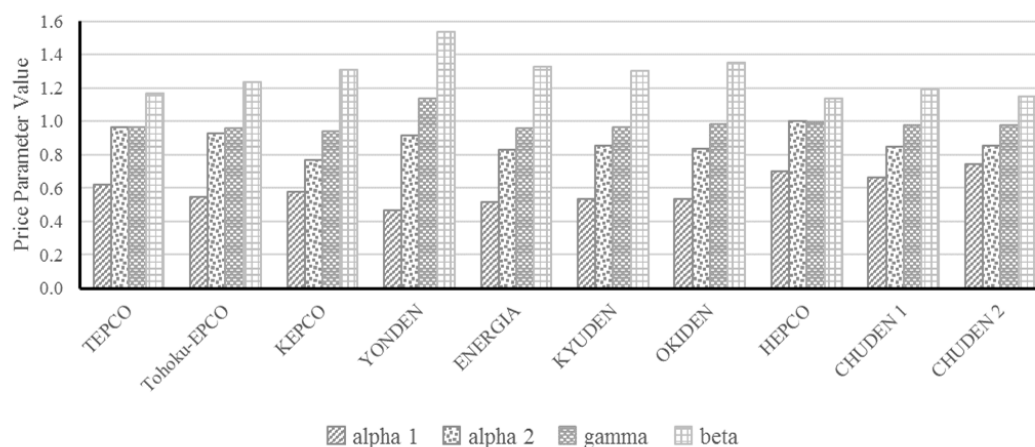


Figure 5.5 Price parameter of utilities in Japan for summer season

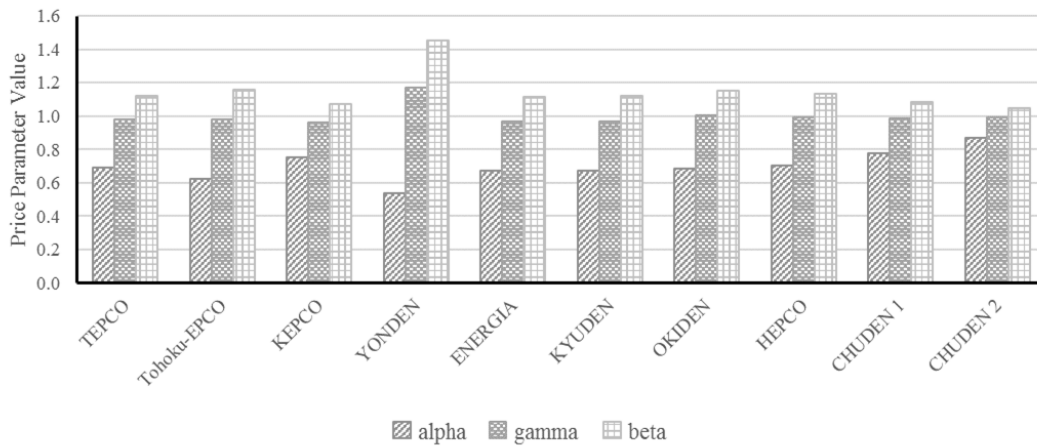


Figure 5.6 Price parameter of utilities in Japan for non-summer season

5.4 Cost Reduction

5.4.1 Cost Reduction Concept

When the peak pricing is applied, there is cheap energy when the demand is low, and expensive one when the demand is high (Figure 5.7). Cost reduction concept is to purchase cheap electricity for charging the battery, and then discharge accumulated energy in battery for reducing the demand to utility. In other words, electricity purchased at low-price time increases, and electricity purchased at high-price time decreases.

There are two main benefits of application of cost reduction concept. First benefit is the possibility to purchase cheaper electricity. Because of the electricity prices will be different depend on the time, when there is a range of cheaper electricity. By shifting the purchasing time into this range, total bill can be reduced. The second one is the opportunity to reduce power capacity contract. When the load is shifted, the peak power will decrease. If the operator can maintain this condition continuously, the contract of power capacity can be reduced (Figure 5.8). However, if the load shifting is not managed well enough, it might over rise the power purchase in low price time. So that, the power capacity contract cannot be reduced, or in the worst case, it might be increased (Figure 5.9).

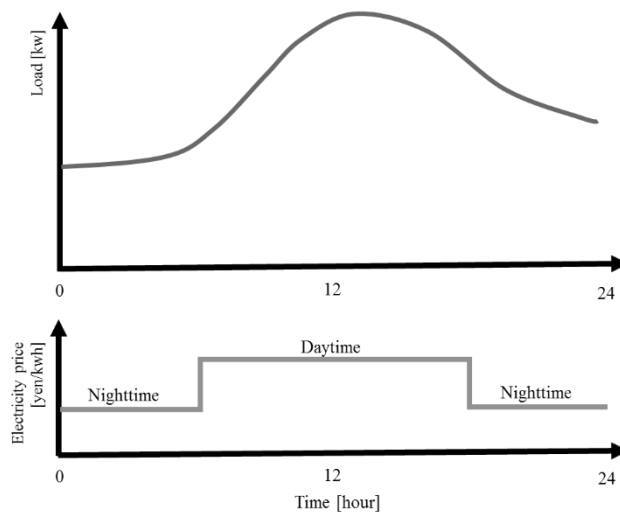


Figure 5.7 Comparison of load profile and electricity price

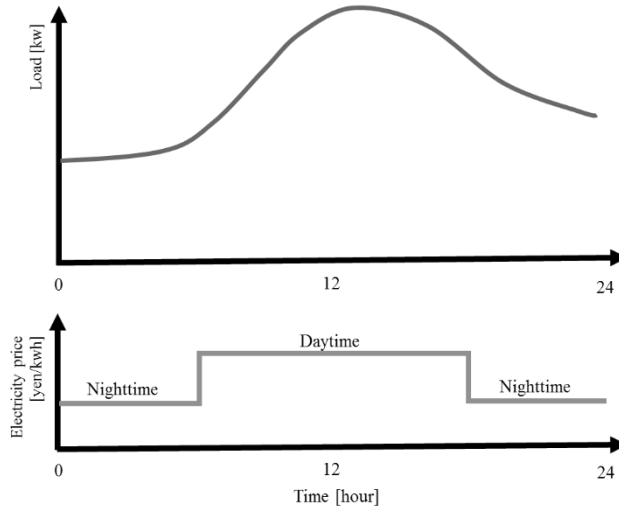


Figure 5.8 Illustration of cost reduction concept

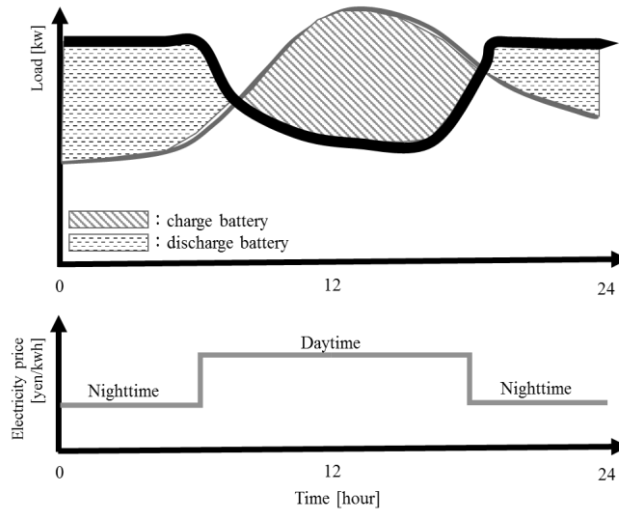


Figure 5.9 Illustration of undesired increase of maximum power

5.4.2 Case Analysis

In order to illustrate the cost reduction concept, following case analysis is used. The building contains PV and battery system is the framework. By observing the sufficiency of PV generation ($P_{PV}(t)$), usable amount of energy storage ($E_{SU}(t)$), and availability space of energy storage ($E_{SA}(t)$), battery operation is decided, whether charge or discharge. Here, power of battery ($P_B(t)$) is assumed to be positive value for charging and negative value for discharging. PV generation sufficiency is calculated by (5.13), where $P_{PV}(t)$ is PV power generation and $P_{LOAD}(t)$ is power demand. Whenever the PV generation is sufficient, there is possibility for charging battery. Considering the stored energy in previous step time ($E_S(t-1)$), minimum allowable SOC (SOC_{min}), and battery capacity (C_B), usable amount of energy storage is calculated by (5.14). Whereas, availability space of energy storage is calculated by (5.15), which is considering the maximum allowable SOC (SOC_{max}). Finally, the consumption power from grid ($P_G(t)$) is determined by considering the total sufficiency power from PV generation and storage ($P_{SUF}(t)$). This sufficiency power is calculated by (5.16). Whenever the total sufficiency power is negative, power from grid should supply the insufficient amount. Any calculation is done for every hour respectively.

$$P_{PVS}(t) = P_{PV}(t) - P_{LOAD}(t) \quad (5.13)$$

$$E_{SU}(t) = E_S(t - 1) - (SOC_{min} \times C_B) \tag{5.14}$$

$$E_{SA}(t) = (SOC_{max} \times C_B) - E_S(t - 1) \tag{5.15}$$

$$P_{SUF}(t) = P_{PVS}(t) - P_B(t) = P_{PV}(t) - P_{LOAD}(t) - P_B(t) \tag{5.16}$$

For the detailed illustration, the following two analysis methods will be used.

5.4.2.1 Analysis Method 1

In analysis method 1, following the flowchart in Figure 5.10, battery will charge using only the sufficiency energy of PV generation. Based on this flowchart, charging battery using power from grid is not allowable. So that, the energy that stored in the battery is only from sufficient power of PV generation.

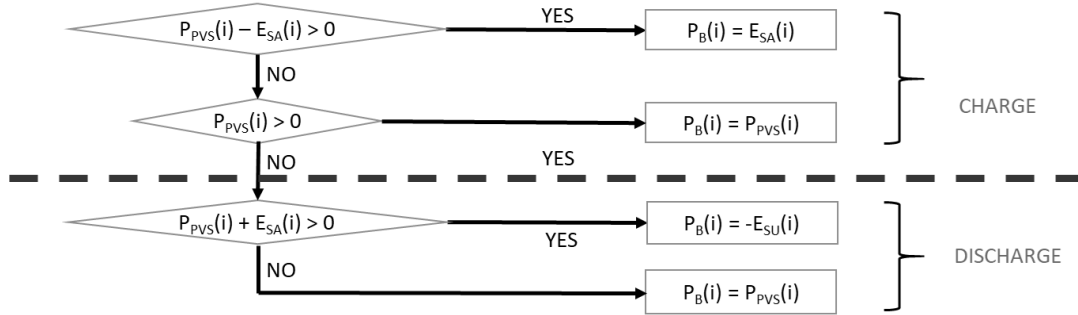


Figure 5.10 Flowchart of battery charge-discharge amount for method 1

5.4.2.2 Analysis Method 2

In analysis method 2, the operation is divided into two cases (Figure 5.11). First case is when low price is occurred, which usually happened on night time, so it called night time price. Because in this period time, the electricity price is low, so charging battery by power from grid is allowable, whenever there is available storage space. Second case is when high price is occurred, which usually happened on day time, so it called day time price. In this case, the decision flow is same as with the flow that is using in analysis method 1.

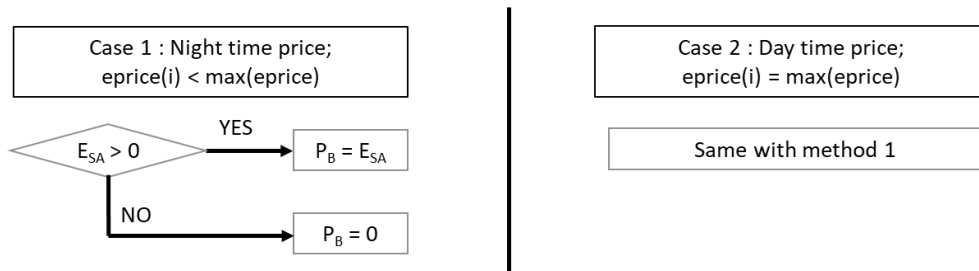


Figure 5.11 Flowchart of battery charge-discharge amount for method 2

5.4.2.3 Analysis Results and Discussion

The analysis is done by assuming there is only one pattern of electricity price, also no difference of summer and other seasons. Here, day-time price is assumed to be constant in 17.96 yen/kWh, then the night-time price is defined by factor α . However, night-time price is applied in whole day for Sunday or holiday as shown in Figure 5.12. Power demand and PV generation assumptions is shown in Figure 5.13. Calculation is done only for one day of weekday type of load, with initial condition of battery is empty, which is equal to SOC minimum. The battery size is assumed to be 1 kWh. In order to see the benefit, the system is comparing to the system without battery.

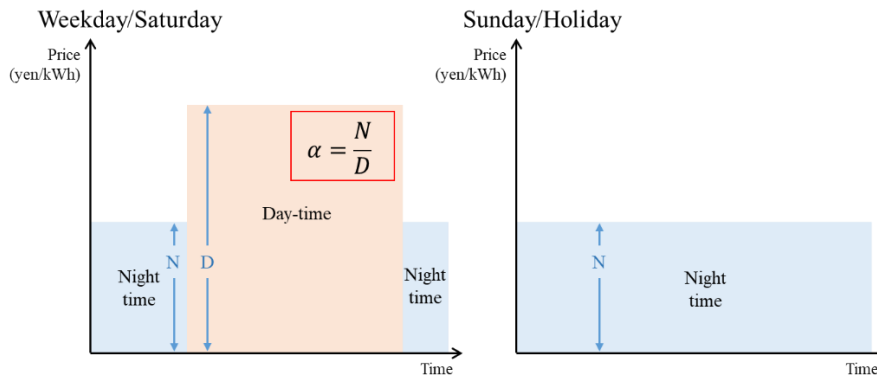


Figure 5.12 Electricity price assumption

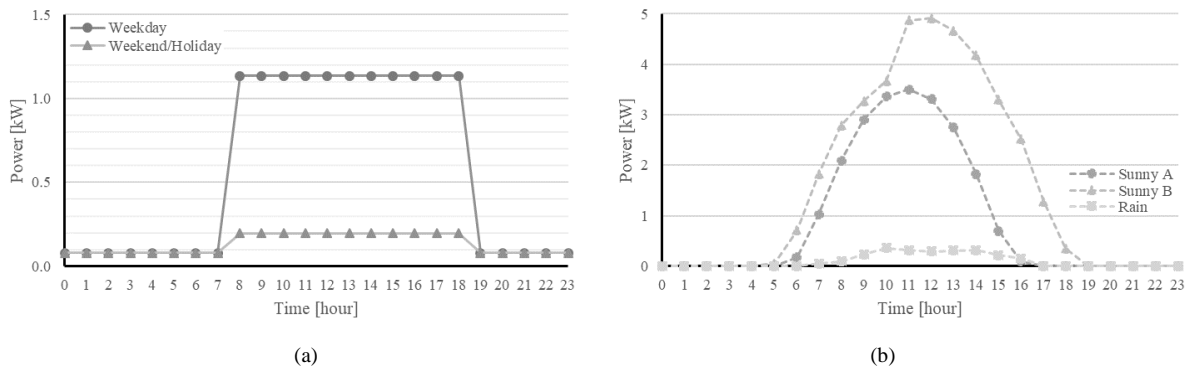


Figure 5.13 Power assumptions for (a) demand and (b) PV generation

The comparison result of analysis method 1 and method 2 is shown in Figure 5.14. It shows that, by using method 1, in sunny day benefit is high but not influenced by alpha value. However, there is no benefit in rainy day. Whilst, in method 2, amount of benefit is influenced by alpha value. The amount of benefit is higher in smaller value of alpha, in both sunny and rainy day. There are alpha values that generate balance point (the benefit is equal to zero).

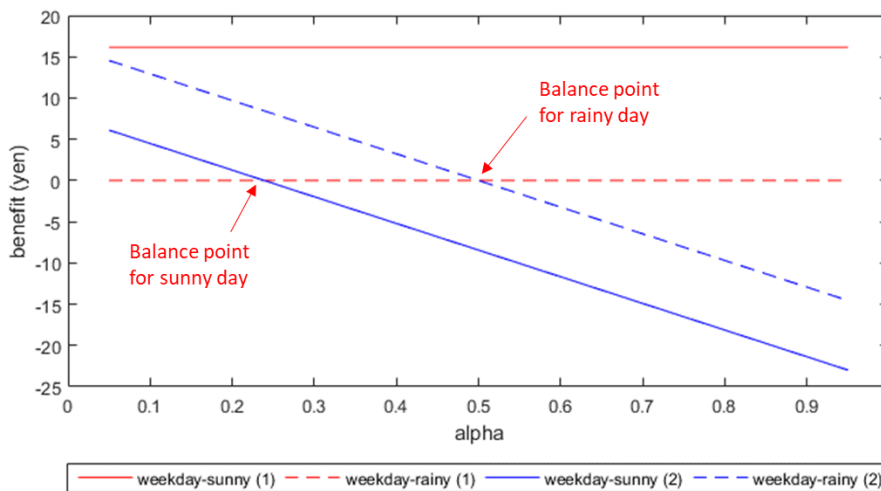


Figure 5.14 Comparison of method 1 and method 2

In addition, we did battery size analysis by using only method 2 for weekday type of load for seeing the impact of alpha value. The initial condition is also set to be an empty battery, which is equal to SOC minimum. Same as previous analysis, the assumption of daytime price is 17.96 yen/kWh. Figure 5.15 shows the analysis result of the battery sizing in cost reduction concept for both sunny and rainy day in weekday type of load. Following the alpha value, the results indicate that the battery size has influence to the benefit value. However, oversized battery gives the decreasing of benefit if it evaluated only in one day. It caused by the energy that have been charged to the battery in the nighttime cannot be used all in daytime but it has to be paid.

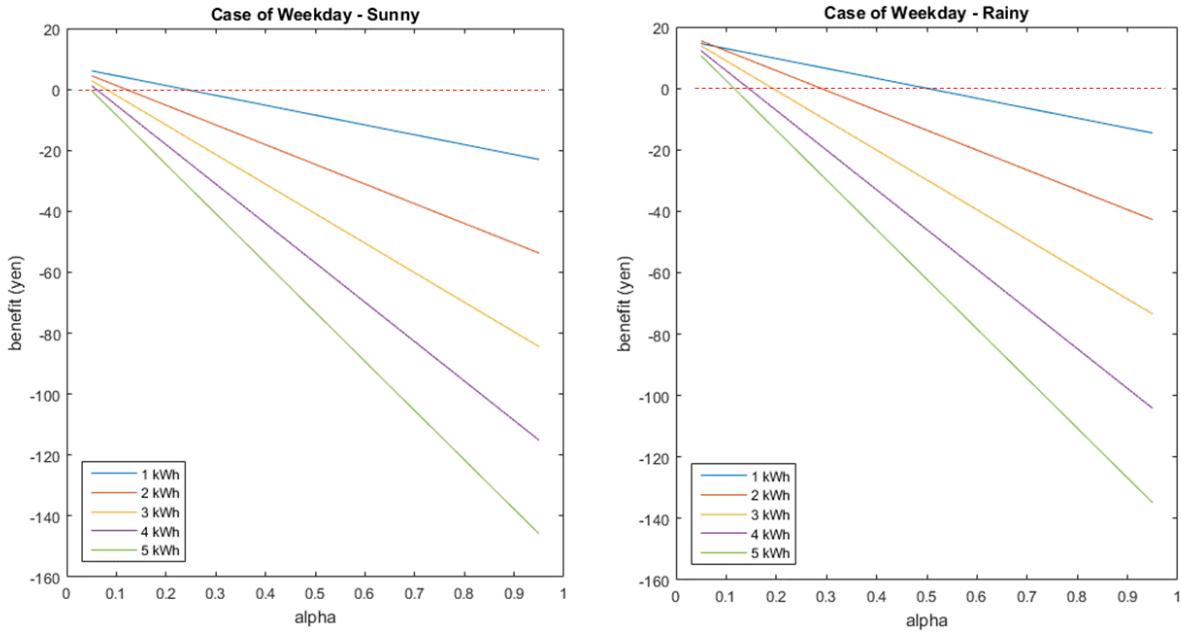


Figure 5.15 Battery size analysis results

5.5 Economic Evaluation in General Model

5.5.1 System Model

5.5.1.1 Electricity Price Model

There are two types of electricity price model that will be considered in this study, which are general and peak-time pricing plan (Figure 5.16). The general pricing plan applies only one standard charge for electricity price which is same along the time. Whereas the peak-time pricing plan applies more expensive charge in the peak-time (usually in day-time) and cheaper charge in the night-time.

In Japan almost all utility companies distinguish prices for the summer, which is more expensive than other seasons. For simplification, all prices are assumed to be no different between summer and other seasons. In addition, the price model taken is a model of the season other than summer, because peak-time is only once.

In order to identify the peak-time pricing plan of electricity charge from many utility companies, we use two proposed parameters. First one is parameter α , as night to day-time electricity price ratio which is stated in (5.17). Second one is parameter β , as day-time to standard charge ratio which is defined by (5.18).

$$\alpha = N/D \tag{5.17}$$

$$\beta = D/B \tag{5.18}$$

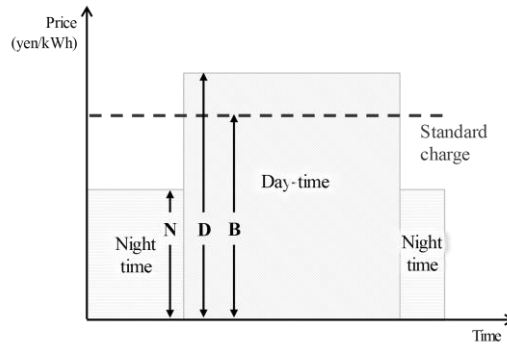


Figure 5.16 Electricity price in general and peak-time pricing plan

5.5.1.2 Power Grids System Model for Building

As a general model of grid system for building (Figure 5.17), loads are supplied by electricity bought from utility grid and generated by photovoltaic (PV) system. Battery system is also included in the grid system. Here, loads can be an ac load and/or dc load. In this general model, the grid system is seen as a black box, where the component that connected the loads to the sources is unknown. By neglecting any loss of components in power grid system and case of selling energy is not allowed, power balance equation for general model is calculated by (5.19). Equation (5.20) is used to calculate the sufficiency power from PV.

$$pgb_t + ppv_t + pbd_t - pbc_t = D_{ac,t} + D_{dc,t} \quad (5.19)$$

$$pvs_t = ppv_t - (D_{ac,t} + D_{dc,t}) \quad (5.20)$$

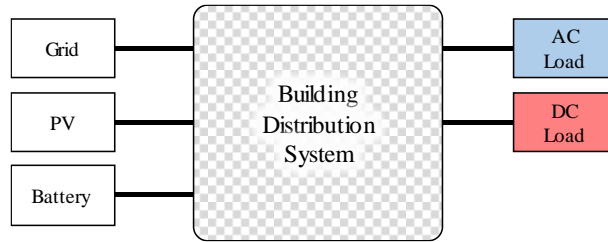


Figure 5.17 General model of power grid system for building

The total electricity cost of system is calculated by (5.21), then by using (5.22), percentage of benefit is calculated.

$$tc_s = \sum_{d=1}^{ND} \sum_{t=1}^{NT} pgb_{t,d} \cdot EC_{t,d} \quad (5.21)$$

$$tb_s = (tc_{base} - tc_s) / tc_{base} \cdot 100\% \quad (5.22)$$

5.5.2 Computational Experiments

5.5.2.1 Data

Time step is hourly. Study horizon is one year. Daily load curve and PV generation curve are shown in Figure 5.18. The load is divided into two types: weekday load and weekend/holiday load. Annual energy consumption is assumed to be 3,720 kWh. PV generation curve is divided into three types: 'Sunny A' for sunny weather in winter and autumn, 'Sunny B' for sunny weather in spring and summer, and 'Rain' for rain weather in all seasons. Here, seasons is classified by the time, where winter is 1 January-31 March, spring is 1 April-30 June, summer is 1 July-30 September, and autumn is 1 October-31 December. Annual PV generation is expected to be 7,925 kWh in total.

Battery size is decided to be 1 kWh with state-of-charge (SOC) is set to 10% for minimum and 100% for maximum value. In case of 2 kWh battery system is defined as the system with 2 pieces of 1 kWh battery which are connected in parallel so that the characteristics of battery is assumed to be not changed.

For electricity price in peak-time pricing plan, daytime price is applied in weekday and Saturday from 8 am to 10 pm. Other than this time will be nighttime price.

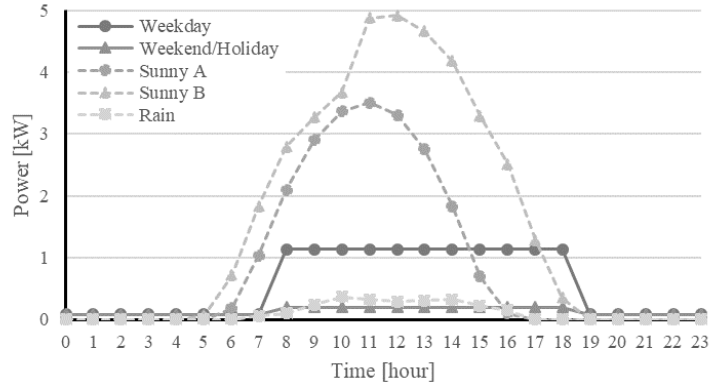


Figure 5.18 Daily load and PV generation curve

5.5.2.2 System Scenarios

5.5.2.2.1 Base Scenario

The building grid system is not use any PV neither battery, then all of the load is supplied by grid, as stated in (5.23). General electricity pricing plan is used, which applies the standard flat charge along the day and there is no difference between weekday and weekend/holiday.

$$p_{gb_t} = D_{ac,t} + D_{dc,t} \quad (5.23)$$

5.5.2.2.2 Scenario 1

PV and battery system is equipped in the building grid system. Peak-time pricing plan is used for the electricity charge. Figure 5.19 shows the algorithm to charge and discharge the batteries in this scenario. It has 5 modes as described below.

Mode 1: PV has excess power that is used to charge the batteries. Batteries charged amount is constrained by the available space in the batteries and maximum current for charging. There is no transfer power from grid. The batteries and grid power are calculated by (5.24). After the batteries are fully charged, the system will change to mode 2.

$$p_{bc_t} = \min(p_{vs_t}, sb_t/\Delta t, PBC_{max}); p_{bd_t} = 0; p_{gb_t} = 0 \quad (5.24)$$

Mode 2: PV has excess power but cannot charge the batteries because of fully charged. In this condition, the batteries have no operation. There is also no transfer power from grid as described in (5.25).

$$p_{bc_t} = 0; p_{bd_t} = 0; p_{gb_t} = 0 \quad (5.25)$$

Mode 3: Cheaper energy in the nighttime is intended to be stored in the batteries. Thus, the batteries will be charged in the limitation of available space in the batteries and maximum current for charging. PV may cannot supply all load or even not generate any power because it is in the nighttime. In order to keep the balance power, grid transfer power as needed as stated in (5.26). When the batteries became fully charged, system will change to mode 4.

$$p_{bc_t} = \min(sb_t/\Delta t, PBC_{max}); p_{bd_t} = 0; p_{gb_t} = D_{ac,t} + D_{dc,t} - ppv_t - p_{bd_t} + p_{bc_t} \quad (5.26)$$

Mode 4: Generation power from PV is not sufficient to supply the loads. Meanwhile the batteries do not operate with two type of conditions. First, it is in the daytime but there is no energy left to be discharged. Second, it is in the nighttime, when the energy from grid is cheap, but the batteries are fully charged, so no more space to be charged. Grid transfer power as needed so that the balance power is maintained as stated in (5.27).

$$pbc_t = 0; pbd_t = 0; pgb_t = D_{ac,t} + D_{ac,t} - ppv_t - pbd_t + pbc_t \quad (5.27)$$

Mode 5: In condition when the electricity price is high, but power generation from PV cannot supply all loads, the batteries will be discharged. The discharged amount will follow the insufficient energy of PV. However, if it reached the discharge limitation, the rest of needed power will be fulfilling by grid as stated in (5.28). When the batteries attain the minimum SOC that is allowed, the system will change to mode 4.

$$pbc_t = 0; pbd_t = \min(-pvs_t, rb_t/\Delta t, PBD_{max}); pgb_t = D_{ac,t} + D_{ac,t} - ppv_t - pbd_t + pbc_t \quad (5.28)$$

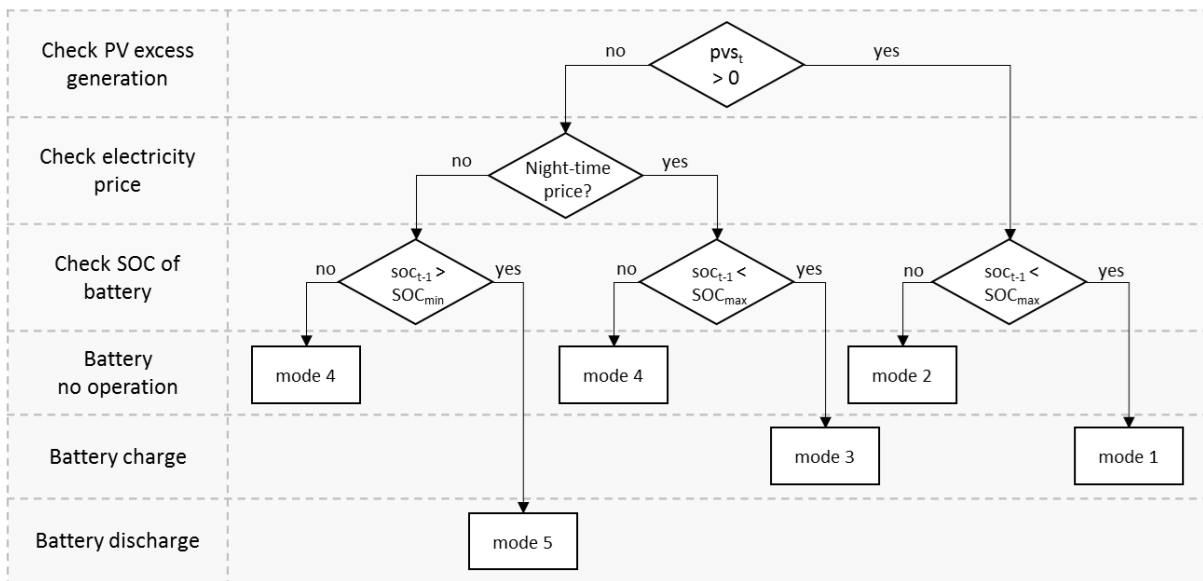


Figure 5.19 Algorithm for charging-discharging battery in scenario 1

5.5.2.3 Results and Analysis

Influence of parameter α to the benefit is evaluated by using general model of power grid system for building. Results in Figure 5.20 show linear relation between percentage of total benefit and value of alpha. Larger size of battery delivers more total benefit. However, the increasing size of battery that offers significance additional benefit for this system is up to 3 x 1 kWh (Figure 5.21).

To validate the use of parameter α , percentage benefit calculated by value α is comparing with the real calculation using factual data. Equation (5.29) is used to calculate percentage error between these two approaches. Comparison results are shown in Table 5.2.

$$e = (|x_{act} - x_{app}|/|x_{act}|) \cdot 100\% \quad (5.29)$$

The percentage error is less than 1% for the systems which have nearest value of parameter β to the reference. This result shows that parameter α itself is not adequate to represent the peak-time electricity-pricing plan.

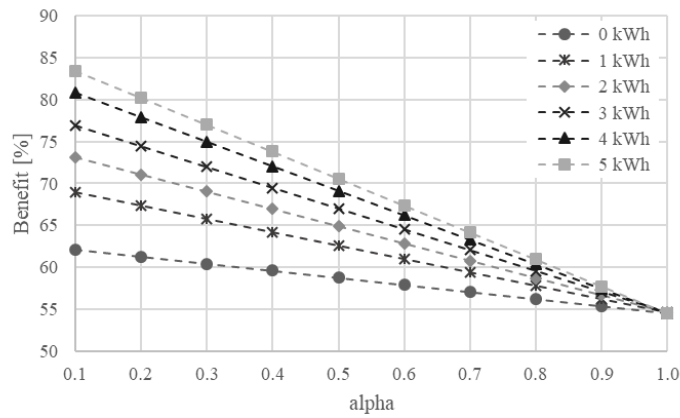


Figure 5.20 Relation of benefit and alpha values with various size of batteries

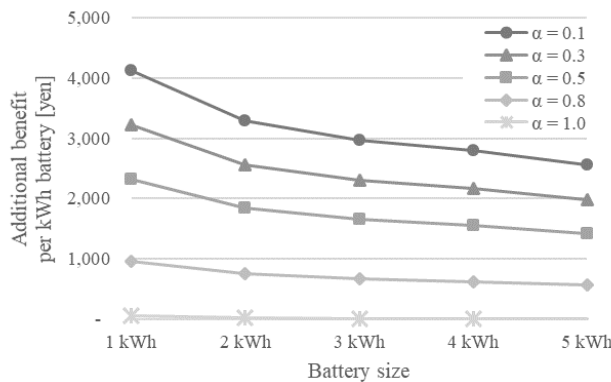


Figure 5.21 Additional benefit per kWh of battery for each system

Table 5.2 Comparison of benefit calculated by value α and real calculation

Utility Company	B	D	N	α	β	tb^1	tb^2	e
TEPCO	16.08	18.05	12.54	0.69	1.12	59.49	59.49	0.00
Tohoku-EPCO	15.34	17.81	11.12	0.62	1.16	60.61	59.26	2.28
KEPCO	16.17	17.36	13.08	0.75	1.07	58.55	60.36	2.99
YONDEN	13.89	20.20	10.82	0.54	1.45	62.03	50.81	22.09
ENERGIA	12.86	14.37	9.68	0.67	1.12	59.83	60.01	0.30
KYUDEN	11.87	13.31	8.93	0.67	1.12	59.87	59.91	0.07
OKIDEN	15.38	17.77	12.15	0.68	1.16	59.67	58.48	2.02
HEPCO	18.12	20.56	14.45	0.70	1.13	59.36	58.92	0.75

1. Estimated by using graph of benefit vs alpha (Figure 5.21)

2. Actual calculation by using factual input data

5.6 Economic Evaluation in Extended Model

5.6.1 System Model

In order to evaluate power grid of building in extended model, it is assumed as a system with pure ac loads and/or pure dc loads. Pure ac load means the load is not converting power to dc inside the equipment. Whereas, pure dc load means the load is not converting power to ac inside the equipment. All of the loads get supply from electricity bought from utility grid and/or generated by photovoltaic (PV) system. Battery system is also included in the building grid system. This study compares two types of building power grid model. They are ac and dc system model (Figure 5.22). The evaluation is done by changing the ratio between ac load and dc load.

Refer to Figure 5.22, a universal model of building power grid system is defined as shown in Figure 5.23. This model is used only for power balance calculation by considering each converter efficiency. Main bus can be ac or dc bus, depends to the system. The list of converters is shown in Table 5.3. In case of ac system, the actual systems use ac bus, and only use converter ①, ②, ③, ④, and ⑤. Meanwhile in case of dc system, the actual systems use dc bus, and only use converter ①, ②, ⑥, and ⑦.

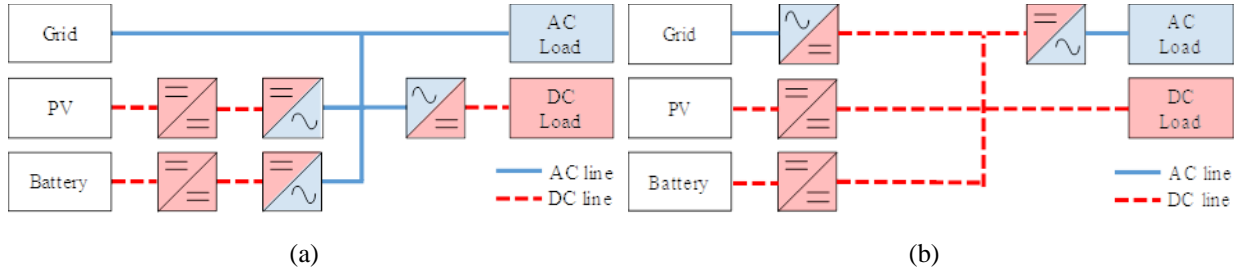


Figure 5.22 Building power grid extended model in (a) ac system and (b) dc system

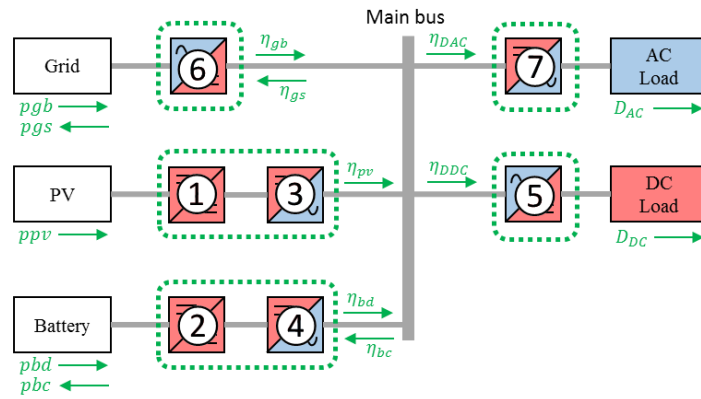


Figure 5.23 Universal model of building power grid system

In this study, by using the universal model in calculation, the not used converters will be assumed to have 100% efficiency, so that they do not affect the calculation result. Efficiency for each converter in every system follows Table 5.4. Power balance equation for the general model is calculated by (5.30). Flowchart in Figure 5.24 shows how the system decides battery response and power purchased from grid. Same with scenario 1 in the previous chapter, the responses are divided into 5 modes, which are referred to excess amount of PV generation, electricity prices, and battery conditions. In mode 1 and 3, battery will be charged, meanwhile it will be discharged in mode 5. Moreover, battery will be in standby mode in mode 2 and 4. Excess amount of PV generation is defined as sufficiency energy from PV after supply all loads, and calculated by (5.31). Equations for battery and grid response in each mode are resumed in Table 5.5.

In order to evaluate the system economically, peak-time pricing plan for electricity purchased from utility grid is applied as shown in Figure 5.25. This pricing plan is assumed has two pattern: weekday pattern and weekend/holiday pattern. Weekday pattern price follows Figure 5.25. It contains two types price, daytime price for hour 9 to 22, and nighttime for others time. Meanwhile, for weekend/holiday pattern, nighttime price is applied for whole day.

Nowadays, peak-time pricing plan is common to be introduced from utility grid. When the price in peak-time is higher than other time, the utility hopes that consumers will reduce their consumption in the peak time or shift their load to the non-peak-time. Here, parameter α , as night to daytime electricity price ratio, is defined as stated in (5.32). Finally, to evaluate the system, total electricity cost is calculated by (5.33) for a long study period.

$$\eta_{gb} \cdot pgb_t - pgs_t/\eta_{gs} + \eta_{pv} \cdot ppv_t + \eta_{bd} \cdot pbd_t - pbc_t/\eta_{bc} = D_{ac,t}/\eta_{Dac} + D_{dc,t}/\eta_{Ddc} \quad (5.30)$$

$$pvs_t = \eta_{pv} \cdot ppv_t - D_{ac,t}/\eta_{Dac} - D_{dc,t}/\eta_{Ddc} \quad (5.31)$$

$$\alpha = N/D \quad (5.32)$$

$$tc = \sum_{d=1}^{ND} \sum_{t=1}^{NT} pgb_{t,d} \cdot EC_{t,d} \quad (5.33)$$

Table 5.3 List of converters

Converter	Descriptions
①	dc/dc converter as pv converter
②	dc/dc converter as battery controller
③, ④, ⑦	dc/ac converter
⑤, ⑥	ac/dc converter

Table 5.4 Efficiency of Converters

	AC System	DC System
η_{gb}	1	η_{6r}
η_{gs}	1	η_{6i}
η_{pv}	$\eta_1 \cdot \eta_3$	η_1
η_{bd}	$\eta_{2d} \cdot \eta_{4d}$	η_{2d}
η_{bc}	$\eta_{2c} \cdot \eta_{4c}$	η_{2c}
η_{DAC}	1	η_7
η_{DDC}	η_5	1

Table 5.5 Equations for battery and grid response in each mode

Mode	Charging & Discharging Power	Purchased Power
Mode 1	$pbc = \min(\eta_{bc} \cdot pvs, sb/\Delta t, PBC_{max}); pbd = 0$	$pgb = \frac{-pvs + pbc_t/\eta_{bc} - \eta_{bd} \cdot pbd_t}{\eta_{gb}}$
Mode 2	$pbc = 0; pbd = 0$	
Mode 3	$pbc = \min(sb/\Delta t, PBC_{max}); pbd = 0$	
Mode 4	$pbc = 0; pbd = 0$	
Mode 5	$pbc = 0; pbd = \min(-pvs/\eta_{bc}, rb/\Delta t, PBD_{max})$	

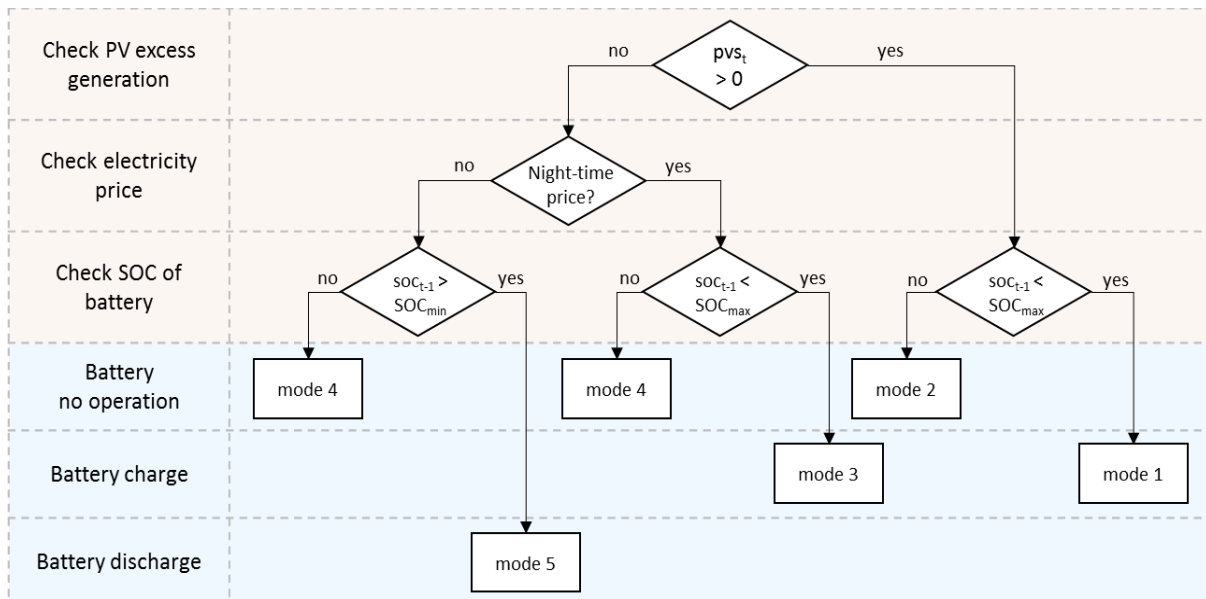


Figure 5.24 Flowchart for deciding battery response and power purchased from grid

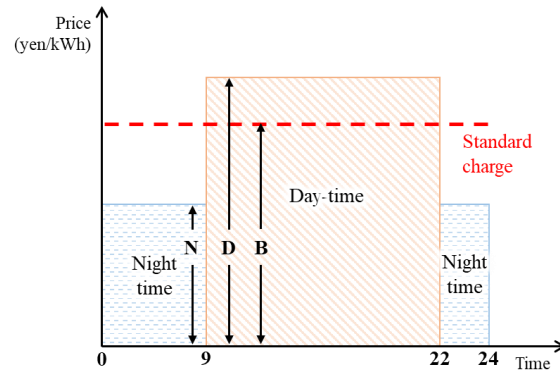


Figure 5.25 Energy price for weekday in peak-time pricing plan

5.6.2 Cost Analysis and Results

The cost analysis is used to economically evaluate the dc system in building comparing to ac system. As the economic evaluation is done by using peak-time pricing ratio, energy price is assumed as 18.05 yen/kWh for day-time price, and 12.45 yen/kWh for night-time price. In this evaluated system, selling energy to the grid is prohibited.

Load curve is also differentiated by weekday or weekend/holiday pattern, as shown in Figure 5.26. PV generation curve is divided into two types of sunny day and one type for rainy day. As shown in Figure 5.26, ‘Sunny A’ is used for winter and autumn, ‘Sunny B’ is used for spring and summer, and ‘Rain’ is used for all seasons. Period of study is one year with hourly time step.

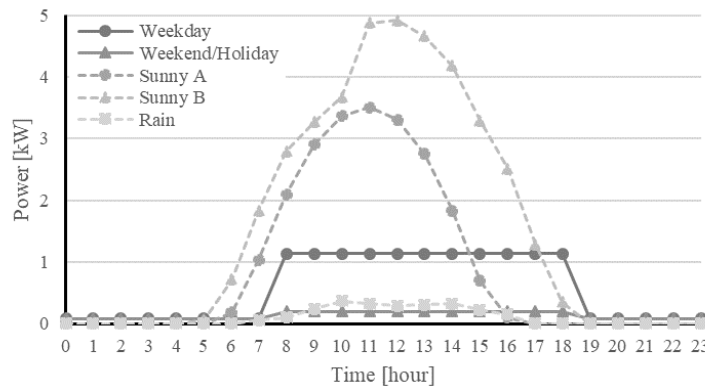


Figure 5.26 Load and PV generation curve

By assuming that every converter has the same efficiency, 95%, total annual cost of dc and ac system is compared in Figure 5.27. The results show that higher portion of dc load increase the annual cost in ac system. On the contrary, the annual cost in dc system is decreased in line with higher dc load. Battery size gives influences whether ac system or dc system which will give minimum cost. In full dc load system, greater battery size will give more reduction when we change ac system to dc system. As shown in Figure 5.28, bigger battery size gives smaller portion of DC load to achieve breakpoint.

By using a different value of efficiency converter, total annual cost of dc and ac system is also compared (Figure 5.29). It shows that with the same battery size, different efficiency converter does not change the breakpoint line. In full dc load system, lower efficiency of converter gives bigger gap of total annual cost reduction if the system is changed from ac system to dc system.

In order to evaluate the effect of value of α to the annual cost, the same efficiency for each converter is used as 95%. It is evaluated by three sizes of battery system. Figure 5.30 shows the percentage benefit of dc system over to ac system as results of this evaluation which is calculated using (5.34). Negative value means ac system gives more percentage benefit compare to dc system, and positive value means the opposite. Value of α gives different effect for negative percentage benefit and positive percentage benefit. In full dc load system, smaller value of α will give more percentage benefit if the dc system is used. Meanwhile, in full ac load system, it will give more percentage benefit if the ac system is used.

$$benefit = ((tc_{ac} - tc_{dc})/tc_{ac}) \cdot 100\% \tag{5.34}$$

By assuming every converter has same efficiency in 95%, load sensitivity analysis is done and Figure 5.31 shows the results. This sensitivity analysis shows that load size affects the border line gradient of critical DC load portion.

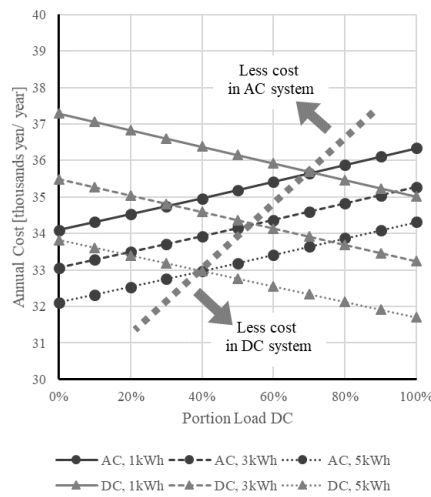


Figure 5.27 Comparison annual total cost by battery size

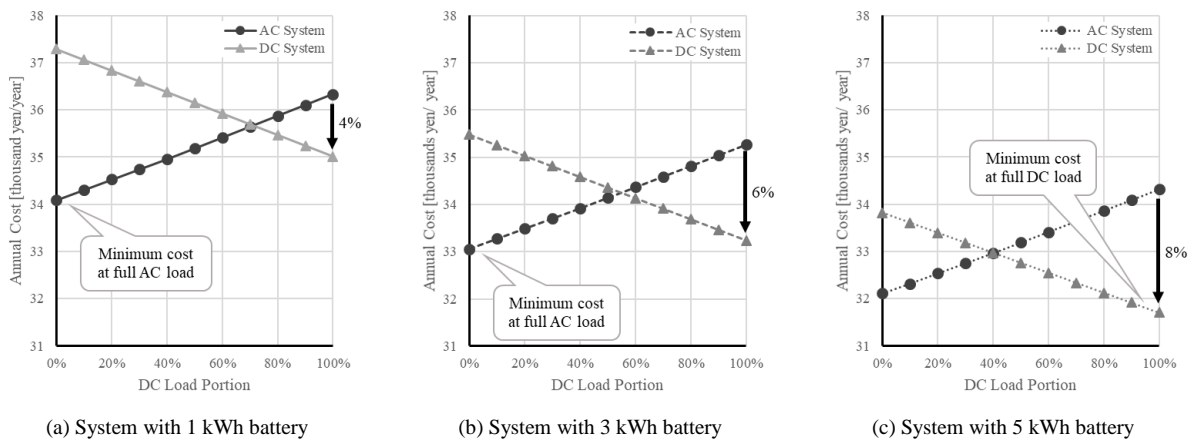


Figure 5.28 Total annual cost vs portion of DC load in battery size comparison

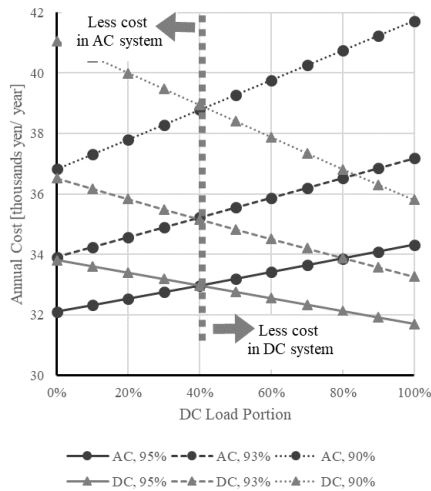


Figure 5.29 Comparison annual total cost by efficiency converter

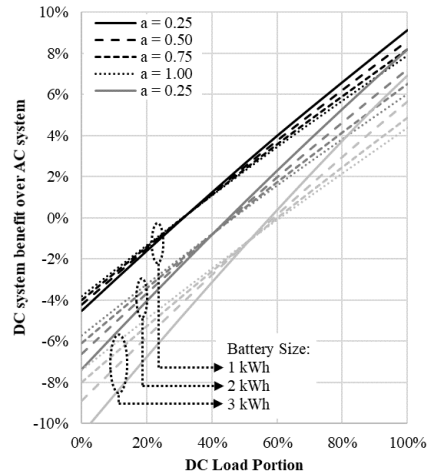
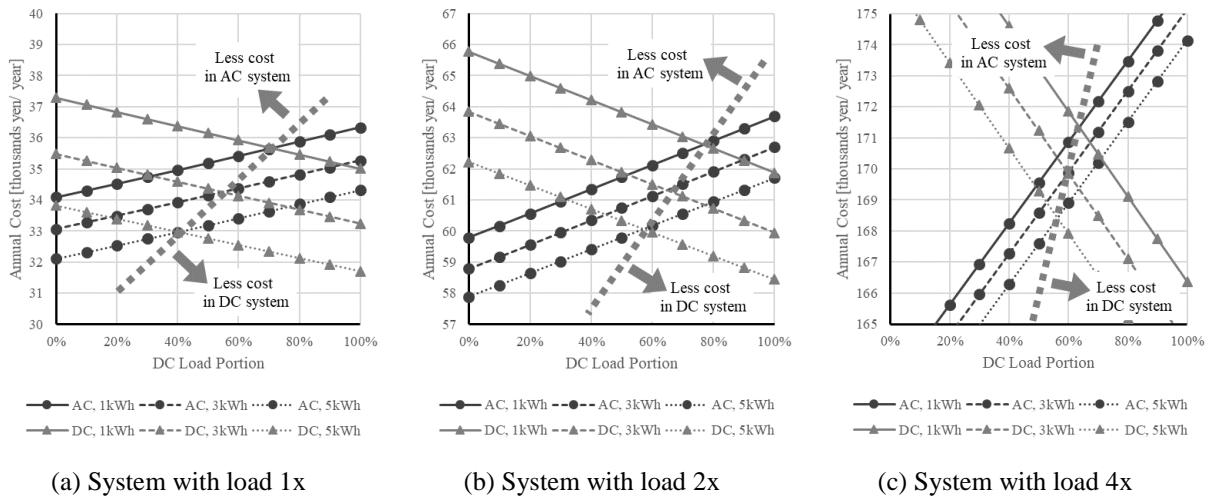


Figure 5.30 Comparison annual total cost by value of alpha and battery size



(a) System with load 1x

(b) System with load 2x

(c) System with load 4x

Figure 5.31 Total annual cost vs portion of DC load for load sensitivity analysis

5.7 Chapter Conclusions

First, the parameter α (night to day-time electricity price ratio) and β (day-time to standard charge ratio) are introduced to identify electricity pricing plan. Influence of parameter α to the benefit is evaluated by using general model of power grid system for building. The computational experiment result shows that there is a linear relation between percentage of total benefit and value of α , where the lower value gives more benefit. It also reveals that parameter α along with parameter β is needed to represent a peak-time electricity pricing plan. The contribution of these parameters is can be used to evaluate the system benefit which is intended to be applied in preliminary economic study of system planning.

Meanwhile, nowadays, AC grid system is commonly used in building grid system. For the time being, photovoltaic and batteries system, which are dc source, become ordinary to be used in building. In the load side, many appliances that used dc inside is also a typical load now. Hence, it is still a deliberation that which system is better to be used, whether ac or dc system.

Here, dc grid system in building is evaluated and compared to ac system by considering efficiency of every converter. This study shows that by using the same converter efficiency, higher portion of dc load increase the annual cost in ac system. Contrariwise, the dc system gives opposite effect where the annual cost is decline in line with higher portion of dc load. In case different size of battery is used, bigger size of battery

will give more reduction when we change ac system to dc system. In case of the same battery size, lower efficiency of converter gives bigger gap of total annual cost reduction when ac system is changed to dc system in full dc load system.

The ratio of night to peak-time electricity price, α , gives different effect for negative percentage benefit and positive percentage benefit. In full dc load system, smaller value of α will give more percentage benefit if the dc system is used. Besides, in full ac load system, it will give more percentage benefit if the ac system is used. The sensitivity analysis shows that load size affects the border line gradient of critical DC load portion.

It can be concluded that dc system will give more benefit when the portion of dc load is high compare to ac load. There is a point that there is no benefit when the ac system is changed to dc system. In case of every converter has same value of efficiency, this point is effected by battery size, but not by converter efficiency.

Chapter 6

Conclusion

6.1 Alignment with Research Issues

Recent environment issues are mostly related to CO₂ emission. Up to now, many international conventions are held in order to initiate the global real act for emission reduction. Countries all over the world are trying to reduce their emission by putting target and declared in these conventions. In COP21, the emission reduction target range in 2030 is -26% to -43% compared to 2005 emission. Japan proposed the target level of GHG emission reduction of 26.0% by fiscal year (FY) 2030 compared to FY 2013. The high share of indirect CO₂ emission of buildings can give significant impact in effort to reduce emission. According to this condition, realizing ZEB can be one of strategies for reducing the emission. Japan aims to realize ZEB in newly-constructed public buildings by 2020 and achieve average number in newly-constructed buildings by 2030.

This research is addressed to answer three mains challenges to achieve ZEB: energy storage, power converter, and economic operation.

Energy storage—Battery lifetime can be indicated by using some indicators, such as SOH, SOL, and RUL. Battery charge control considering this lifetime parameter such as SOH can be used for preventing over usage of battery by limiting its degradation. So that, we can expect the battery lifetime become longer compared to common operation. In addition, PV with battery system has a potential to reduce the electricity charge. Then, the optimization of battery charge-discharge schedule may increase the reduction.

Power converter—Avoid low power operation is necessary to keep high performance of converter. The datasheet will show only the efficiency average in rating power operation. Nevertheless, analysis result of recorded data shows that operation in power lower than its rating bring low efficiency. Except the sizing design, the operation controls also hold significant effect of maintaining efficiency converter in operation condition. Besides, by minimizing the total electricity charge, optimizing power schedule of PV system with batteries also can be achieved by minimizing converter loss. Considering the role of converters, the reliability evaluation in commercial building indicates reliability of dc-grids can be higher than the usual ac-grids.

Economic operation—Peak-time electricity pricing started to be common used recently. This research proposed some price parameters, which can be used to evaluate the system benefit that is intended to be applied in preliminary economic study of system planning. Hence, it is still a deliberation that which system is better to be used, whether ac or dc system. This study shows that by using the same converter efficiency, higher portion of dc load increase the annual cost in ac system. Contrariwise, the dc system gives opposite effect where the annual cost is decline in line with higher portion of dc load. Each converter efficiency and battery size have influence the annual cost reduction. Load composition also has impact of the potential benefit if we change from current ac-system to dc-system.

6.2 Further Research Development

As future work, the energy management system, which includes SOH consideration, can be developed by using the proposed control. This kind of management system is expected will extend battery lifetime while optimizing the operation cost. Consideration of converter loss also can be added into the optimization operation.

Furthermore, the reliability study can be expanded to cover more on-site generation types and their state of conditions. Most popular on-site generation types on the scale of a small or medium-sized building is photovoltaic and small wind turbines. In case of large-sized building or complex of building, on-site generation such as internal combustion engine, cogeneration or combined heat and power (CHP), also can be used.

In order to obtain a deeper economic analysis, consideration of investment cost, such as storage battery price, PV panel price, and installation cost, will be necessary. In other side, consideration of demand response can be applied in energy management optimization.

References

- [1] J. R. C. (J.) / Netherlands E. A. A. (P.) European Commission, “Total greenhouse gas emissions (kt of CO₂ equivalent),” 2012. [Online]. Available: https://data.worldbank.org/indicator/EN.ATM.GHGT.KT.CE?end=2012&name_desc=false&start=1970&type=shaded&view=chart&year=2012. [Accessed: 08-Mar-2018].
- [2] J. Friedrich, M. Ge, and A. Pickens, “This Interactive Chart Explains World’s Top 10 Emitters, and How They’ve Changed,” *World Resour. Inst.*, 2017.
- [3] Climate Watch, “Global Historical Emissions,” 2018.
- [4] IPCC, “Climate Change 2014: Synthesis Report,” 2014.
- [5] C. Zou, Q. Zhao, G. Zhang, and B. Xiong, “Energy revolution: From a fossil energy era to a new energy era,” *Nat. Gas Ind. B*, vol. 3, no. 1, pp. 1–11, 2016.
- [6] *Rencana Umum Energi Nasional*. 2017, pp. 1–227.
- [7] Y. Ito, “A Brief History of Measures to Support Renewable Energy: 1 . Overview of implementation of measures to support renewable energy in Japan and abroad,” *IEEEJ*, vol. October, pp. 1–22, 2015.
- [8] ASEAN Centre for Energy, *ASEAN Renewable Energy Policies*, no. SEPTEMBER 2013. 2016.
- [9] M. Wulandari, “Renewable Energy Power Pricing in Indonesia,” 2017. [Online]. Available: <http://www.aseanenergy.org/blog/renewable-energy-power-pricing-in-indonesia/>. [Accessed: 08-Mar-2018].
- [10] P. Torcellini, S. Pless, M. Deru, and D. Crawley, “Zero Energy Buildings: A Critical Look at the Definition,” in *ACEEE Summer Study Pacific Grove*, 2006, p. 15.
- [11] SHASEJ, “Zebの定義と評価方法,” 2015.
- [12] H. Pang, E. Lo, and B. Pong, “DC Electrical Distribution Systems in Buildings,” in *2006 2nd International Conference on Power Electronics Systems and Applications*, 2006, pp. 115–119.
- [13] M. Starke, L. M. Tolbert, and B. Ozpineci, “AC vs. DC distribution: A loss comparison,” *Transm. Distrib. Expo. Conf. 2008 IEEE PES Powering Towar. Futur. PIMS 2008*, 2008.
- [14] R. Asad and A. Kazemi, “A Quantitative Analysis of Effects of Transition from AC to DC System, on Storage and Distribution Systems,” *Asia-Pacific Power Energy Eng. Conf.*, pp. 1–5, 2012.
- [15] K. W. Park, J. B. Kim, and D. Z. Lee, “Applying the DC distribution system constructed commercial buildings,” *2012 Int. Conf. Renew. Energy Res. Appl. ICRERA 2012*, 2012.
- [16] A. J. Wood and B. F. Wollenberg, *Power Generation, Operation, and Control*, Second. John Wiley & Sons Inc, 1996.

- [17] Q. Xu, J. Xiao, P. Wang, and C. Wen, "A Decentralized Control Strategy for Economic Operation of Autonomous AC, DC, and Hybrid AC/DC Microgrids," *IEEE Trans. Energy Convers.*, vol. 32, no. 4, pp. 1345–1355, 2017.
- [18] P. Tian, X. Xiao, K. Wang, and R. Ding, "A Hierarchical Energy Management System Based on Hierarchical Optimization for Microgrid Community Economic Operation," *IEEE Trans. Smart Grid*, vol. 7, no. 5, pp. 2230–2241, 2016.
- [19] L. Che and M. Shahidehpour, "DC microgrids: Economic operation and enhancement of resilience by hierarchical control," *IEEE Trans. Smart Grid*, vol. 5, no. 5, pp. 2517–2526, 2014.
- [20] J. Sachs and O. Sawodny, "A Two-Stage Model Predictive Control Strategy for Economic Diesel-PV-Battery Island Microgrid Operation in Rural Areas," *IEEE Trans. Sustain. Energy*, vol. 7, no. 3, pp. 903–913, 2016.
- [21] Y. Guo, J. Xiong, S. Xu, and W. Su, "Two-Stage Economic Operation of Microgrid-Like Electric Vehicle Parking Deck," *IEEE Trans. Smart Grid*, vol. 7, no. 3, pp. 1703–1712, 2016.
- [22] S. Chakraborty, T. Ito, T. Senjyu, and A. Y. Saber, "Intelligent economic operation of smart-grid facilitating fuzzy advanced quantum evolutionary method," *IEEE Trans. Sustain. Energy*, vol. 4, no. 4, pp. 905–916, 2013.
- [23] C. Chen, S. Duan, T. Cai, B. Liu, and G. Hu, "Smart energy management system for optimal microgrid economic operation," *IET Renew. Power Gener.*, vol. 5, no. 3, p. 258, 2011.
- [24] H. Farzin, M. Fotuhi-Firuzabad, and M. Moeini-Aghaie, "A Stochastic Multi-Objective Framework for Optimal Scheduling of Energy Storage Systems in Microgrids," *IEEE Trans. Smart Grid*, vol. 8, no. 1, pp. 117–127, 2017.
- [25] J. Y. Joo and M. D. Ilić, "An information exchange framework utilizing smart buildings for efficient microgrid operation," *Proc. IEEE*, vol. 104, no. 4, pp. 858–864, 2016.
- [26] H. Ge and Z. Zhao, "Security Analysis of Energy Internet with Robust Control Approaches and Defense Design," *IEEE Access*, vol. 3536, no. c, pp. 1–1, 2018.
- [27] D. Zhu, Y. Guo, J. Chen, Y. Li, and H. Jiang, "Architecture and security protection scheme for distributed new energy public service platform with hybrid cloud system," *J. Eng.*, vol. 2017, no. 13, pp. 2203–2206, 2017.
- [28] W. Chin, W. Li, and H. Chen, "Energy Big Data Security Threats in IoT-Based Smart Grid Communications," no. October, pp. 70–75, 2017.
- [29] M. Rossi, A. Toppo, and D. Brunelli, "Real-time Optimization of the Battery Banks Lifetime in Hybrid Residential Electrical Systems," *Proc. Conf. Des. Autom. Test Eur.*, p. 139:1----139:6, 2014.
- [30] S. A. Pourmousavi, R. K. Sharma, and B. Asghari, "A framework for real-time power management of a grid-tied microgrid to extend battery lifetime and reduce cost of energy," *2012 IEEE PES Innov. Smart Grid Technol. ISGT 2012*, pp. 1–8, 2012.
- [31] D. J. Spiers and A. A. Rasinkoski, "Limits to battery lifetime in photovoltaic applications," *Sol. Energy*, vol. 58, no. 4–6, pp. 147–154, 1996.
- [32] A. El Mejdoubi, A. Oukaour, H. Chaoui, H. Gualous, J. Sabor, and Y. Slamani, "State-of-Charge and State-of-Health Lithium-Ion Batteries' Diagnosis According to Surface Temperature Variation," *IEEE Trans. Ind. Electron.*, vol. 63, no. 4, pp. 2391–2402, 2016.
- [33] P. Fortenbacher, J. L. Mathieu, and G. Andersson, "Modeling, identification, and optimal control of batteries for power system applications," *2014 Power Syst. Comput. Conf.*, pp. 1–7, 2014.
- [34] B. Zhao, X. Zhang, J. Chen, C. Wang, and L. Guo, "Operation optimization of standalone

- microgrids considering lifetime characteristics of battery energy storage system,” *IEEE Trans. Sustain. Energy*, vol. 4, no. 4, pp. 934–943, 2013.
- [35] Y. Riffonneau, S. Bacha, F. Barruel, and S. Ploix, “Optimal Power Flow Management for Grid Connected PV Systems With Batteries,” *IEEE Trans. Sustain. Energy*, vol. 2, no. 3, pp. 309–320, 2011.
- [36] M. Gholizadeh and F. R. Salmasi, “Estimation of state of charge, unknown nonlinearities, and state of health of a lithium-ion battery based on a comprehensive unobservable model,” *IEEE Trans. Ind. Electron.*, vol. 61, no. 3, pp. 1335–1344, 2014.
- [37] N. Watrin, B. Blunier, and A. Miraoui, “Review of adaptive systems for lithium batteries state-of-charge and state-of-health estimation,” *2012 IEEE Transp. Electrification Conf. Expo, ITEC 2012*, no. 3, 2012.
- [38] K. C. Divya and J. Østergaard, “Battery energy storage technology for power systems-An overview,” *Electr. Power Syst. Res.*, vol. 79, no. 4, pp. 511–520, 2009.
- [39] X. Hu, C. Zou, C. Zhang, and Y. Li, “Technological Developments in Batteries: A Survey of Principal Roles, Types, and Management Needs,” *IEEE Power Energy Mag.*, vol. 15, no. 5, pp. 20–31, 2017.
- [40] Nokia Bell Labs, “Lead-Acid Battery: Foreword,” *Bell Syst. Tech. J.*, vol. 49, 1970.
- [41] M. Reyes and T. Novak, “Injury surveillance and safety considerations for large format lead-acid batteries used in mining applications,” *IEEE Trans. Ind. Appl.*, vol. 52, no. 2, pp. 1–1, 2015.
- [42] H. Kakigano, Y. Miura, T. Ise, and R. Uchida, “DC Micro-grid for Super High Quality Distribution — System Configuration and Control of Distributed Generations and Energy Storage Devices —,” *37th IEEE Power Electron. Spec. Conf.*, pp. 1–7, 2006.
- [43] S. Ebbesen, P. Elbert, and L. Guzzella, “Battery State-of-Health Perceptive Energy Management for Hybrid Electric Vehicles,” *IEEE Trans. Veh. Technol.*, vol. 61, no. 7, pp. 2893–2900, 2012.
- [44] S. Ben-Yaakov, “Spice simulation of PWM DC-DC convertor systems: voltage feedback, continuous inductor conduction mode,” *Electron. Lett.*, vol. 25, no. 16, p. 1061, 1989.
- [45] A. Matsumoto, A. Fukui, T. Takeda, K. Hirose, and M. Yamasaki, “Development of 400 Vdc power distribution system and 400 Vdc output rectifier,” in *INTELEC, International Telecommunications Energy Conference (Proceedings)*, 2009.
- [46] A. Matsumoto, A. Fukui, T. Takeda, and M. Yamasaki, “Development of 400-Vdc output rectifier for 400-Vdc power distribution system in telecom sites and data centers,” in *Intelec 2010*, 2010, pp. 1–6.
- [47] D. Marquet *et al.*, “Pre roll-out field test of 400 VDC power supply: The new alliance of Edison and Tesla towards energy efficiency,” in *2011 IEEE 33rd International Telecommunications Energy Conference (INTELEC)*, 2011, no. 1, pp. 1–8.
- [48] T. Iino, K. Hirose, M. Noritake, T. Yuba, H. Miyazawa, and J. Sekikawa, “Development of 400 Vdc plug and socket-outlet for DC distribution system,” in *INTELEC, International Telecommunications Energy Conference (Proceedings)*, 2012, no. 2.
- [49] K. Garbesi, V. Vossos, and H. Shen, “Catalog of DC Appliances and Power Systems,” Berkeley, 2012.
- [50] Carbon Trust, “Renewable energy sources: Opportunities for businesses,” 2010.
- [51] A. K. Nayak, K. B. Mohanty, K. Thakre, and V. S. Kommukuri, “Comparative reliability study of existing & proposed configurations of a PV plant,” in *2016 IEEE 7th Power India International Conference (PIICON)*, 2016, pp. 1–5.

- [52] Japan Sustainable Building Consortium, “Data-base for energy consumption of commercial building (DECC),” 2012.
- [53] Japan Sustainable Building Consortium, “Urgent proposal involved in summer power-saving measures for commercial buildings based on the DECC (available in Japanese language),” 2011.
- [54] Japan Sustainable Building Consortium, “Recommendations relating to winter power-saving measures for commercial buildings based on the DECC (Available in Japanese language),” 2011.
- [55] R. Billinton and R. N. Allan, *Reliability Evaluation of Power Systems*. Boston, MA: Springer US, 1996.
- [56] Syafaruddin, H. Narimatsu, and H. Miyauchi, “Optimal Energy Utilization of Photovoltaic Systems Using the Non-Binary Genetic Algorithm,” *Energy Technol. Policy*, vol. 2, no. 1, pp. 10–18, 2015.
- [57] T. Patterson, “U.S. electricity blackouts skyrocketing,” 2010. [Online]. Available: <http://edition.cnn.com/2010/TECH/innovation/08/09/smart.grid/>.
- [58] A. Jain, S. C. Tripathy, and R. Balasubramanian, “Reliability and economic analysis of a power generation system including a photovoltaic system,” *Energy Convers. Manag.*, vol. 36, no. 3, pp. 183–189, Mar. 1995.
- [59] M. Noritake, K. Yuasa, T. Takeda, H. Hoshi, and K. Hirose, “Demonstrative research on DC microgrids for office buildings,” *2014 IEEE 36th Int. Telecommun. Energy Conf.*, pp. 1–5, 2014.
- [60] TEPCO, “業務用季節別時間帯別電力（契約電力500kW未満）,” 2016. [Online]. Available: <http://www.tepco.co.jp/e-rates/corporate/charge/charge08-j.html>.
- [61] F. Oldewurtel, a. Ulbig, a. Parisio, G. Andersson, and M. Morari, “Reducing peak electricity demand in building climate control using real-time pricing and model predictive control,” *Decis. Control (CDC), 2010 49th IEEE Conf.*, pp. 1927–1932, 2010.
- [62] Z. Wang and R. Paranjape, “Optimal Residential Demand Response for Multiple Heterogeneous Homes With Real-Time Price Prediction in a spaceMultiagent Framework,” *IEEE Trans. Smart Grid*, vol. 8, no. 3, pp. 1173–1184, 2015.
- [63] Z. Liu, C. Zhang, M. Dong, B. Gu, Y. Ji, and Y. Tanaka, “Markov-decision-process-assisted consumer scheduling in a networked smart grid,” *IEEE Access*, vol. 5, pp. 2448–2458, 2017.
- [64] T. C. Chiu, Y. Y. Shih, A. C. Pang, and C. W. Pai, “Optimized Day-Ahead Pricing with Renewable Energy Demand-Side Management for Smart Grids,” *IEEE Internet Things J.*, vol. 4, no. 2, pp. 374–383, 2017.
- [65] M. Muratori and G. Rizzoni, “Residential Demand Response: Dynamic Energy Management and Time-Varying Electricity Pricing,” *IEEE Trans. Power Syst.*, vol. 31, no. 2, pp. 1108–1117, 2016.
- [66] Y. Wang, S. Member, X. Lin, S. Member, M. Pedram, and A. Integrating, “A Near-Optimal Model-Based Control Algorithm for Households Equipped With Residential Photovoltaic Power Generation and Energy Storage Systems,” *IEEE Trans. Sustain. Energy*, vol. 7, no. 1, pp. 1–10, 2015.
- [67] J. Lin, W. Yu, and X. Yang, “Towards Multistep Electricity Prices in Smart Grid Electricity Markets,” *IEEE Trans. Parallel Distrib. Syst.*, vol. 27, no. 1, pp. 286–302, 2016.
- [68] M. Parvania and R. Khatami, “Continuous-time marginal pricing of electricity,” *IEEE Trans. Power Syst.*, vol. 32, no. 3, pp. 1960–1969, 2017.
- [69] P. Yang, S. Member, G. Tang, and A. Nehorai, “A Game-Theoretic Approach for Optimal Time-

- of-Use Electricity Pricing,” vol. 28, no. 2, pp. 884–892, 2012.
- [70] R. S. Sachdev and O. Singh, “Consumer’s demand response to dynamic pricing of electricity in a smart grid,” in *2016 International Conference on Control, Computing, Communication and Materials (ICCCCM)*, 2016, pp. 1–6.
- [71] M. Alamaniotis, D. Bargiotas, N. G. Bourbakis, and L. H. Tsoukalas, “Genetic Optimal Regression of Relevance Vector Machines for Electricity Pricing Signal Forecasting in Smart Grids,” *IEEE Trans. Smart Grid*, vol. 6, no. 6, pp. 2997–3005, 2015.
- [72] M. Shahidehpour and L. Wu, “A hybrid model for integrated day-ahead electricity price and load forecasting in smart grid,” *IET Gener. Transm. Distrib.*, vol. 8, no. 12, pp. 1937–1950, 2014.
- [73] C. Joe-Wong, S. Sen, S. Ha, and M. Chiang, “Optimized day-ahead pricing for smart grids with device-specific scheduling flexibility,” *IEEE J. Sel. Areas Commun.*, vol. 30, no. 6, pp. 1075–1085, 2012.
- [74] Federal Energy Regulatory Commission (FERC), “Assessment of Demand Response and Advanced Metering,” *Dep. Energy EEUU*, p. 130, 2012.
- [75] Y. Qiu, L. Kirkeide, and Y. D. Wang, “Effects of Voluntary Time-of-Use Pricing on Summer Electricity Usage of Business Customers,” *Environ. Resour. Econ.*, vol. 69, no. 2, pp. 417–440, 2018.
- [76] Y. Wang and L. Li, “Time-of-use electricity pricing for industrial customers: A survey of U.S. utilities,” *Appl. Energy*, vol. 149, pp. 89–103, 2015.
- [77] P. Faria and Z. Vale, “Demand response in electrical energy supply: An optimal real time pricing approach,” *Energy*, vol. 36, no. 8, pp. 5374–5384, 2011.
- [78] M. Kii, K. Sakamoto, Y. Hangai, and K. Doi, “The effects of critical peak pricing for electricity demand management on home-based trip generation,” *IATSS Res.*, vol. 37, no. 2, pp. 89–97, 2014.

List of Publications

List of Publications during Ph.D Course at Shibaura Institute of Technology.

Journal article

- [A1] P. O. Hadi and G. Fujita, "Battery Charge Control by State of Health Estimation," *Indonesian Journal of Electrical Engineering and Computer Science*, vol. 5, no. 3, p. 508-514, 2017.
- [A2] P. O. Hadi, K. Tagami, Y. Tanaka, G. Fujita, "Peak-Time Ratio in Time-Based Electricity Pricing for Economic Evaluation of Distribution System in Zero Energy Building," *Energies*, 2018. (Under review process, per August 2018)

International conference proceedings

- [B1] P. O. Hadi and G. Fujita, "Reliability of DC-Grids for Commercial Buildings," *Proceeding of International Conference on Electrical Engineering, Informatics, and Its Education*, Malang, Indonesia, 2015.
- [B2] P. O. Hadi and G. Fujita, "Optimizing Power Schedule of Grid Connected PV System with Batteries Based on Converter Loss," *Proceeding of International Conference on Electrical Engineering*, Okinawa, Japan, 2016.
- [B3] P. O. Hadi and G. Fujita, "Battery Charge Control by State of Health Estimation," *Proceeding of International Conference on Electrical, Electronic, Communication and Control Engineering*, Johor Bahru, Malaysia, 2016.
- [B4] P. O. Hadi and G. Fujita, "SOH-Estimated Battery Charge Control Using Average Model Simulation," *Proceeding of South East Asian Technical University Consortium (SEATUC) Symposium*, Ho Chi Minh, Vietnam, 2017.
- [B5] P.O. Hadi, G. Fujita, Y. Tanaka, K. Tagami, "Peak-Time Pricing Ratio for Economic Evaluation of Power Grids System in Zero Energy Building," *International Universities Power Engineering Conference (UPEC)*, Glasgow, United Kingdom, 2018.

Other proceeding

- [C1] P. O. Hadi and G. Fujita, "Evaluation of DC Power Distribution System in Commercial Building: Social Significance," *Proceeding of Intensive Workshop in SEATUC*, Tokyo, Japan, 2016.